10-21-2010

Thermal Conductivity of Soils from the Analysis of Boring Logs

Nicole M. Pauly
University of South Florida

Follow this and additional works at: http://scholarcommons.usf.edu/etd

Part of the American Studies Commons

Thermal Conductivity of Soils from the Analysis of Boring Logs

by

Nicole M. Pauly

A thesis submitted in partial fulfillment
of the requirements for the degree of
Master of Science in Civil Engineering
Department of Civil and Environmental Engineering
College of Engineering
University of South Florida

Major Professor: A. Gray Mullins, Ph.D.
Rajan Sen, Ph.D.
Mike Stokes, Ph.D.

Date of Approval:
October 21, 2010

Keywords: Thermal Conductivity, Diffusivity, Integrity Testing, Drilled Shaft,
Standard Penetration Test

Table of Contents

List of Tables

List of Figures

List of Symbols and Abbreviations

ρ dry density (g/cm^3)

γ unit weight (lb/ft^3) and (N/m^3)

Q   heat flow (W/m)

λ thermal conductivity (W/m-K)

c   specific heat (kJ/g-K)

C   Heat Capacity (J/cm^3-K)

k   diffusivity (m^2/s)

T   temperature (°C)

t   time (s)

Abstract

Recent interest in "greener" geothermal heating and cooling systems as well as developments in the quality assurance of cast-in-place concrete foundations has heightened the need for properly assessing thermal properties of soils. Therein, the ability of a soil to diffuse or absorb heat is dependent on the surrounding conditions (e.g. mineralogy, saturation, density, and insitu temperature). Prior to this work, the primary thermal properties (conductivity and heat capacity) had no correlation to commonly used soil exploration methods and therefore formed the focus of this thesis.

Algorithms were developed in a spreadsheet platform that correlated input boring log information to thermal properties using known relationships between density, saturation, and thermal properties as well as more commonly used strength parameters from boring logs. Limited lab tests were conducted to become better acquainted with ASTM standards with the goal of proposing equipment for future development.

Finally, sample thermal integrity profiles from cast-in-place foundations were used to demonstrate the usefulness of the developed algorithms. These examples highlighted both the strengths and weaknesses of present boring log data quality leaving room for and/or necessitating engineering judgment.

Chapter 1 - Introduction

Much of civil engineering practice involves the use of empirical relationships that cross reference available physical measurements to design parameters that are often difficult to define. This is particularly true in the specialty of soil mechanics where literally hundreds of correlations have been developed for the Standard Penetration Test, SPT, (Kulhawy 1990). Despite numerous advances in subsurface exploration (e.g. cone penetration test, seismic refraction, ground penetrating radar, etc), the SPT remains the most commonly used and is the primary choice of most design engineers. With regards to bridge foundations, this simple test provides the necessary information to estimate end bearing, side shear, or lateral stiffness of supporting elements such as driven piles, drilled shafts, and auger cast-in-place piles (ACIP).

The Standard Penetration Test as defined by ASTM D1586 entails driving a standard-sized split spoon sampler into the ground with a 140 lb hammer, dropped 30 inches. The recorded measurements include the number of hammer blows to advance the sampler 1 ft into the soil and the characteristics of the physical samples of the soil recovered from the split spoon. By augering or wash boring down to various depths of interest, SPT information can be obtained as a function of depth thereby providing both a strength and soil type profile.

In recent years, the need has arisen to find additional soil information that cannot be commonly discerned from present SPT correlations. This need comes in the wake of new developments in the quality assurance of cast-in-place foundation as well as trends

toward developing "greener" heating/cooling systems. In these cases, the ability of the soil to diffuse or provide thermal energy can only be assessed by knowing the thermal properties, specific heat and thermal conductivity, as well as ambient temperature conditions.

A new method of assessing the integrity of cast-in-place concrete measures the internal temperature of curing concrete that stems from the hydration reactions of the cementitious material (Mullins, 2009, 2007, 2005, 2004; Kranc, 2007). When intact concrete is present, a recognizable temperature signature / profile is present. When part of the concrete cross section is missing, the signature is interrupted. Figure 1.1 shows an example of a drilled shaft that exhibited dramatic loss of concrete cross-section and emphasizes the severity of an anomaly formation. Accurate knowledge of how the surrounding soils dissipate the curing temperature of concrete is presently difficult to define given the lack of rational correlations between commonly used soil exploration methods and the thermal properties.

Figure 1.1: Drilled Shaft with Concrete Void

The same disconnect exists in the emerging fields of geothermal heating and cooling systems. Many of these systems use shallow, buried heat exchange coils or extract and replace ground water from deep wells to dissipate the heat from condensing refrigerants. Well-type, water exchange systems are less susceptible to soil heat transfer, but systems using buried cooling loops, coils or similar rely on the surrounding soil type, ambient temperature, depth, and thermal properties of the soil to optimize such a system design. Figure 1.2 shows a geothermal ground loop located in the Tampa, Florida area that used cooling loops made of polyethylene tubing, buried in underground trenches, as one method of increasing air conditioning efficiency (Maynard, 2010).

Figure 1.2: Geothermal Ground Loop

Although the process used to install the polyethylene coils (as shown) disturbs the natural state of the soil and the associated thermal properties (increasing or decreasing density), the use of standard soil exploration methods would provide the system designer a rationale for specifying a finished state or at least provide boundaries for the possible range of thermal properties that are likely to result.

The focus of this study was to provide correlations between the boring log data from the SPT test and thermal properties of the soils present in the boring log. To that end, an Excel spreadsheet was created to take the blow counts and soil profile from the boring log and use them to calculate the thermal conductivity at any depth based on published, predictive approaches. This was supplemented with thermal conductivity testing in the laboratory to validate the results of the previously published relationships.

By calculating the thermal properties of soils, a better understanding of how the surrounding soils react through the ground when hot water or liquid concrete is pumped into it. The thermal conductivity and specific heat values of the soil will show how the ground reacts to the heat that it is receiving, and how much of that heat can be stored. This is especially helpful to the future of geotechnical engineering when designing geothermal systems and analyzing the structural integrity of concrete drilled shafts.

1.1 Organization of Thesis

This thesis is organized into four ensuing chapters describing the background, testing, results, and finally applications of the thesis findings with conclusions.

Chapter 2 outlines the historical evolution of the modern day understanding of thermal properties of soil. This includes not only the testing and predictive efforts to

define these properties, but also the applications that were instrumental in motivating research to that end.

Chapter 3 provides the process for developing the algorithms used to design the spreadsheet. Each component of the spreadsheet is broken down into a separate section with a thorough explanation included for each. These provide the reader a step-by-step overview of the process.

Chapter 4 discusses the testing and evaluation of thermal properties. The testing section discusses the equipment used and procedures followed for the laboratory tests conducted, along with the evaluation of these tests. This includes the recorded data, calculations, and an analysis of the results showing how the experimental data correlates with published thermal conductivity values. Chapter 4 concludes with the evaluation of the theoretical algorithms where a simple boring log is presented to aid as example of how the spreadsheet functions.

Chapter 5 concludes the report by summarizing the results and solidifying the correlation between boring log data and thermal properties. This chapter also provides information on current applications and recommendations for future studies on this topic.

Chapter 2 - Literature Review

A thorough literature review was conducted to initiate and focus the scope of this thesis. The topics of this literature review include an overview of thermal properties and usage, a history of thermal conductivity testing, standard soil testing methods, and existing correlations defining the thermal properties of soils.

2.1 Overview

Thermal conductivity and specific heat are the primary parameters affecting the transfer of heat energy through a given material. This transfer is commonly referred to as conductive heat flow when it uses these parameters, but often mechanisms including convection or radiation also contribute to the overall transfer, particularly in fluids or gases. For solids or particulates, the conductive mechanism overwhelmingly controls. Thermal properties for common materials have been well documented and some examples are listed in Table 2.1.

Table 2.1: Thermal Properties of Common Materials

Material Name	Thermal Conductivity (W/m-K)	Specific Heat (J/kg-K)
Dry Air	0.024	775
Saturated Air	0.1	940
Wood, Pine	0.147	240
Fresh Water	0.6	4184
Salt Water	0.8	3850
PCV Plastic Pipe	1.04	1340
Concrete (w=44%)	1.9	850
Concrete (w=40%)	2	900
Concrete (w=36%)	2.3	1100
Steel	14	470
Aluminum	250	900
Silver	429	233

Some values for soils can be found, but they vary widely in value likely caused by being poorly defined. Variations in temperature, density, and moisture content directly affect thermal properties making it difficult to accurately assess them without this information.

The correlations between thermal and mechanical properties of soil particles have been cited as being affected by close contact and density whereby thermo-elastic waves transmit heat. Farouki (1966) translated this concept from Debye (1914) where heat flow through a crystalline material occurs as warm atoms vibrate more than cooler atoms causing waves to travel through the material proportional to bond strength between the atoms.

From a computational standpoint, these concepts are applied using the general heat equation below which takes into account the heat production from an added heat source, Q, and the heat dissipation in the x, y, and z directions (second term) to calculate the change in temperature, T, with respect to time, t.

$$\frac{\partial T}{\partial t} = \frac{Q}{C} + k \left(\frac{\partial^2 T}{\partial x^2} + \frac{\partial^2 T}{\partial y^2} + \frac{\partial^2 T}{\partial z^2} \right)$$

Diffusivity, k, is defined as the ratio of thermal conductivity, λ, to heat capacity, C

$$k = \frac{\lambda}{C}$$

where thermal conductivity is the heat flow passing through a unit area, A, given a unit temperature gradient

$$\lambda = \frac{Q}{A \cdot \Delta T / l}$$

and, heat capacity is the product of the mass specific heat, c, and the density of the soil, ρ.

$$C = \rho \cdot c$$

In the application of geothermal heating/cooling systems, the source of heat is the hot water or coolant from the H.V.A.C. heat exchanger and can be considered a relatively constant heat flow for a given season. For shaft integrity applications, the heat source only exists during concrete curing, after which the second term of the general heat equation dominates the resultant temperature of the concrete.

2.2 Thermal Conductivity of Soils (Background)

Thermal testing of standard construction materials such as wood, concrete, plaster, and insulations are relatively straight forward when compared to soils. Until the late 1940's, little research had been performed on the thermal conductivity of soils. At that time, Miles S. Kersten conducted a significant amount of research on this topic at the University of Minnesota.

Studies were performed on 19 different soil types, consisting of a variety of sands, gravels, sandy loams, clays, minerals, crushed rocks, and organics. To quantify the thermal properties of these soils, numerous influential variables were identified including; mineralogy, density, moisture content, and moisture state. The primary focus of this research was to study the effects of the thermal conductivity of soils in permafrost regions in order to address complications arising from construction in these regions. A strong knowledge base of thermal properties was thought to help correct this problem (Kersten 1949).

From the extensive soil testing, Kersten developed a ratio between the thermal conductivity of the dry soil state, λ_0, and the saturated soil state, λ_1, denoted as the Kersten number, K_e.

$$K_e = (\lambda - \lambda_0)/(\lambda_1 - \lambda_0)$$

Kersten then developed empirical correlations between this number and the degree of saturation, S_r. For unfrozen soils, the Kersten number was defined as:

$$K_e = \left\{ \begin{array}{ll} 0.7\ Log S_r + 1.0 & S_r > 0.05\ coarse \\ log S_r + 1.0 & S_r > 0.1\ fine \end{array} \right\}$$

For frozen soils it is simply equal to the degree of saturation.

$$K_e = S_r$$

According to Oistein Johansen, the previous methods for calculating thermal conductivity were based on empirical correlations that were simply approximate determinations with wide tolerance limits (Johansen 1977). Johansen developed and used empirical correlations to develop theoretical equations to calculate thermal conductivity. Therein, the geometric mean of the thermal conductivity of air, water, and soil was given as

$$\lambda = \lambda_a^{n_a} \cdot \lambda_w^{n_w} \cdot \lambda_s^{n_s}$$

where λ and n represent the thermal conductivity and volumetric fraction of the phase components: air, water, and solids. For a saturated soil, the term for air can be ignored and this equation reduces to

$$\lambda_{sat} = \lambda_s^{(1-n)} \cdot \lambda_w^{n}$$

where n is the volumetric fraction of water. Johansen further developed a method for predicting thermal conductivity of soils by combining the conductivity at the two moisture extremes (dry and saturated) with the empirical relationship between the Kersten number and the degree of saturation (Johansen 1975).

$$\lambda = \lambda_0 + (\lambda_1 - \lambda_0) \cdot K_e(S_r)$$

Omar Farouki (1982) compiled thermal conductivity research from seven different sources, among which were Kersten and Johansen. The remaining five researchers were Mickley, Gemant, De Vries, Van Rooyen, and McGaw. Each researcher had devised a method for calculating thermal conductivity for fine grained and coarse grained soils. The data was provided in the form of either constant moisture content curves or constant degree of saturation curves of thermal conductivity vs. dry density graphs. The data are plotted in Figures 2.1 though 2.14. In practice, soil is rarely found in its dry state (degree of saturation = 0); however, data from dry soils was provided from Mickley, De Vries, Van Rooyen, and Johansen.

Much of the early research was performed on either frozen or freeze/thaw soils. Duarte (2006) published a study on unsaturated, tropical soils in Brazil. A sandy-clay and a clayey-sand were tested using a 1.5 mm diameter ALMEMO thermal probe which functions by heating up the soil sample until the thermal energy being passed into the soil and the thermal energy dissipated from the soil reach equilibrium.

Duarte concluded that much of the earlier work dealt with soils from frozen regions and was therefore not applicable to tropical climates. This conclusion stemmed from the study findings which reported four-fold lower thermal conductivity values for like soils. Amazingly, the findings were never disputed even though the thermal conductivity probe used for the study was severely limited and could not measure thermal conductivity values in excess of 0.420 W/m-K. All other sources predicted thermal conductivity values as high as 2.0 W/m-K. As would be expected, all soils tested reported values less than the equipment limit. Duarte presents the experimental data from the limited ALMEMO probe for the clayey-sand (coarse grained) and the sandy clay (fine

grained) in thermal conductivity vs. percent saturation curves. Duarte provides this data along with data from Johansen. This data is plotted in Figure 2.15.

Although the data from this source cannot be considered reliable, the paper does provide an excellent theoretical thermal conductivity history, along with the current probe method for measuring thermal conductivity. The large apparatus Kersten constructed in 1949 has evolved over the years and has been simplified into a probe with dimensions in millimeters connected to a small data-logger instead of a device the size of a room.
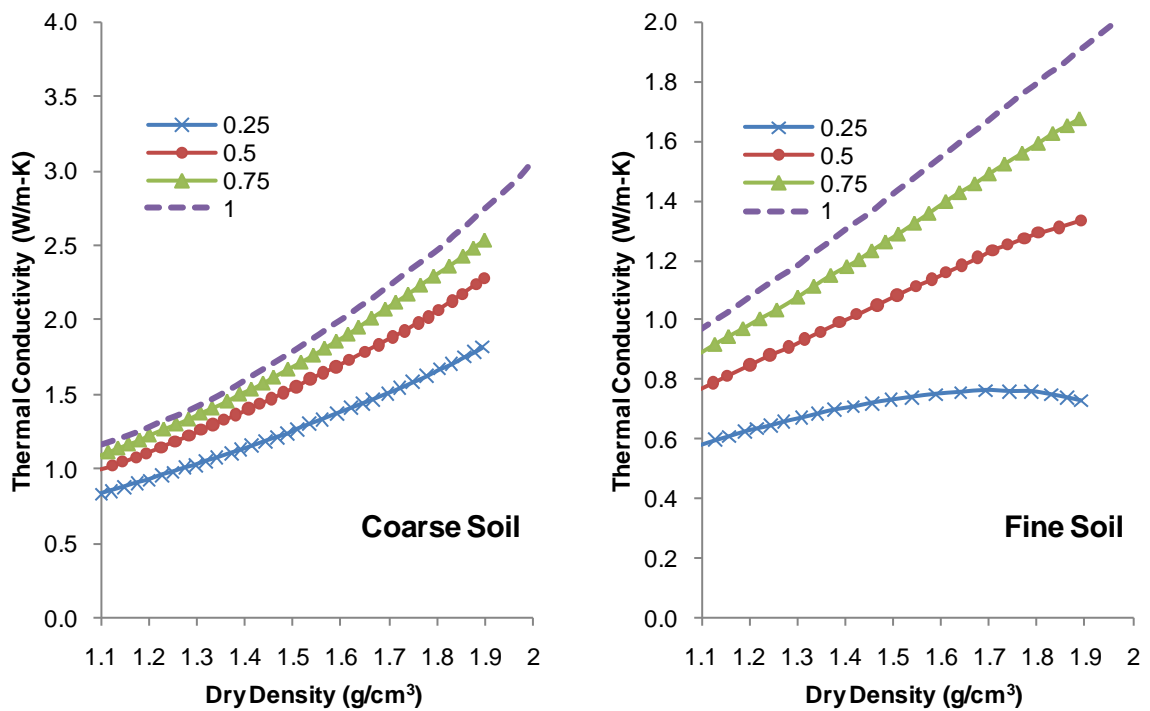
Figure 2.1: Conductivity vs. Density at varied Saturation (Kersten)
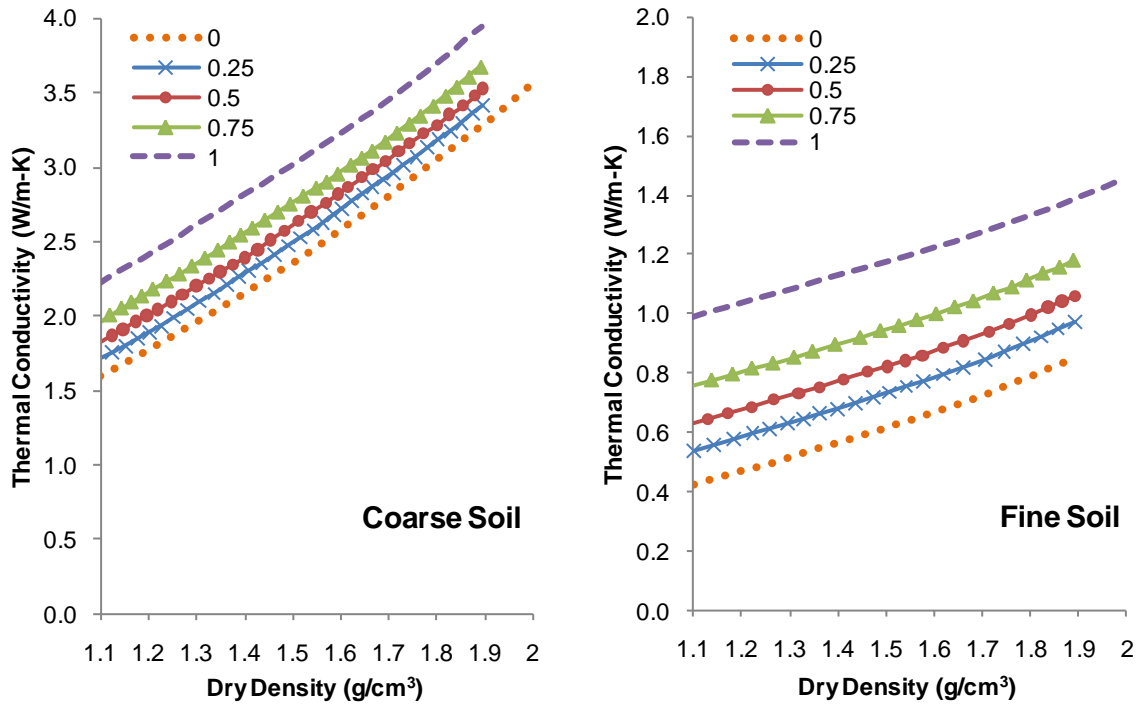
Figure 2.2: Conductivity vs. Density at varied Saturation (Mickley)
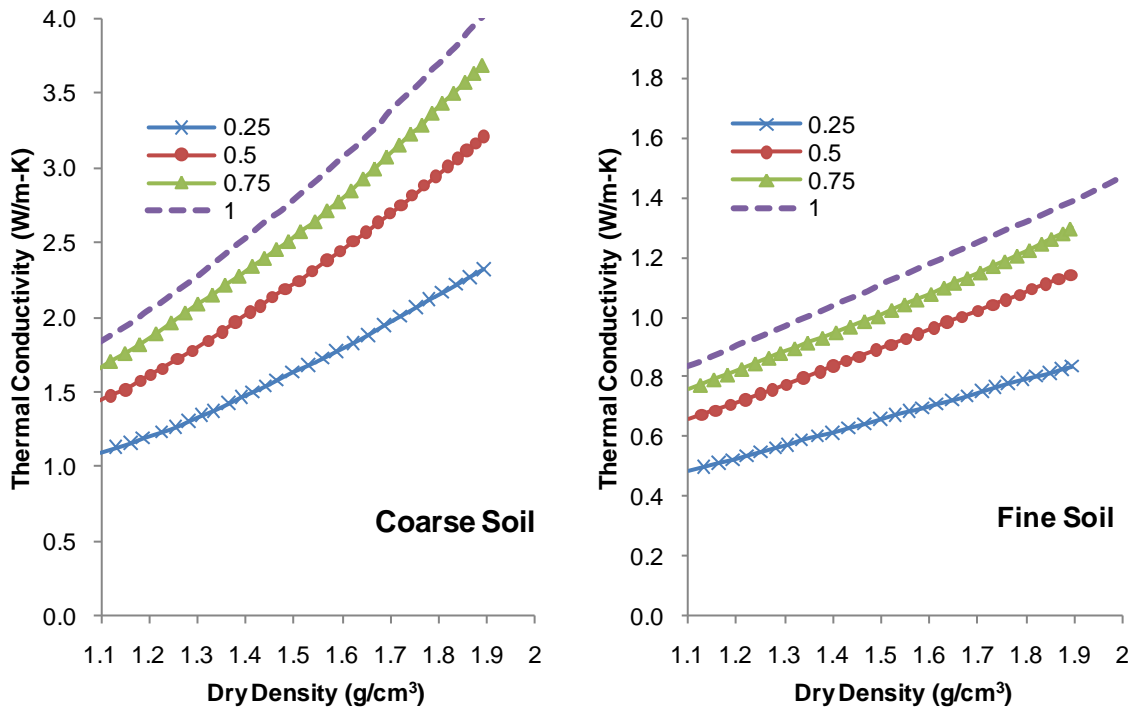
Figure 2.3: Conductivity vs. Density at varied Saturation (Gemant)
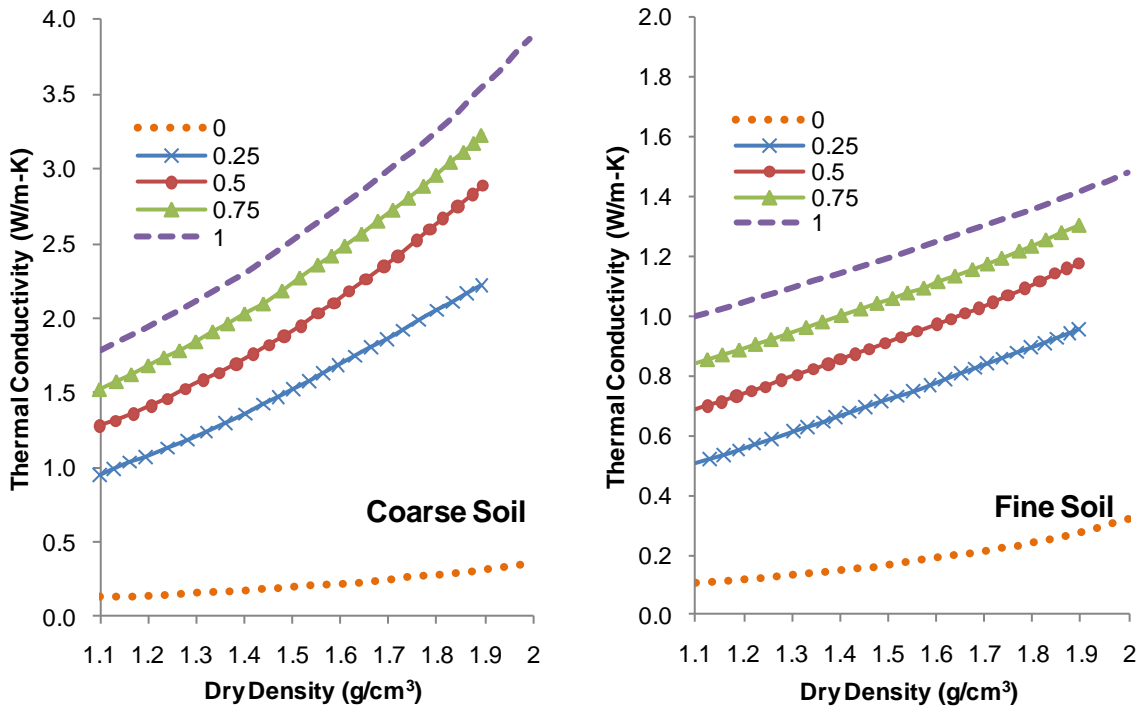
Figure 2.4: Conductivity vs. Density at varied Saturation (De Vries)
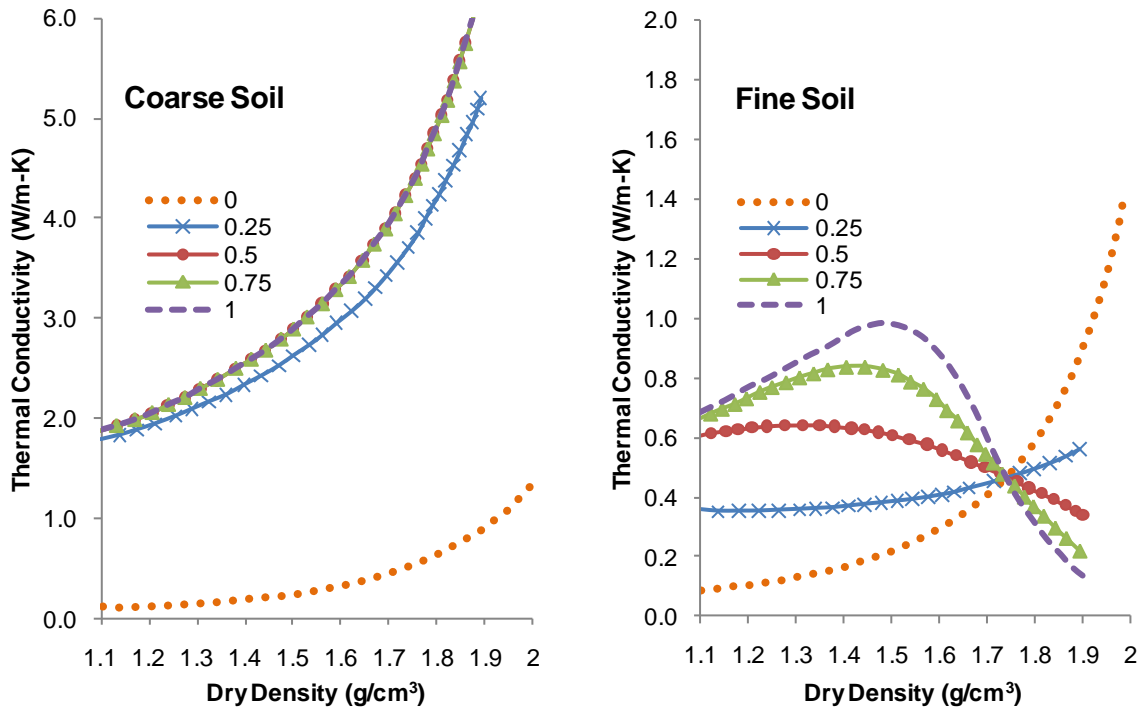
Figure 2.5: Conductivity vs. Density at varied Saturation (VanRooyen)
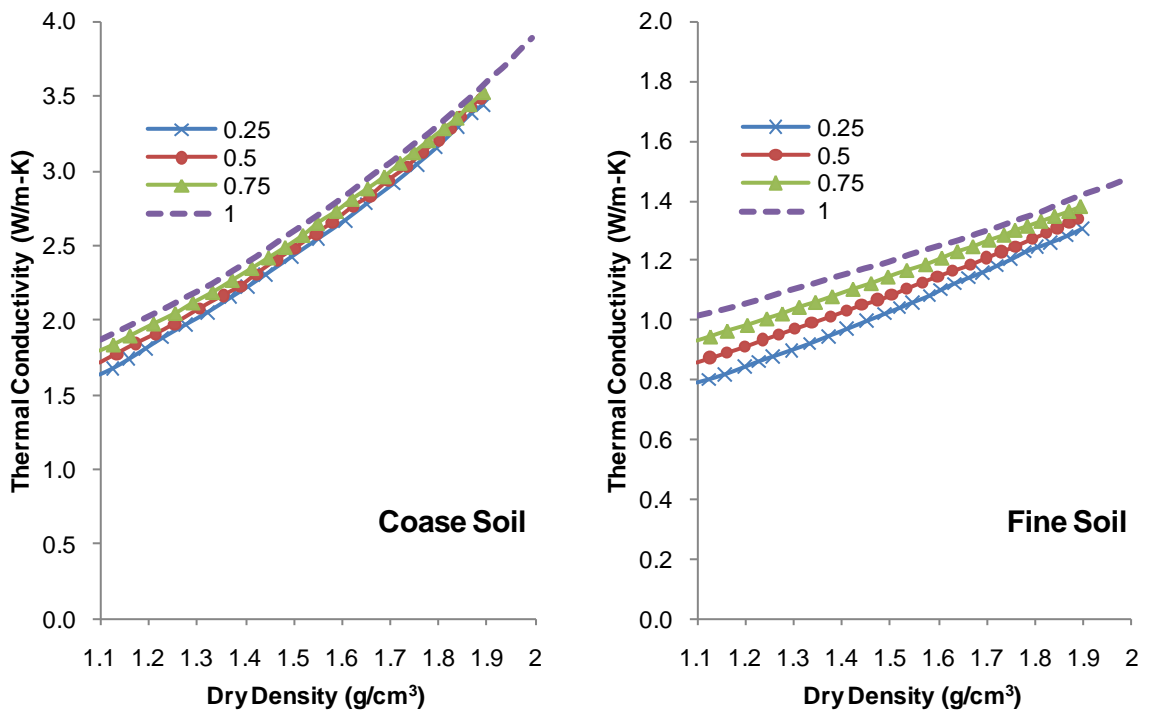
Figure 2.6: Conductivity vs. Density at varied Saturation (McGaw)
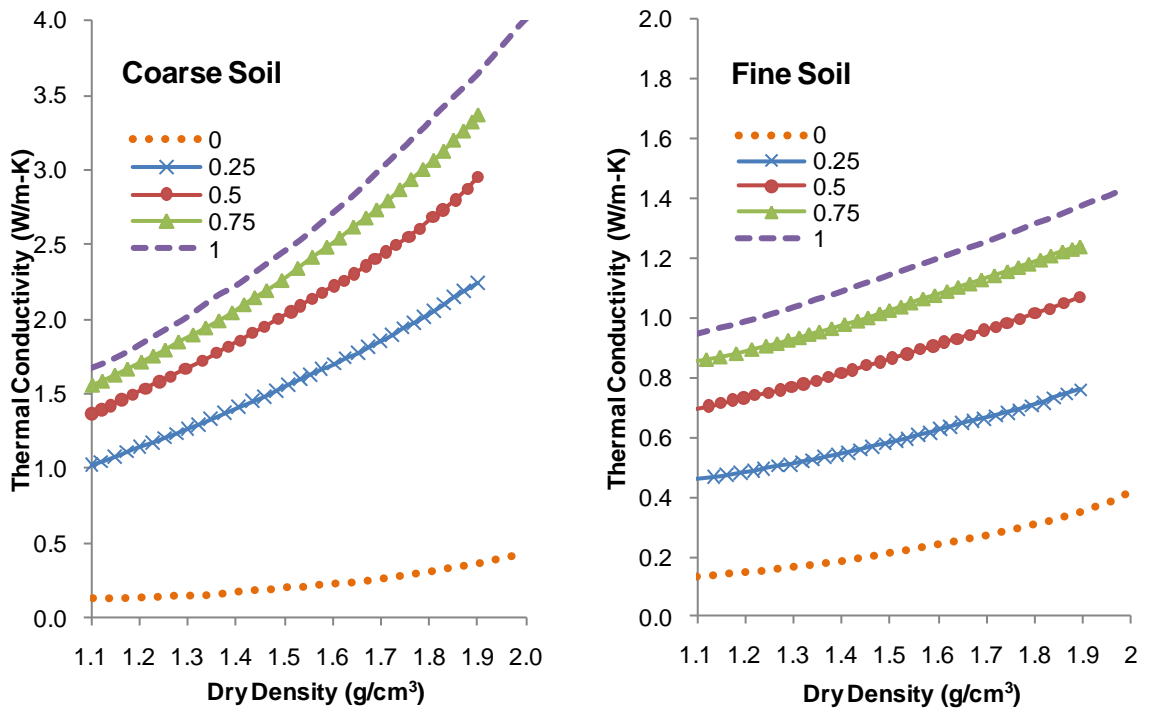
Figure 2.7: Conductivity vs. Density at varied Saturation (Johansen)
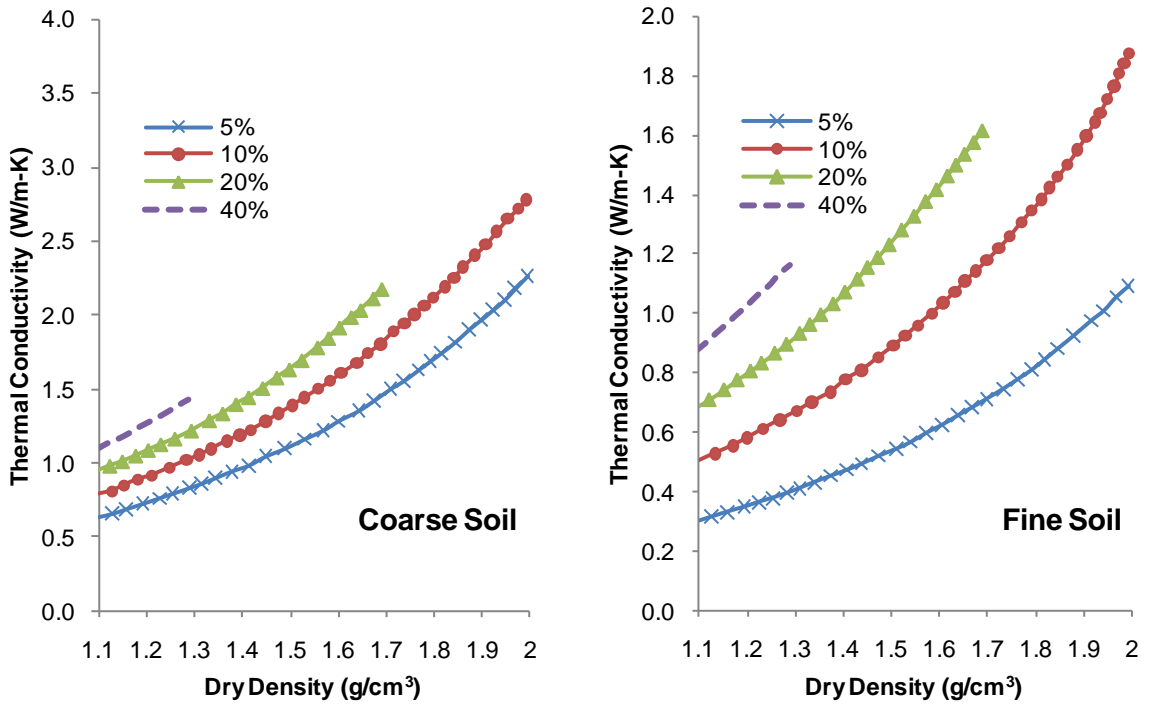
Figure 2.8: Conductivity vs. Density at varied Moisture Contents (Kersten)
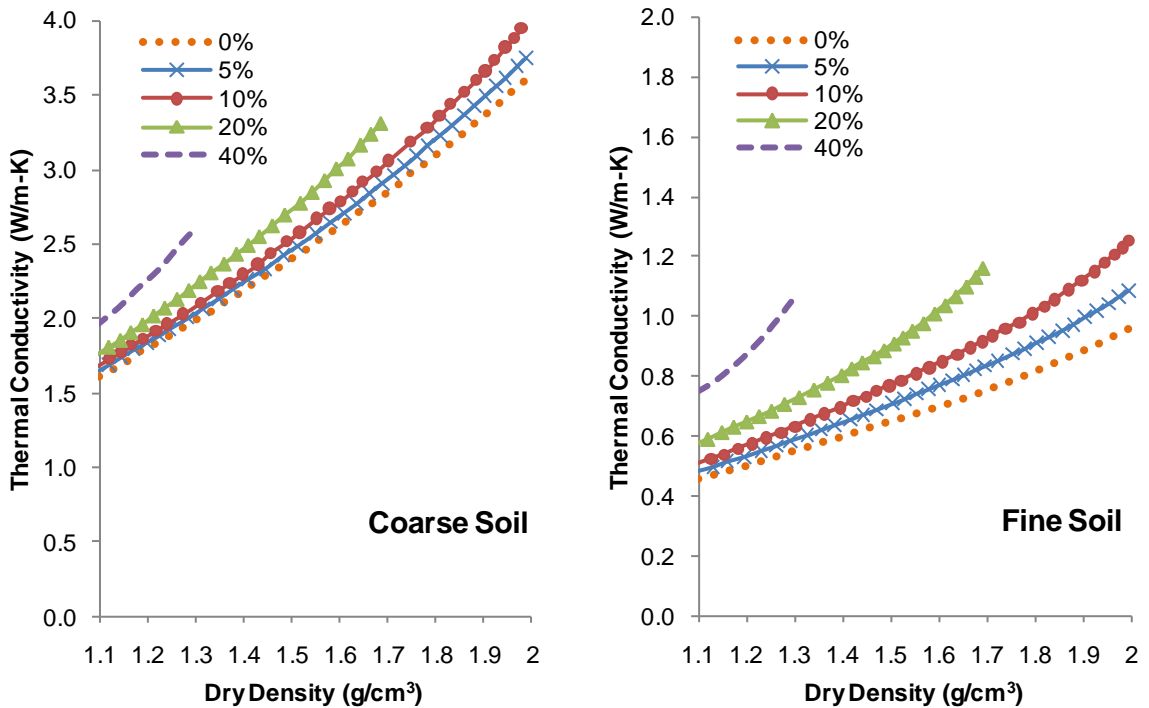
Figure 2.9: Conductivity vs. Density at varied Moisture Contents (Mickley)
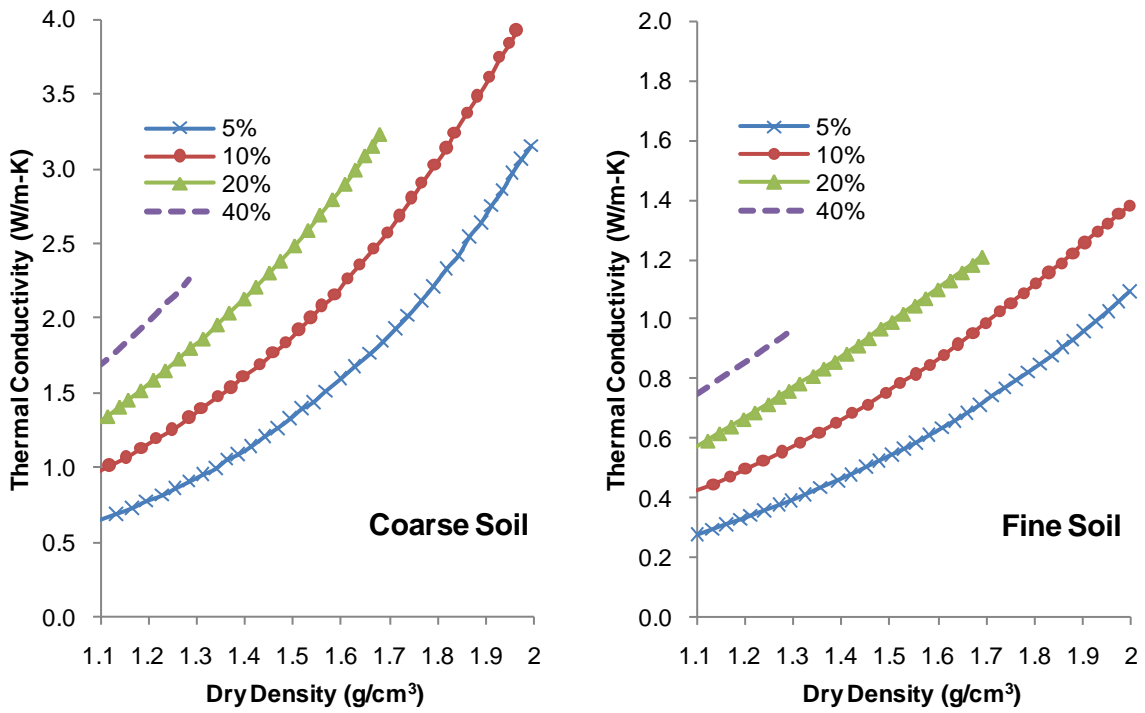
Figure 2.10: Conductivity vs. Density at varied Moisture Contents (Gemant)
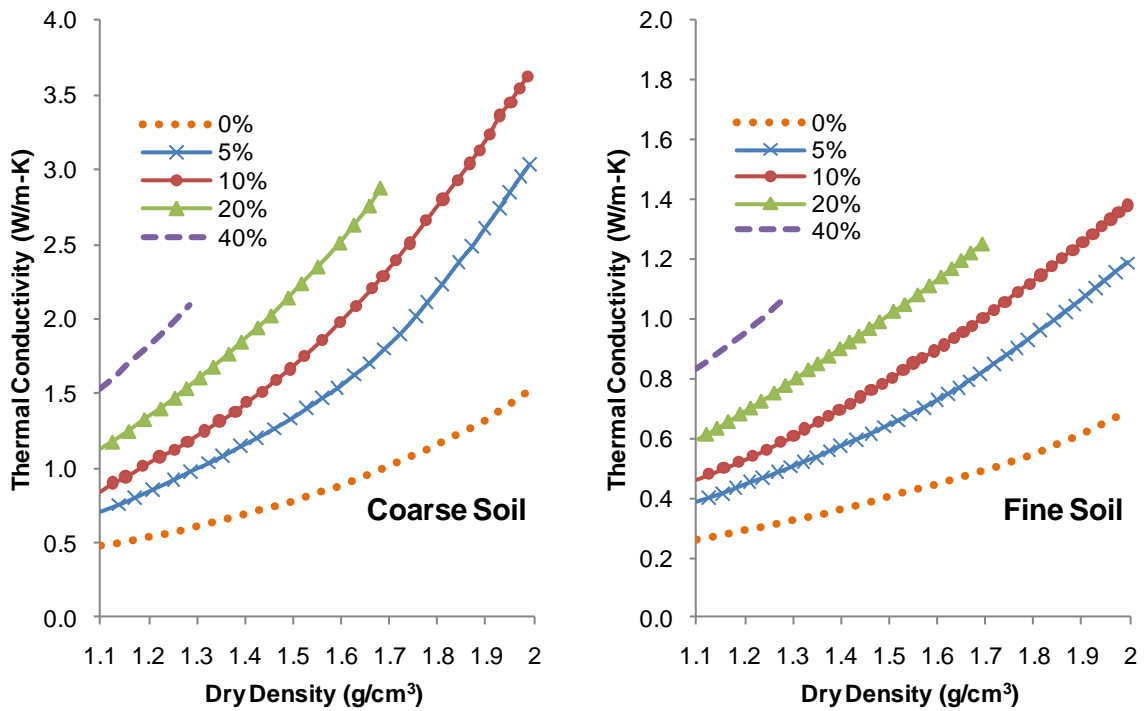
Figure 2.11: Conductivity vs. Density at varied Moisture Contents (De Vries)
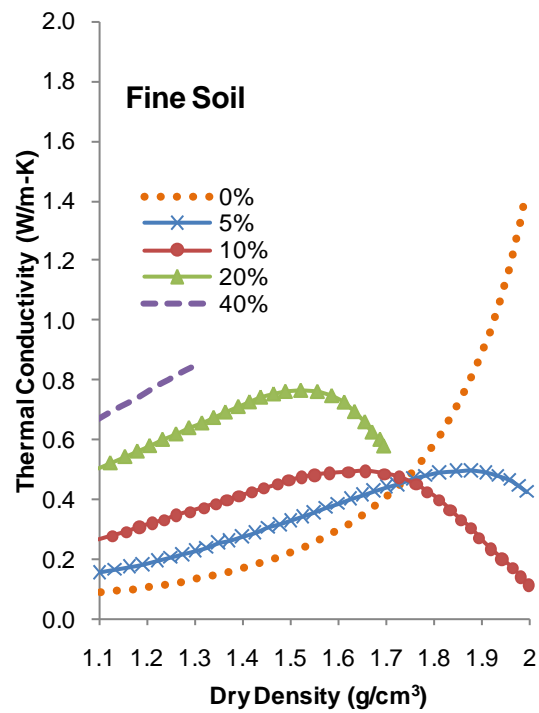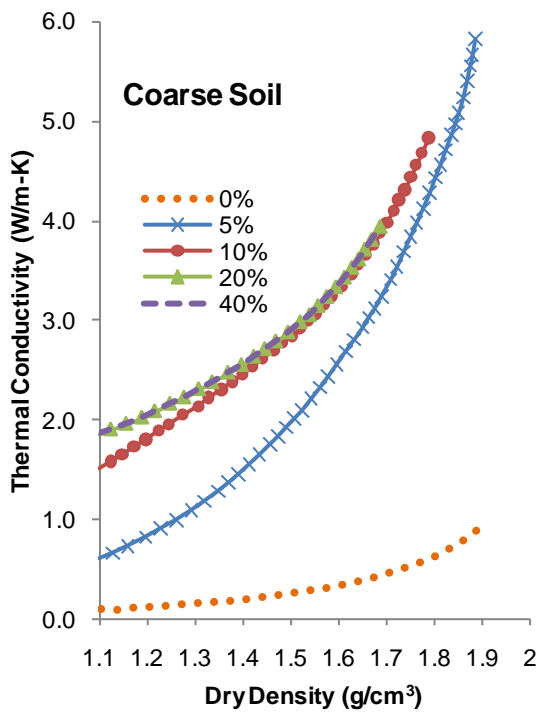
Figure 2.12: Conductivity vs. Density at varied Moisture Content(VanRooyen)
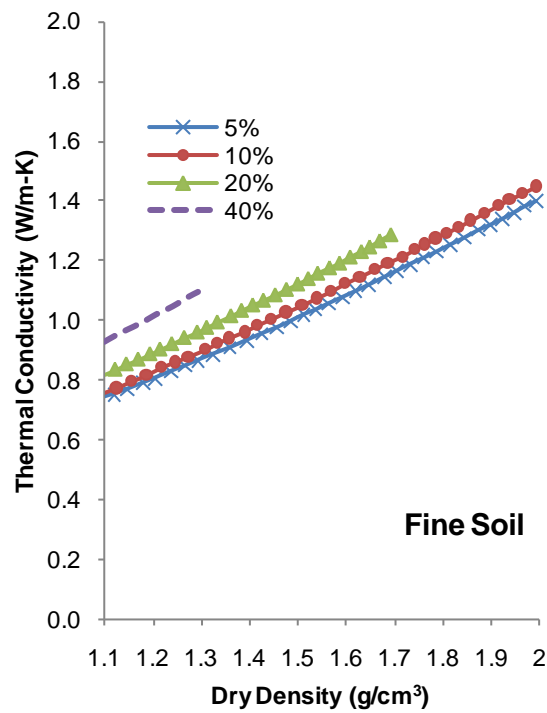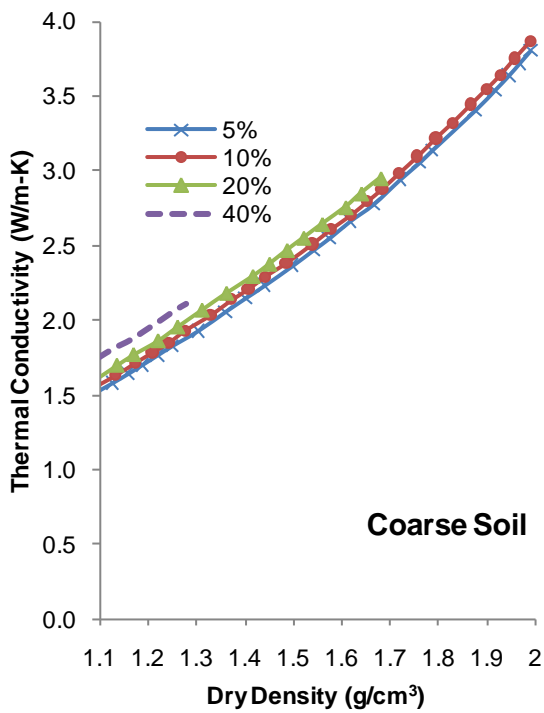
Figure 2.13: Conductivity vs. Density at varied Moisture Contents (McGaw)

17
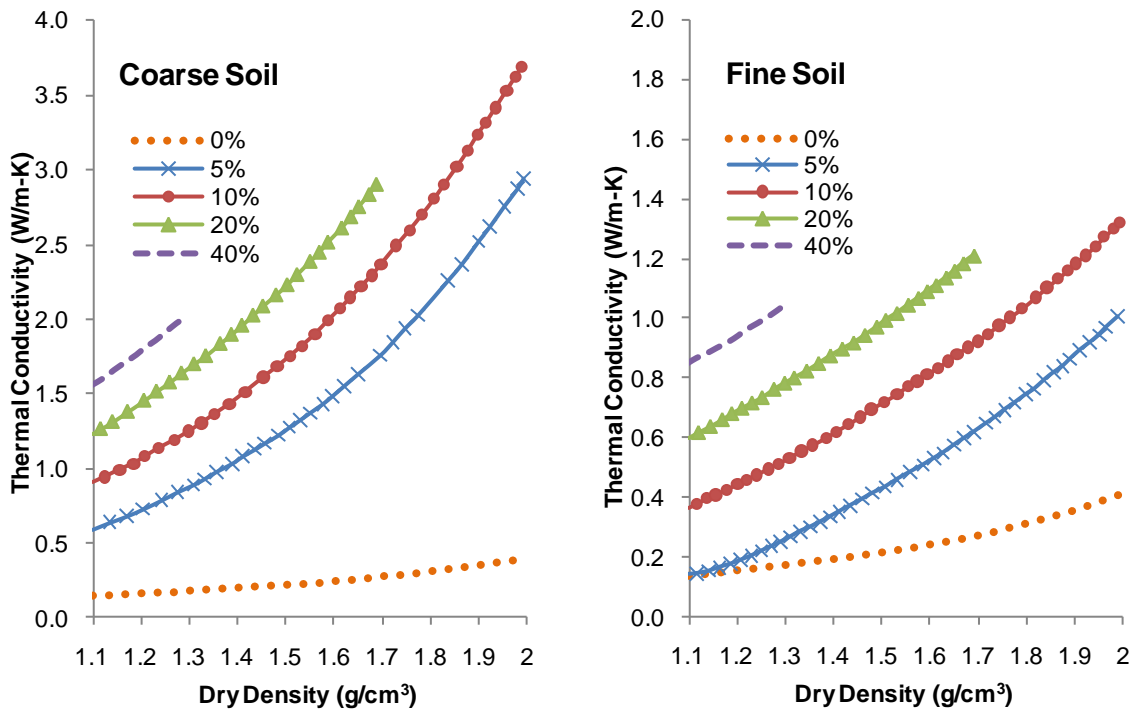
Figure 2.14: Conductivity vs. Density at varied Moisture Contents (Johansen)
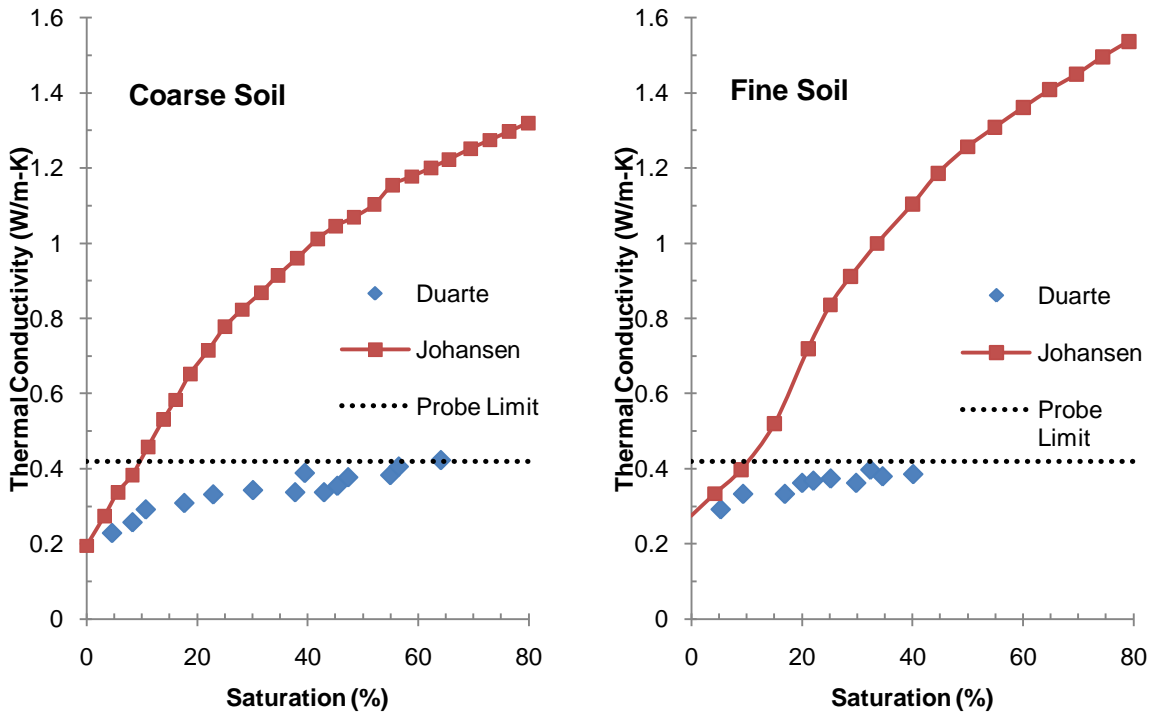
Figure 2.15: Thermal Conductivity vs. % Saturation (Duarte)

2.3 Properties and Measurement Correlations

2.3.1 Boring Log Measurements

A boring log is a compilation of the data from a Standard Penetration Test. Boring logs display blow count and soil type as a function of depth and often include moisture content information for fine grain or clayey soils. The soil extracted from the split-spoon sampler at each depth is placed in jars and taken to a laboratory to be classified using the USCS standards to identify the soil type as well as moisture content.

2.3.2 Density

Density is typically referred to as the amount of mass present in a unit volume, but often times in design applications, density is presented in the form of weight per unit volume, or unit weight. A correlation exists between unit weight and SPT blow counts for clays, silts, and sands. This correlation is depicted in Figure 2.16.
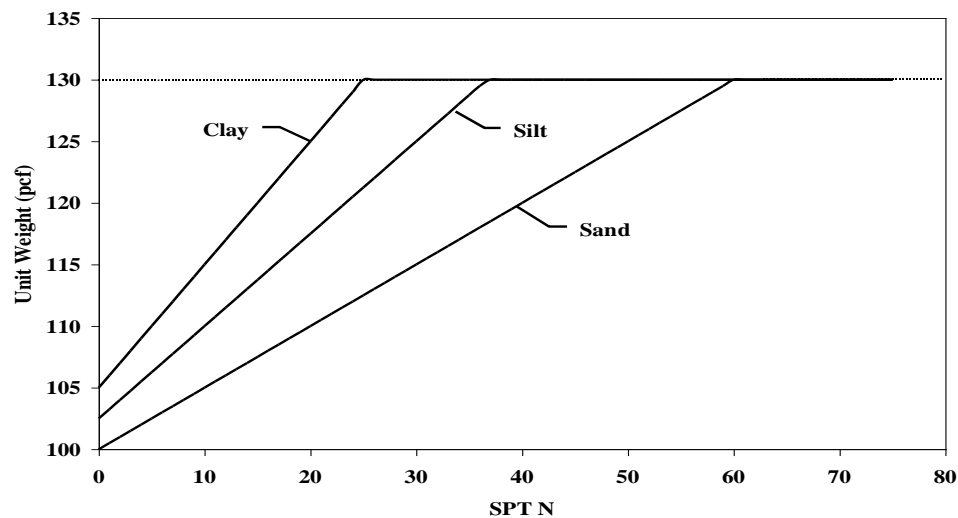
Figure 2.16: Curves for Density vs. Blow Count Correlation (Mullins 2004)

Any correlations hereafter involving unit weight are converted to density and presented in units of g/cm^3.

19

2.3.3 Moisture Content

Moisture content is the ratio of the weight of water to dry soil expressed as a percentage. Moisture contents vary between different soil types and the location relative to the water table. Depending on the soil type, capillary action will pull moisture from the water table up into the soil above the phreatic surface. The data shown in Figure 2.17 represents the result of capillary action at elevations above the water table for three common soil types.
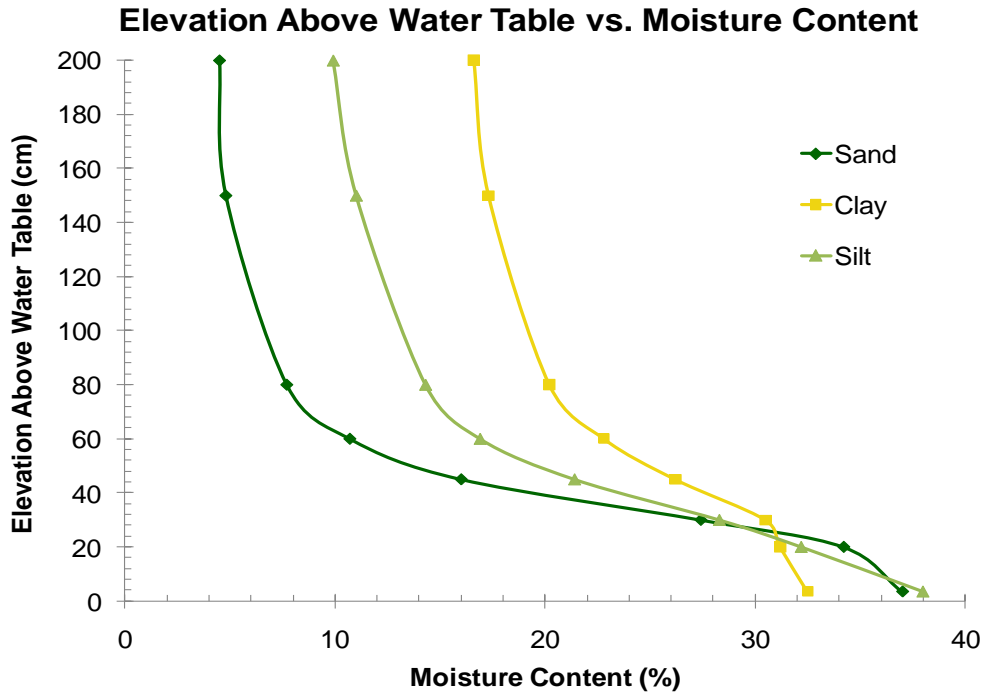
Figure 2.17: Water Table Effects on Moisture Contents of Florida Soils (Trout 2010)

2.3.4 Temperature

For all temperature dissipation scenarios involving soil, the temperature of the soil is an important parameter. Although the soil surface is subjected to seasonal variation, at depths greater than 30 feet below the surface, the soil temperature remains relatively constant. This soil temperature is dictated by the mean annual ground temperature and is

20

dependent on its geographic location. Figure 2.18 shows the mean annual ground temperatures for the United States (Virginia Tech 2010).
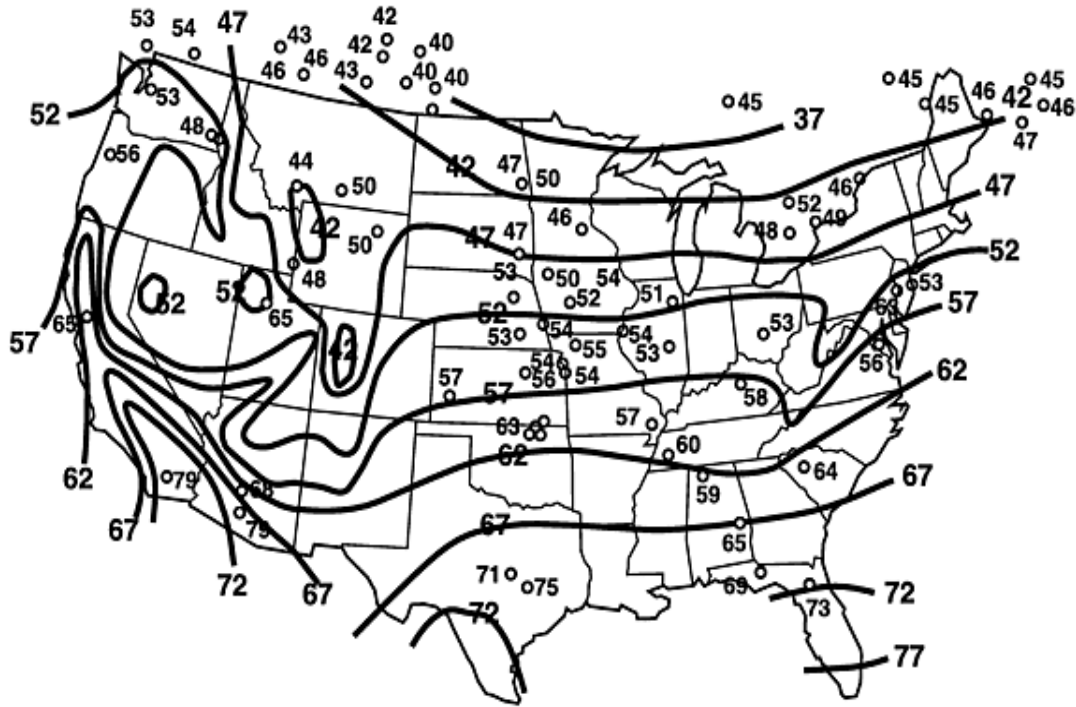
Figure 2.18: Mean Annual Ground Temperatures in the United States

2.4 Standard Soil Testing Methods

Standardized methods for soil testing are published in section 4 of the Annual Book of ASTM Standards by the American Society for Testing and Materials International. ASTM standards are technically competent standards that have been critically examined and used as the basis for commercial, legal or regulatory actions (ASTM 1996). In order for a test to conform to ASTM standards, it must meet all pertinent requirements prescribed for the method. The ASTM standards that are applicable to this thesis are the standards for standard penetration tests, thermal conductivity tests, relative density tests, and classification of soils. A brief overview of each is provided herein.

2.4.1 Standard Penetration Test

The standard penetration test (briefly discussed in Chapter 1) consists of a split-barrel sampler which is driven into the ground to obtain a soil sample. The resistance of the soil to the penetration of the sampler, referred to as a blow count or SPT N, represents the number of hammer blows necessary to advance the sampler 1 ft. The procedure for the SPT test is outlined in ASTM D1586, the Standard Test Method for the Penetration Test and Split-barrel Sampling of Soils. This test is conducted to provide a soil sample for laboratory soil classification tests. The SPT N value can be correlated to a variety of different applications (ASTM 1996).

Sampling rods with an inside diameter of 1 1/8 inch are used to connect the split-barrel sampler to the drive-weight assembly, which consists of a hammer and anvil. The requirements for the hammer are that it should weigh 140 lbs, consist of a solid rigid metallic mass, and make steel on steel contact with the anvil when it is dropped. Figure 2.19 provides the components and dimensions for the split-barrel sampler.

A = 1.0 to 2.0 in
B = 18.0 to 30.0 in
C = 1.375 ± 0.005 in
D = 1.50 ± 0.05 in
E = 0.10 ± 0.02 in
F = 2.00 ± 0.05 in
G = 16.0° to 23°
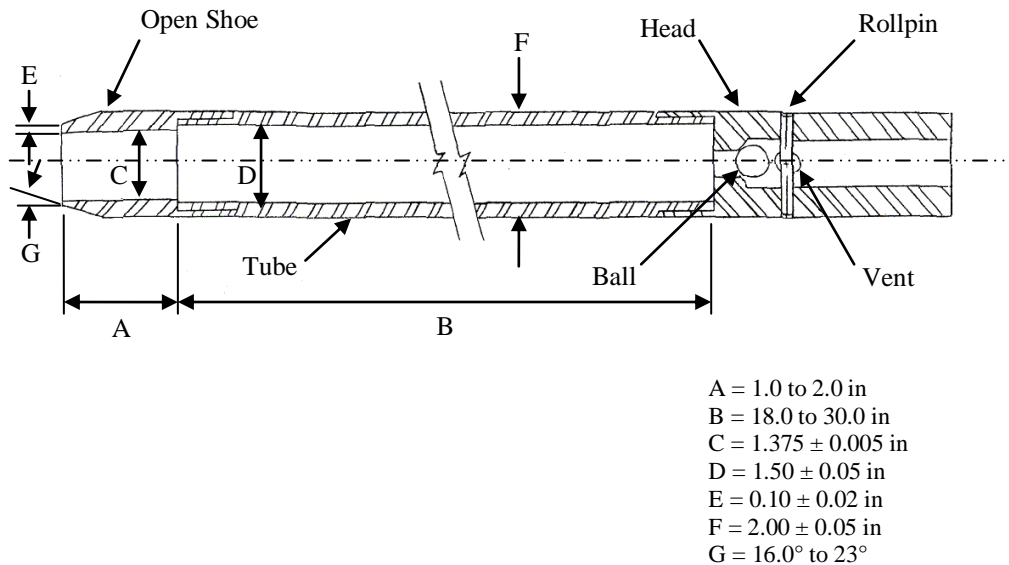
Figure 2.19: Split-Barrel Sampler

Once a boring has been advanced to desired elevation, the split-barrel sampler is attached to the sampling rods and lowered into the hole. The drive-weight is then positioned above and the anvil is attached to the sampling rods. The dead weight of the sampler, rods, anvil and drive weight are rested on the bottom of the boring and a seating blow is applied. The hammer is continuously dropped and the blows are counted over three increments of 6 inches. The sampler is to be tested over the entire 18 inches unless the soil is dense enough such that 50 blows have been applied over any 6 inch test, a total of 100 blows have been applied, or there is no noticeable advance during the application of 10 blows.

When compiling the data into a boring log, the first 6 inches is referred to as the seating drive and those blows are omitted. The blow counts of the second and third 6 inch penetrations are summed to provide the number of blow counts from that test. If 6 inches has not been reached within 50 blows, the blows per number of inches penetrated are recorded.

2.4.2 Thermal Conductivity Testing

Methods for measuring thermal conductivity include the transient method and the steady state method, the first of which is the most common. The Standard Test Method for Determination of Thermal Conductivity of Soil and Soft Rock by Thermal Needle Probe, ASTM D5334, is the approved transient heat method for thermal conductivity testing of soils. This method is approved for use in both wet and dry soils, but as moisture increases, percent error increases. Moisture can cause errors in the readings from the redistribution of water due to thermal gradients resulting from heating of the probe (ASTM 2008). This

error increases with greater heating times; therefore, either total heat added should be minimized or heating time should be reduced for soils with high moisture contents.

The equipment required for the test is a thermal needle probe, a constant current source, a multimeter, and a data collection device that collects both temperature and time readings. A probe with a large length to diameter ratio is required to simulate an infinitely thin heating source. The typical probe design consists of a copper-constantan thermocouple and either manganin or nichrome wire for the heating element encased in a stainless steel or similar thin-walled, closed-end tube. The heating element connects to a circuit with a constant current source which generates heat in the probe from the wire resistance when energized. The thermocouple wires are connected to the data collection device which monitors the temperature changes over time. The typical probe design according to ASTM 5334-08 is depicted in Figure 2.20.
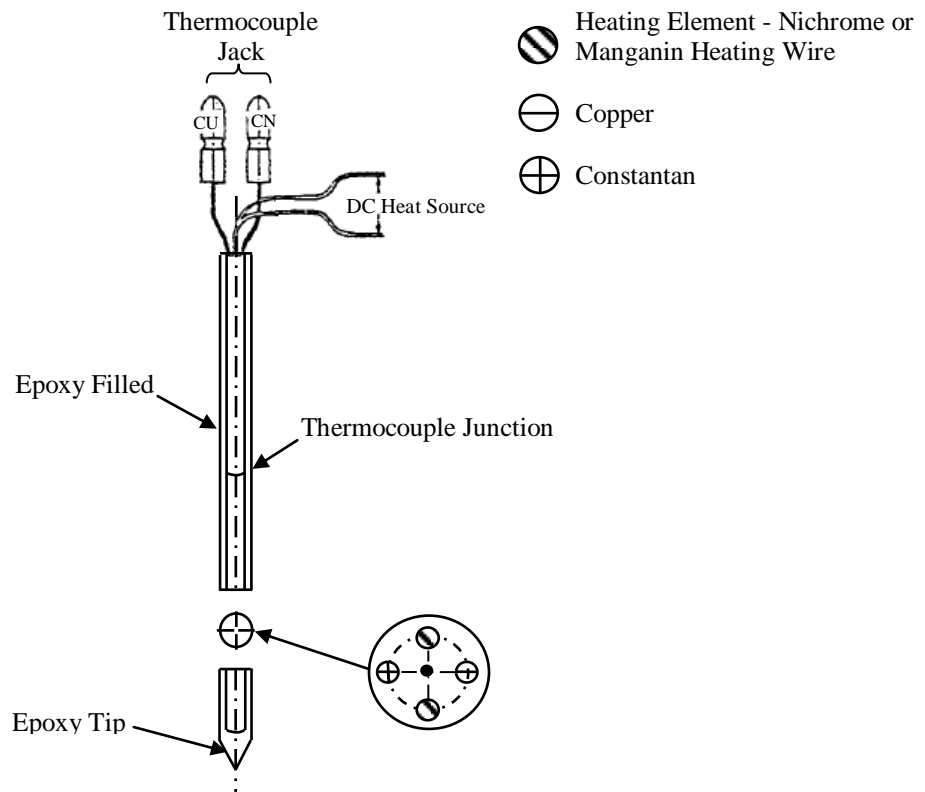
Figure 2.20: ASTM D5334-08 – Typical Probe Components

24

When conducting tests, known amounts of current and voltage are applied to the probe and temperature rises are recorded over a period of time. A minimum of 20 to 30 readings should be recorded for each test. Once the data is collected, temperature is plotted versus time on a semi-log time scale and the linear, steady-state portion of the curve is selected. The slope of this portion of the temperature vs. time curve is used to calculate the thermal conductivity. Figure 2.21 shows the temperature vs. time plot, delineating the non-steady state regions to exclude. The transient portion and the portion dominated by edge and end effects should not be used when fitting the curve to determine the slope. Figure 2.22 shows the linear portion of the curve from which the slope is determined and used in the thermal conductivity calculation.
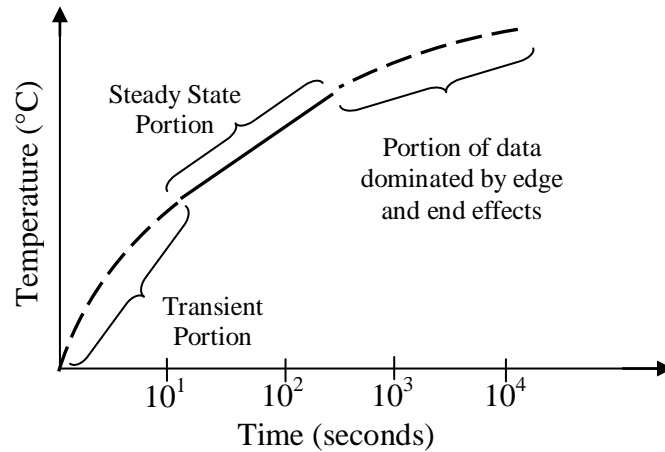
Figure 2.21: ASTM D5334-08 – Temperature vs. Time Curve
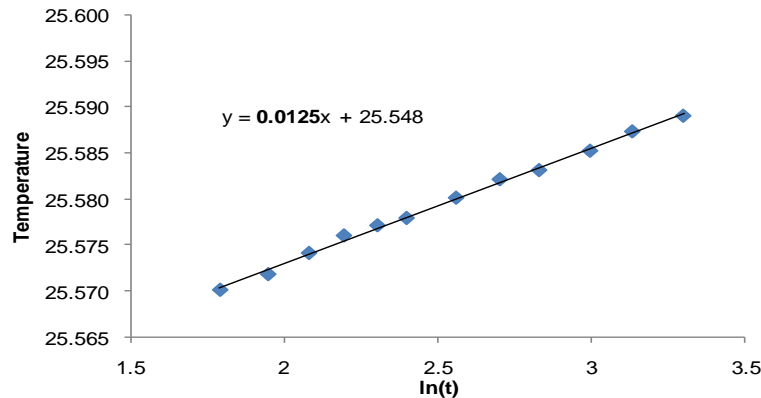
Figure 2.22: Steady-State Portion of Temperature vs. Time Curve

25

Thermal conductivity is determined from the slope of the temperature vs. time graph, S, the heat input, Q, and the calibration factor of the probe, C

$$\lambda = \frac{CQ}{4\pi S}$$

where the heat input is the product of the current, I, and the voltage, V, divided by the length of the probe, L.

$$Q = \frac{VI}{L}$$

2.4.3 Relative Density Test

The Standard Test Method for Maximum Index density and Unit Weight of Soils Using a Vibratory Table, ASTM D4253, is used to determine the density index for cohesionless, free-draining soils. This test is typically done to evaluate the state of compactness of a soil sample. Two procedures, one for dry soils and one for wet soils, are outlined in this standard. For this test to be applicable, 100 percent of the soil sample must pass a 3 in sieve and at most, 15 percent of it can pass the No. 200 sieve. Regardless of the percent fines, if the soil does not have the characteristics of a cohesionless, free-draining soil, it does not meet ASTM standards for this test.

The testing apparatus comprises a vibrating table and mold assembly. The mold assembly consists of the mold, the guide sleeve, the surcharge weight, the surcharge base-plate, and the dial gage holder and indicator. Two standard mold options are available; the 0.1 ft^3 and the 0.5 ft^3 mold. Each mold has a specifically sized guide sleeve, weight, and base-plate. To assemble the components, the mold is first attached to the table and the surcharge base-plate is place on top. The guide sleeve is then attached to mold, and the

surcharge weight is lowered through the guide sleeve onto the base-plate. The assembly
described in ASTM D4253 is shown in Figure 2.23.
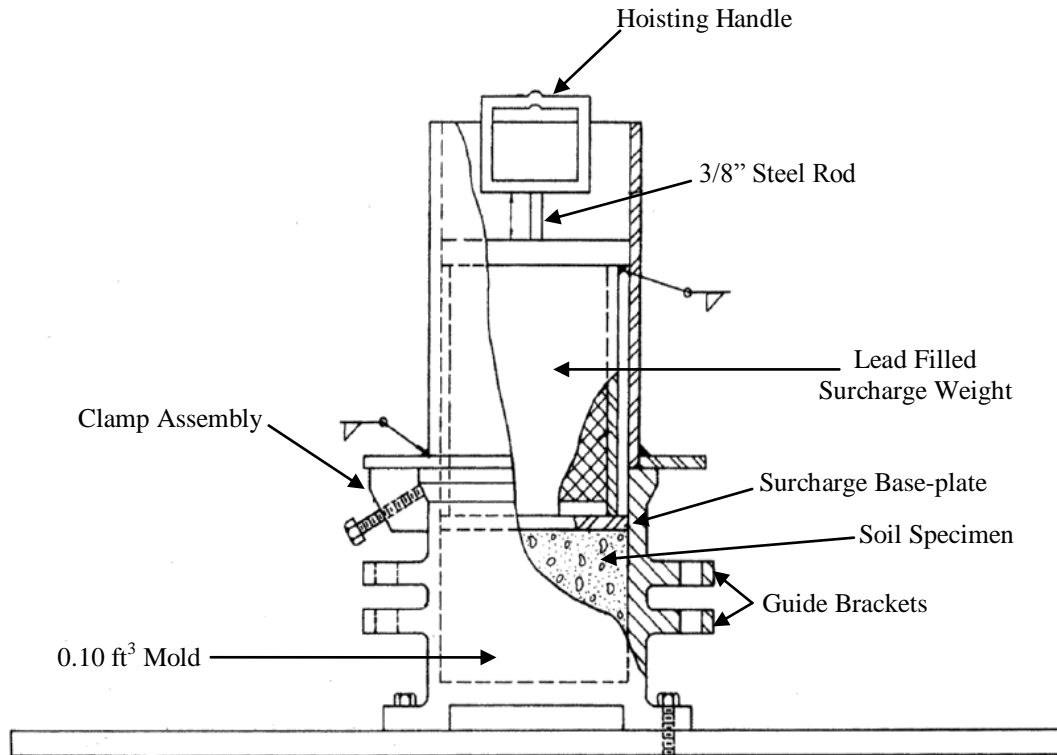
Figure 2.23: Relative Density Test - Mold Assembly

For the dry method, the mold is filled with oven dried soil and vibrated for 8 to12
minutes, depending on if a frequency of 50 or 60 Hertz is chosen. Initial measurements
include the mass of the empty mold, the mass of the mold with soil filled in the loosest
possible state, and the initial dial gage reading. Final measurements included the total
elapsed time and the final dial gage reading. From the dial gage readings, the initial and
final volumes can be calculated. The minimum dry density, ρ_{dmin}, is the mass of the soil
divided by the initial volume of the soil sample, and the maximum dry density, ρ_{dmax}, is
the mass of the soil divided by the final sample volume. The relative density can be
calculated at any point between these two values using the following equation:

$$D_d = \frac{\rho_{dmax}(\rho_d - \rho_{dmin})}{\rho_d(\rho_{dmax} - \rho_{dmin})} x\ 100$$

The only variation between the dry and wet methods is that for the wet method, the mold is initially attached to the table and wet soil is gently placed in it over a period of 5 to 6 minutes while the table is vibrating. This is done prior to attaching the guide sleeve, base-plate, and weight to the mold. Because the mold is already bolted to the table when the soil is placed in it, the mold and soil must be dried and weighed at the end of test.

2.4.4 Soil Classification

The Unified Soil Classification System (USCS) is presented in ASTM D2487, the Standard for the Classification of Soils for Engineering Purposes. This standard classifies soils into groups based on their particle size characteristics, liquid limit, and plasticity index.

Soils are classified into four main groups: gravel (G), sand (S), silt (M), and clay (C). Gravel and sand are classified as coarse-grained soils, while silt and clay are classified as fine-grained. To be considered coarse-grained, at least 50 percent of the soil mass must be retained on the No. 200 sieve, while 50 percent has to pass the No. 200 sieve to be considered fine-grained. Gravels and sands are separated by the No. 4 sieve. If the soil is retained on the No. 4 sieve, it is classified as a gravel whereas if it passes the No. 4 sieve and is retained on the No. 200, it is classified as a sand. Silts and clays require additional tests before they can be classified. These tests are provided in ASTM D4318.

To classify a soil sample, a particle size distribution must be obtained. This entails performing a sieve analysis for the entire soil sample using a series of sieves which should include the 3 in, No. 4, and No. 200 sieves, along with several others. The soil sample is weighed and sieved. Each sieve is weighed and the weight retained is recorded. Using the

weight retained, the weight passing and the percent passing each sieve is calculated. For fine-grained soils, the liquid limit and plastic limit must be determined. Once this information is know, the USCS classification chart can be followed to classify the soil. The USCS classification chart is provided in Table 2.2.

Table 2.2: USCS Soil Classification Chart

Criteria for Assigning Group Symbols and Names			Group Symbol	Group Name
Coarse-Grained Soils More than 50% retained on No. 200 sieve	Gravels 50% or more retained on No. 4 sieve	Clean Gravels	GW	Well-graded gravel
			GP	Poorly-graded gravel
		Gravels with Fine	GM	Silty gravel
			GC	Clayey gravel
	Sands 50% or more passes the No. 4 sieve	Clean Sands	SW	Well-graded sand
			SP	Poorly-graded sand
		Sands with Fines	SM	Silty sand
			SC	Clayey sand
Fine-Grained Soils 50% or more passes No. 200 sieve	Silts and Clays liquid limit less than 50		ML	Silt
			CL	Lean clay
			OL	Low plasticity Organic silts and clays
	Silts and Clays liquid limit 50 or more		MH	Elastic Silt
			CH	Fat clay
			OH	High plasticity Organic silts and clays
Highly Organic Soils			PT	Peat

2.4.5 Thermal Integrity Profiling

The Thermal Integrity Profiler uses the temperature generated by curing cement (hydration energy) to assess the quality of cast in place concrete foundations (i.e. drilled shafts or ACIP piles). Whereas other methods of integrity testing are limited to specific regions of the foundation cross-section (e.g. inside the reinforcing cage, between tubes, or within a few inches of an access tube), TIP measurements are sensitive to the concrete quality from all portions of the cross-section.

In general, the absence of intact / competent concrete is registered by relative cool regions (necks or inclusions); the presence of additional / extra concrete is registered by relative warm regions (over-pour bulging into soft soil strata). Anomalies both inside and outside the reinforcing cage not only disrupt the normal temperature signature for the nearest access tube, but the entire shaft; anomalies (inclusions, necks, bulges, etc.) are also detected by more distal tubes (but with progressively less effect).

Analysis of the data has multiple levels of intricacy, but in general it depends on the concrete mix design, shape, and geometry of the concrete tested as well as the diffusion field (e.g. air, soil, water). As a result, the thermal properties of the soil surrounding the concrete structure are important and form one focus of this thesis.

Chapter 3 - Algorithm Development

The primary focus of this thesis was to provide design parameters for engineering problems requiring thermal properties of soils. As the most common soil exploration methodology involves SPT borings, a concentrated effort was put forth to relate both thermal conductivity and specific heat to this form of soil data. To that end, presently available correlations between SPT (N) and density were employed along with correlations from density to thermal conductivity. This chapter provides detailed development of such algorithms to correlate the link between SPT (N) to thermal properties.

An Excel spreadsheet was created using correlations where the data from a SPT boring log could be inputted and these thermal properties could be calculated. The necessary input data for the spreadsheet consists of depth, soil type, blow count, ground surface elevation and the elevation of the water table. Ground surface elevation and water table elevation are both single entry inputs, whereas depth, blow count, and soil type are arrays requiring multiple entries for each field. Using these inputs, the soil structure, moisture content, and density can be properly assigned. Once these values are known, the thermal conductivity calculations are simply determined from a series of polynomial equations. The parameters listed above are the deciding factors on which one of these equations should be used for each entry.

Boring logs are provided in terms of either depth or elevation. Both are acceptable, but depth was chosen as the input parameter for this spreadsheet. To provide the elevation

corresponding to each depth, the input depth is subtracted from the ground surface

elevation. Figure 3.1 shows a screen shot of the spreadsheet main page. The spaces for the

inputs are shaded to distinguish between the outputs. Numbers must be typed into these

boxes for ground surface elevation, water table elevation, depth, and blow count, whereas

drop-down menus are provided for soil type. Figure 3.2 shows a close up of the required

spreadsheet inputs.

Figure 3.1: Spreadsheet Default Settings

Figure 3.2: Spreadsheet Inputs

3.1 Command Buttons

Six command buttons control the spreadsheet. The first command button changes the input units back and forth between English (feet) and Metric (meters). Thermal Conductivity and Density outputs remain in Metric units to be consistent with historical data, but elevations and depths can be inputted in either system of measurement. The second command button clears the calculated data, but all inputs remain. The third command button, *Clear All*, clears all inputted and calculated data, leaving the spreadsheet ready for new data. The fourth command button is the *Calculate* button. This calculates density and thermal conductivity, and plots the selected methods. Below this button is the *Update* button. If methods are selected or deselected, clicking the update button will update the graph. Command button 6 is the *Help* button which, when clicked, brings up a detailed list of each object and its function.

3.2 Soil Classification

There are multiple ways to classify soils (e.g. USCS, AASHTO); therefore, a drop-down menu (Figure 3.2) was created to avoid typographical errors. The soil choices provided are clay, silt, sand, limestone, silty sand, clayey sand, silty limestone, clayey limestone, sandy silt, sandy clay, and organics. From the soil type, a soil structure can be determined. If the soil passes the #200 sieve, it is considered a fine grained soil. Clay, silt, and organic soils fall under this category. If any of these soil types are chosen, computations for fine grained soils are performed. Sand and limestone are retained on or above the #200 sieve, so they are categorized as coarse grained. If sand or limestone are selected, the soil will be identified as coarse grained for that entry and processed

accordingly. For the soil types consisting of a mix of coarse and fine grained soils, the soil structure is labeled as "mixed" and computations include raising the thermal conductivity of both fine and coarse grained soils to their respective volumetric fractions.

3.3 Moisture Content

The moisture content of a soil changes with its position relative to the water table. At the water table and below, it can be assumed that the soil is saturated for most cases. Above the water table, soil type and distance above the water table must be taken into account. The University of South Florida performed studies on the changes in moisture content with relation to the water table for many soil. Three common Florida soils were chosen from this analysis: one with a high clay content, one with a high silt content, and one with a high sand content. Limestone was not present in this study, but because it is typically found below the water table, it can be considered saturated for this application. Because sand and limestone are coarse grained soils, limestone above the water table is assumed to have the wicking characteristics of sand. Figures 3.3 through 3.5 show the changes in moisture content with respect to elevation above the water table for the chosen clay, silt, and sand. The equations used to calculate thermal conductivity require moisture contents to be separated into 5%, 10%, 20% and saturated to match available thermal conductivity correlations. To do this, the graphs were sectioned off and labeled accordingly.

Figure 3.3 shows the effect that the water table has on the moisture content of a clayey soil. From the water table to approximately 80 cm above it, the soil has over 20% moisture and is identified as saturated. Clay typically retains at least 12% moisture, but the data from the study was only collected to 200 cm above the water table, so a line was

34

extrapolated, following the same slope, to extend up to a moisture content of 12%. This point was 780 cm above the water table. Between 80cm and 780 cm, the soil is labeled as having a moisture content of 20%. Data for 12% moisture is not available; therefore, the 10% moisture content curves are used for clayey soils greater than 780 cm above the water table.
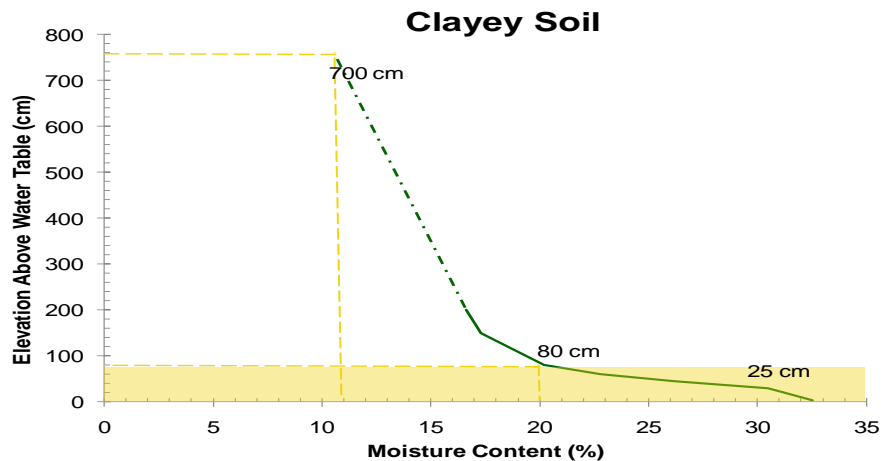
Figure 3.3: Moisture Content above Water Table for a Clayey Soil

Since clay is a very fine soil that can absorb large currents of water, there is no surprise that it retains a higher moisture content than the other soils. Even though silt is a fine grained soil, the properties are often similar to sand. The moisture content of silt at each elevation above the water table should fall in between a typical sand and clay. Figure 3.4 shows the effect that the water table has on the moisture content of a silty soil. At 200 cm, this silty soil has already reached 10% moisture. Because the graph data cuts off at 200 cm like that of clay, the relationship was extrapolated to where it would provide information for 5% moisture. From the water table to approximately 50 cm above it, the soil can be considered saturated. Above that point but below 150 cm, the moisture content is classified as 20% moisture. Between 150 cm and 430 cm, the moisture content is 10%, and above that it is considered to be 5%.
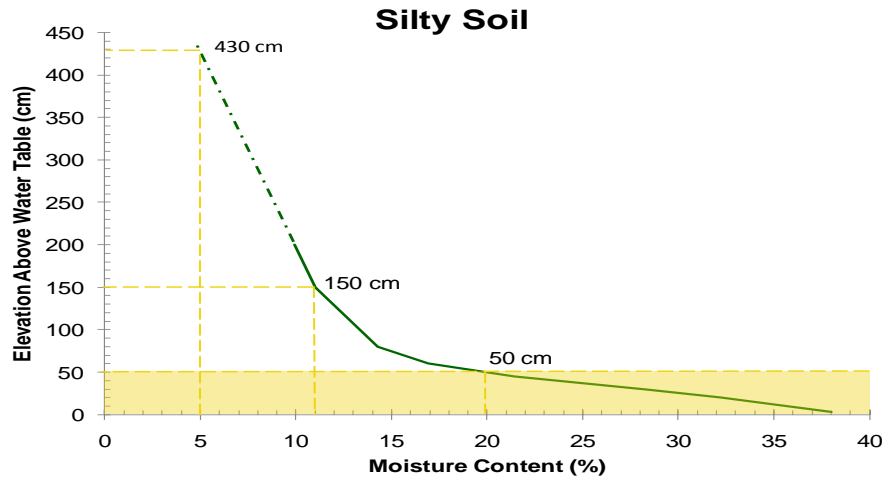
Figure 3.4: Moisture Content above Water Table for a Silty Soil

Figure 3.5 shows the effect that the water table has on the moisture content of a common sand in Florida, Myakka Fine Sand. Up to 40 cm above the water table, the moisture content is already reduced to 20%; therefore, anything between this height and the water table is considered saturated. Only 20 cm above that, at 60 cm above the water table, the soil is at 10% moisture. When the elevation reaches 150 cm, an almost vertical slope shows that it has leveled off at a moisture content of 5%. This is a typical moisture content value near the ground surface for Florida soils.
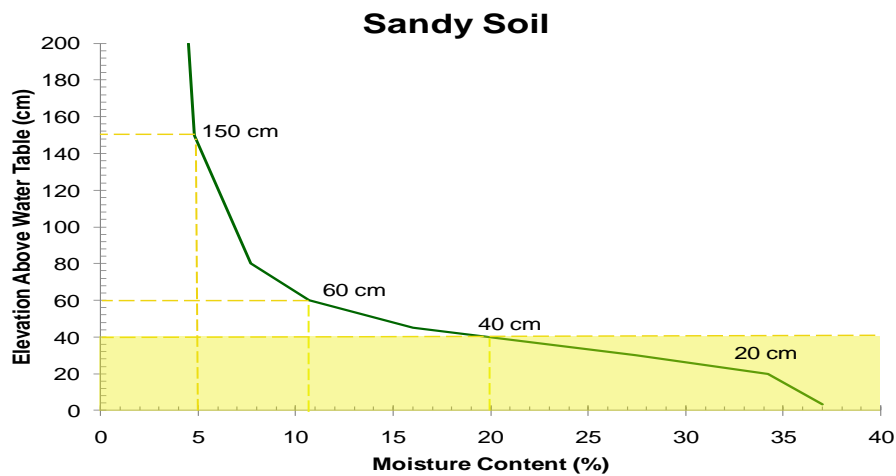
Figure 3.5: Moisture Content above Water Table for a Sandy Soil

3.4 Density

The relationships cited in Chapter 2 for thermal conductivity all relate to the density of the soil as well as the saturation and structure. As a result, making use of correlations from SPT data to density was a necessary first step. This could also be used to establish the void ratio and saturation when the soil is not submerged. See Figure 2.16 in Chapter 2 for the linear correlation between number of blows and the unit weight of clay, silt, and sand.

A correlation for limestone was detained from a study on cohesionless soil performed by the University of Florida (University of Florida 2009). Therein, the unit weight varied from 90lb/ft^3 to 130lb/ft^3 for soft to medium/hard limestone. A linear relationship was assumed where 90 lb/ft^3 represents the density at zero blow counts and 130 lb/ft^3 as the density at 60 blow counts. The line has a slope of 0.667 and a y-intercept of 90.

The data from Figure 2.16 was reproduced and plotted in Figure 3.6, along with the values produced for limestone. Trendlines were fitted to the data of each soil type in order to obtain the equation of each line. The spreadsheet uses the inputted soil type to select the appropriate equation. It then uses that equation to calculate density, where blow count is the independent variable (x-value) and density is the dependent value (y-value). The densities that result from using the equations in Figure 3.6 are in terms of lb/ft^3. The thermal conductivity calculations require density to be converted to the metric units of g/cm^3. A conversion factor of 0.016g/cm^3 per 1 lb/ft^3 is automatically applied to each resulting density in the spreadsheet.

Blow Count vs. Unit Weight of Soil
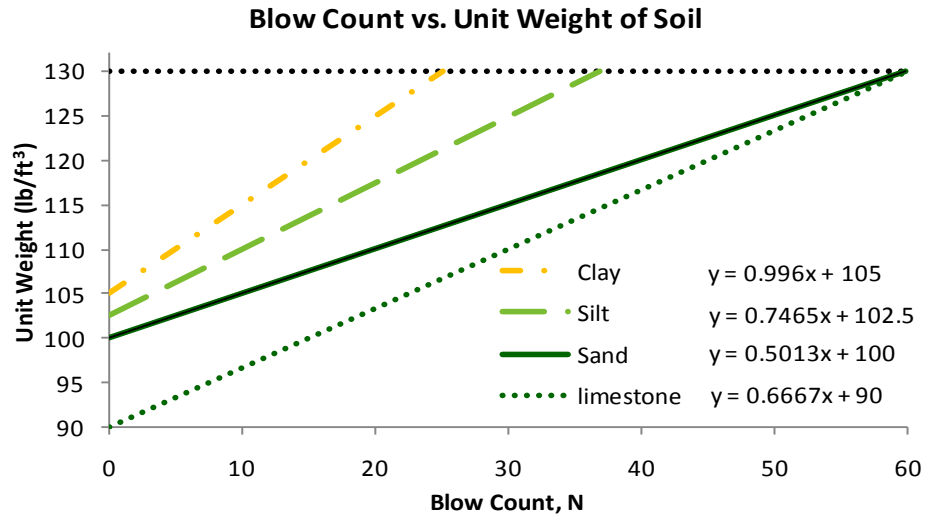
Figure 3.6: Blow Count vs. Unit Weight of Soil Graph Showing Slopes

3.5 Thermal Conductivity

The equations for thermal conductivity were fitted from a series of curves developed from the seven methods cited in Chapter 2. These curves present data for thermal conductivity as a function of dry density with varying degrees of saturation or moisture contents for both coarse and fine grained soils. According to the data presented in Section 3.3, the required curves needed to construct this spreadsheet were based on 5% moisture, 10% moisture, 20% moisture, and fully saturated. These four curves are provided for both coarse and fine grained soils for each method in Figures 3.7 through 3.13.

A trendline was fitted to each curve to obtain the equation of the function. All of the trendlines were a "perfect" fit out to three decimal places (i.e. $R^2=1$). For each equation, the x-value represents density and the y-value represents thermal conductivity. Knowing these equations and the algorithms that lead to calculating density, thermal conductivity can be calculated at any depth given the specified blow count and soil type at that depth.

38

Thermal Conductivity vs. Dry Density for Coarse Soil

5% $y = 6.8484x6 - 64.482x5 + 250.87x4 - 515.29x3 + 589.57x2 - 355.52x + 88.601$

10% $y = -0.6617x4 + 4.6871x3 - 10.553x2 + 10.928x - 3.7348$

20% $y = 0.6637x3 - 0.9938x2 + 0.9205x + 0.2615$

Saturated $y = 1.4721x4 - 9.154x3 + 22.116x2 - 22.41x + 9.0948$
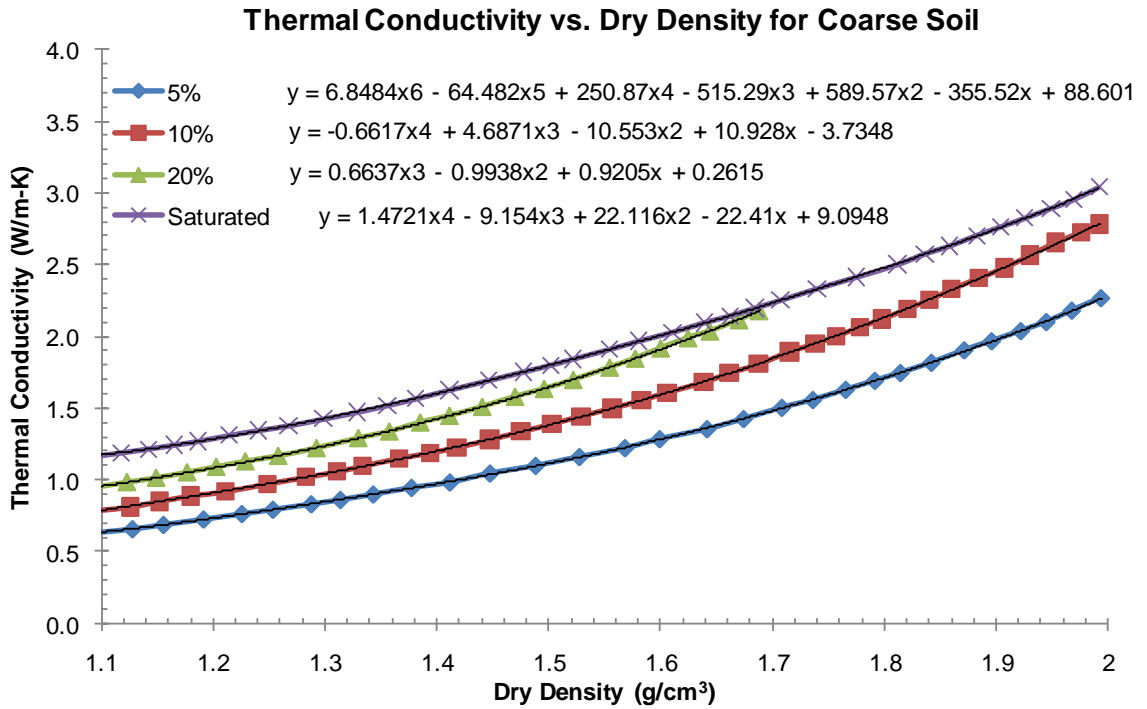
Figure 3.7: Thermal Conductivity vs. Density for a Coarse Soil (Kersten)

Thermal Conductivity vs. Dry Density for Fine Soil

5% $y = 0.4099x^3 - 1.2852x^2 + 1.839x - 0.712$

10% $y = 5.6859x^5 - 42.11x^4 + 124.16x^3 - 181.26x^2 + 131.54x - 37.634$

20% $y = -2.1307x^4 + 11.752x^3 - 23.061x^2 + 20.444x - 6.4165$

Saturated $y = -0.213x^3 + 1.1012x^2 - 0.6446x + 0.6296$
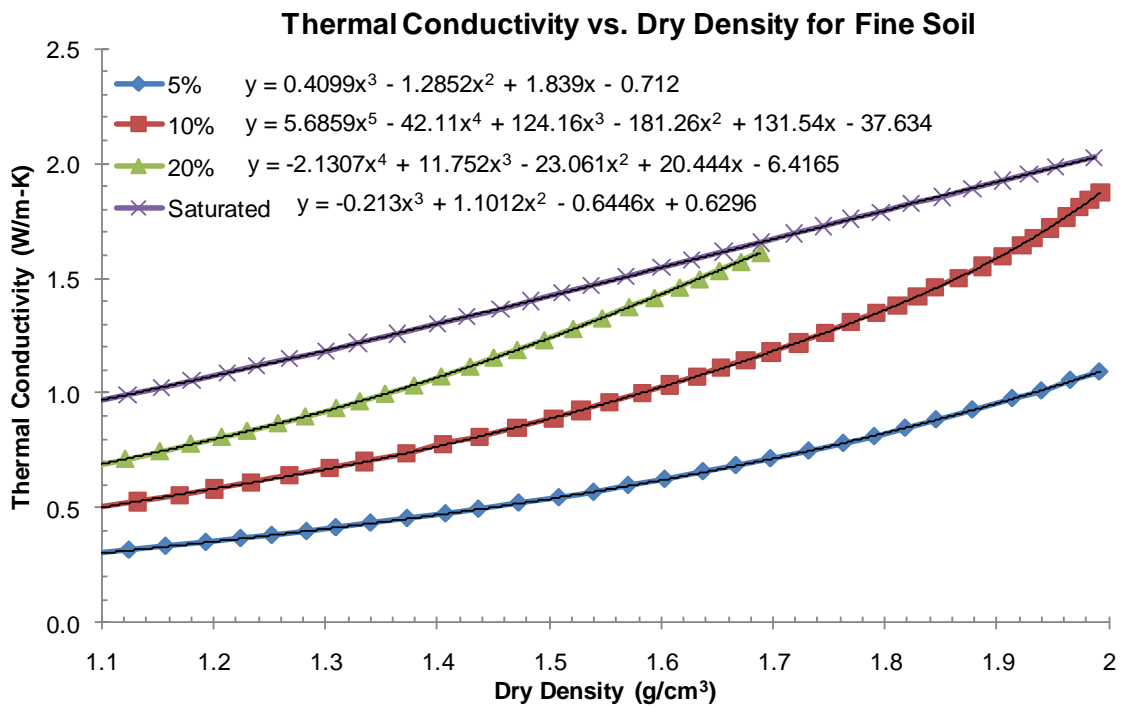
Figure 3.8: Thermal Conductivity vs. Density for a Fine Soil (Kersten)

39
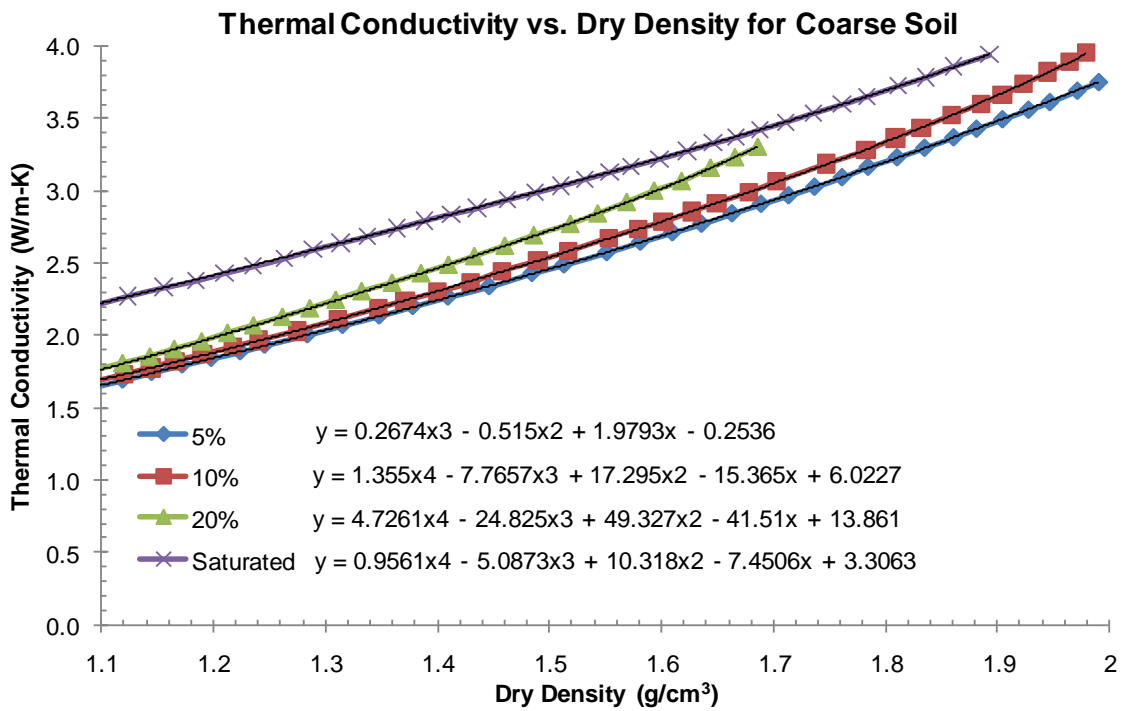
Figure 3.9: Thermal Conductivity vs. Density for a Coarse Soil (Mickley)

The equations shown in the Coarse Soil chart:

5%: $y = 0.2674x^3 - 0.515x^2 + 1.9793x - 0.2536$

10%: $y = 1.355x^4 - 7.7657x^3 + 17.295x^2 - 15.365x + 6.0227$

20%: $y = 4.7261x^4 - 24.825x^3 + 49.327x^2 - 41.51x + 13.861$

Saturated: $y = 0.9561x^4 - 5.0873x^3 + 10.318x^2 - 7.4506x + 3.3063$
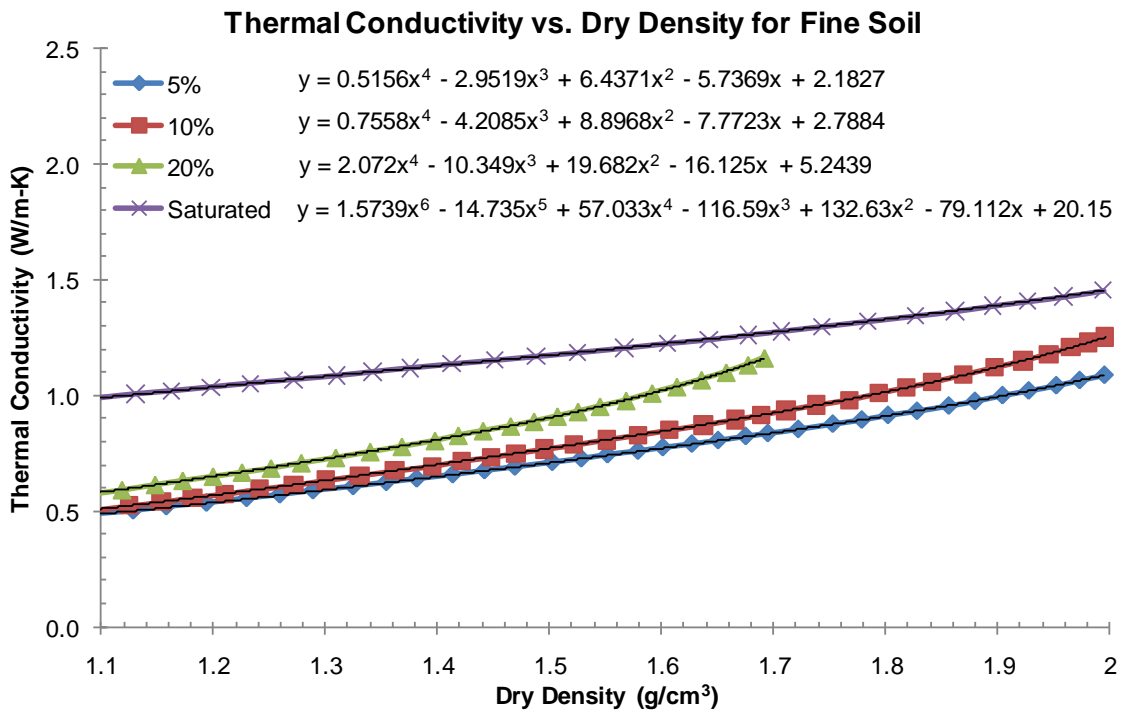
Figure 3.10: Thermal Conductivity vs. Density for a Fine Soil (Mickley)

The equations shown in the Fine Soil chart:

5%: $y = 0.5156x^4 - 2.9519x^3 + 6.4371x^2 - 5.7369x + 2.1827$

10%: $y = 0.7558x^4 - 4.2085x^3 + 8.8968x^2 - 7.7723x + 2.7884$

20%: $y = 2.072x^4 - 10.349x^3 + 19.682x^2 - 16.125x + 5.2439$

Saturated: $y = 1.5739x^6 - 14.735x^5 + 57.033x^4 - 116.59x^3 + 132.63x^2 - 79.112x + 20.15$

40
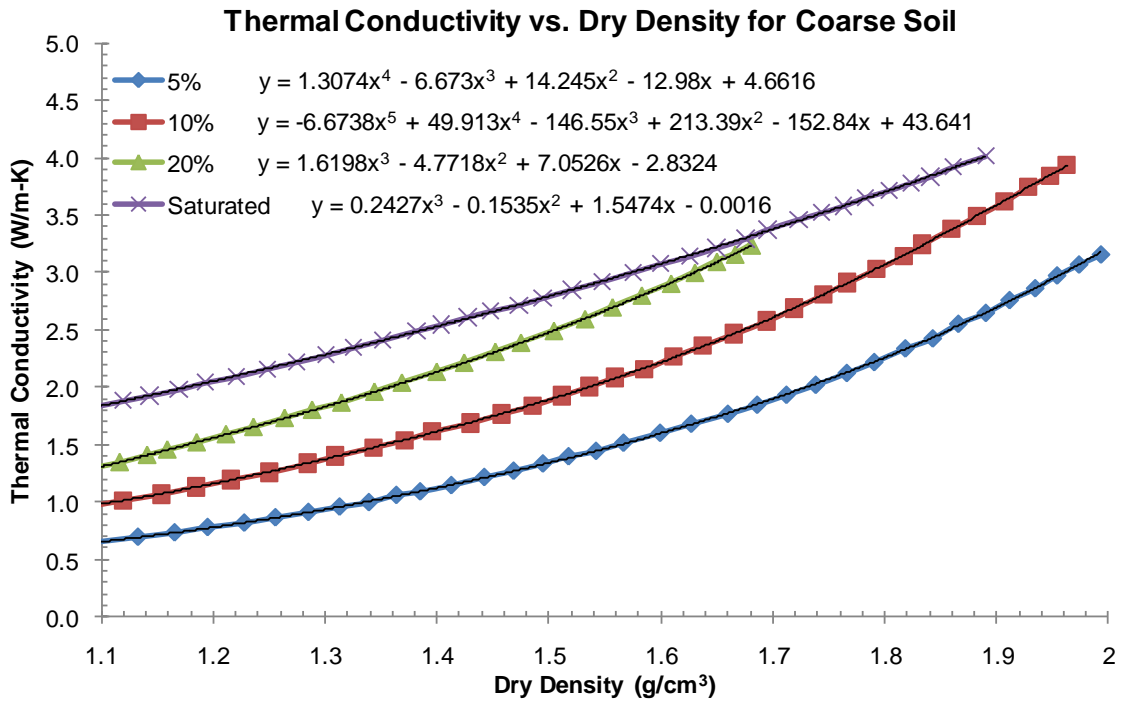
Figure 3.11: Thermal Conductivity vs. Density for a Coarse Soil (Gemant)
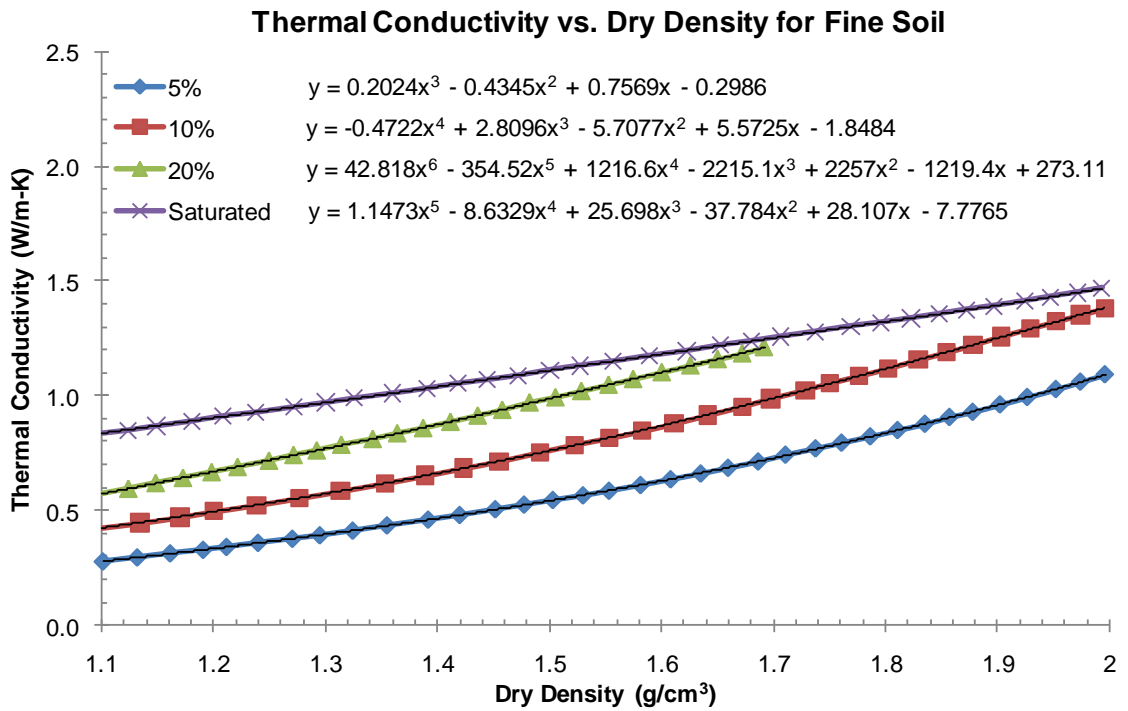
Figure 3.12: Thermal Conductivity vs. Density for a Fine Soil (Gemant)

41
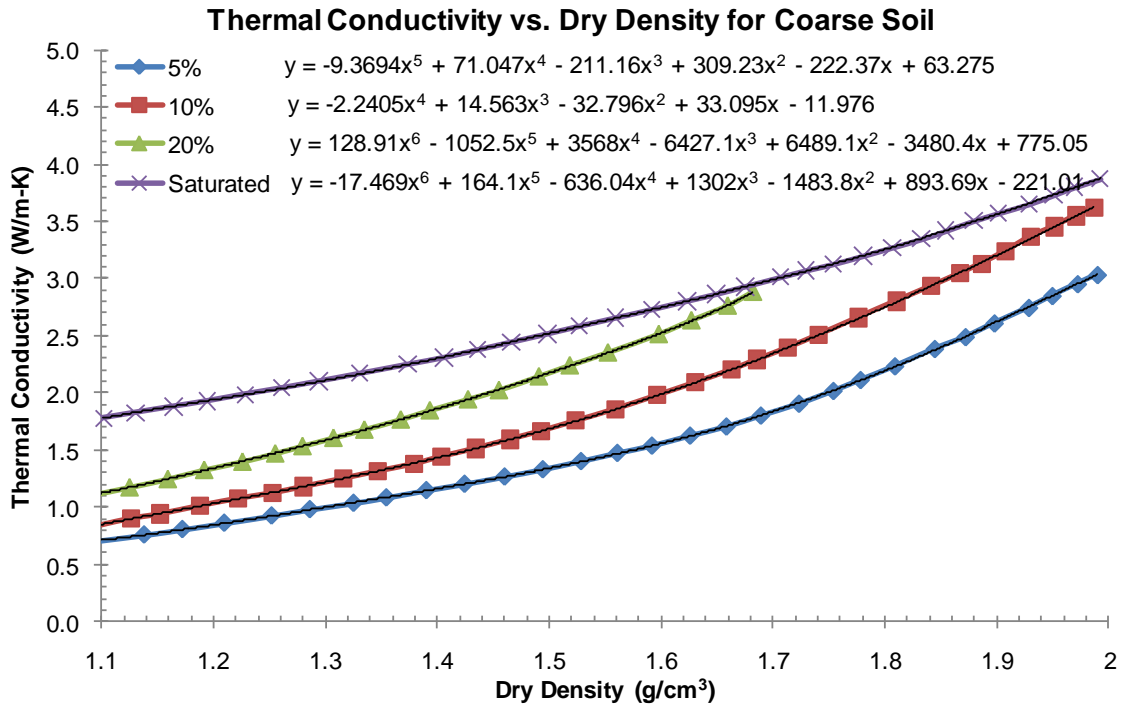
Figure 3.13: Thermal Conductivity vs. Density for a Coarse Soil (De Vries)
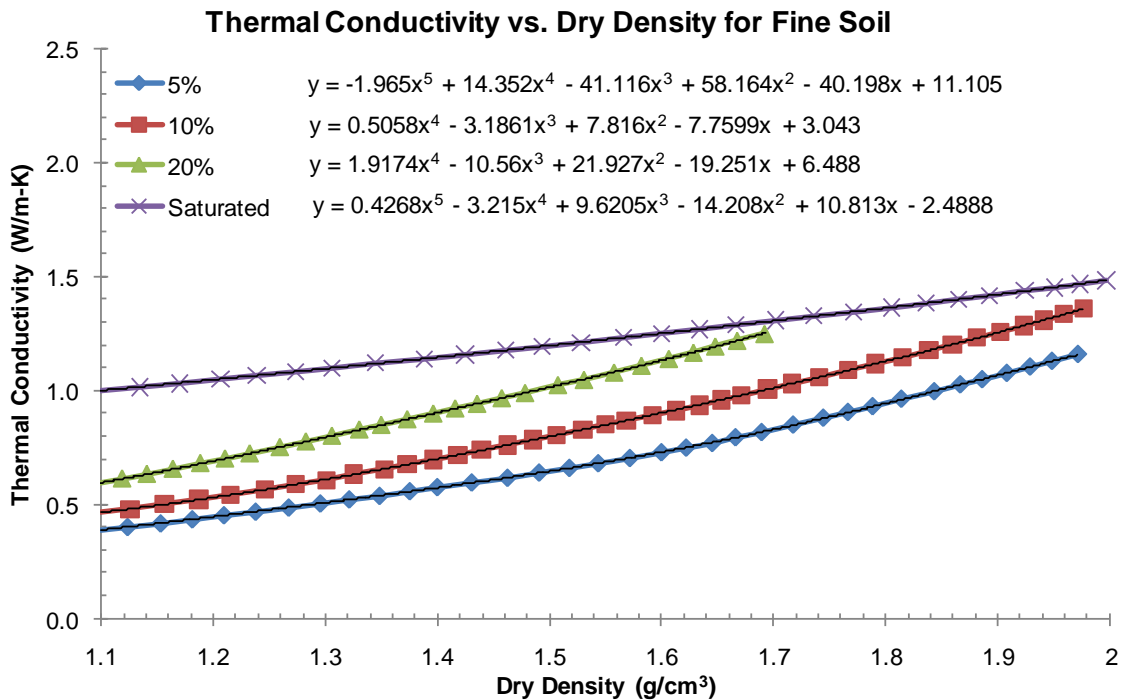
Figure 3.14: Thermal Conductivity vs. Density for a Fine Soil (De Vries)

Thermal Conductivity vs. Dry Density for Coarse Soil

5% $y = 47.697x^5 - 339.23x^4 + 963.08x^3 - 1358.7x^2 + 952.87x - 265.6$
10% $y = 14.25x^4 - 72.677x^3 + 139.55x^2 - 116.35x + 36.516$
20% $y = 15.888x^4 - 81.906x^3 + 160.07x^2 - 137.98x + 45.721$
Saturated $y = 20.834x^4 - 112.34x^3 + 228.94x^2 - 206.09x + 70.596$
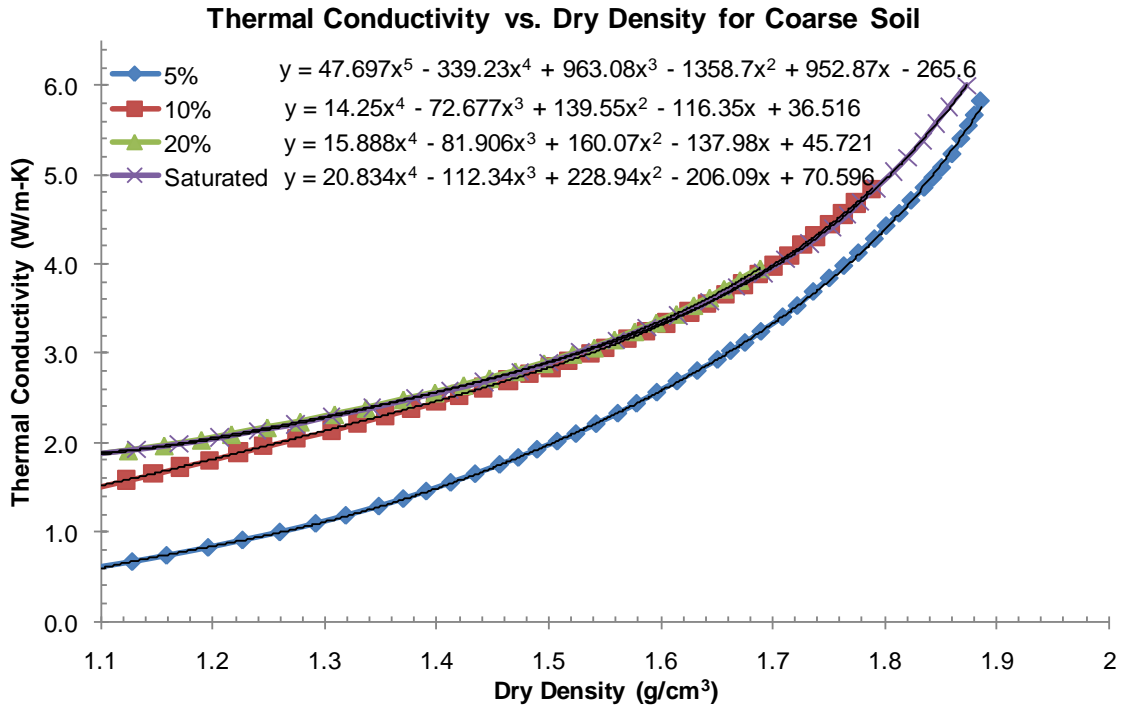
Figure 3.15: Thermal Conductivity vs. Density for Coarse Soil (Van Rooyen)

Thermal Conductivity vs. Dry Density for Fine Soil

5% $y = -4.272x^5 + 30.686x^4 - 88.076x^3 + 126.45x^2 - 90.432x + 25.808$
10% $y = 16.57x^6 - 144.09x^5 + 515.66x^4 - 973.97x^3 + 1025.4x^2 - 570.56x + 131.26$
20% $y = -9.1789x^4 + 45.438x^3 - 84.068x^2 + 69.599x - 21.368$
Saturated $y = -95.877x^6 + 904.54x^5 - 3504.2x^4 + 7136x^3 - 8060.6x^2 + 4792.9x - 1172.6$
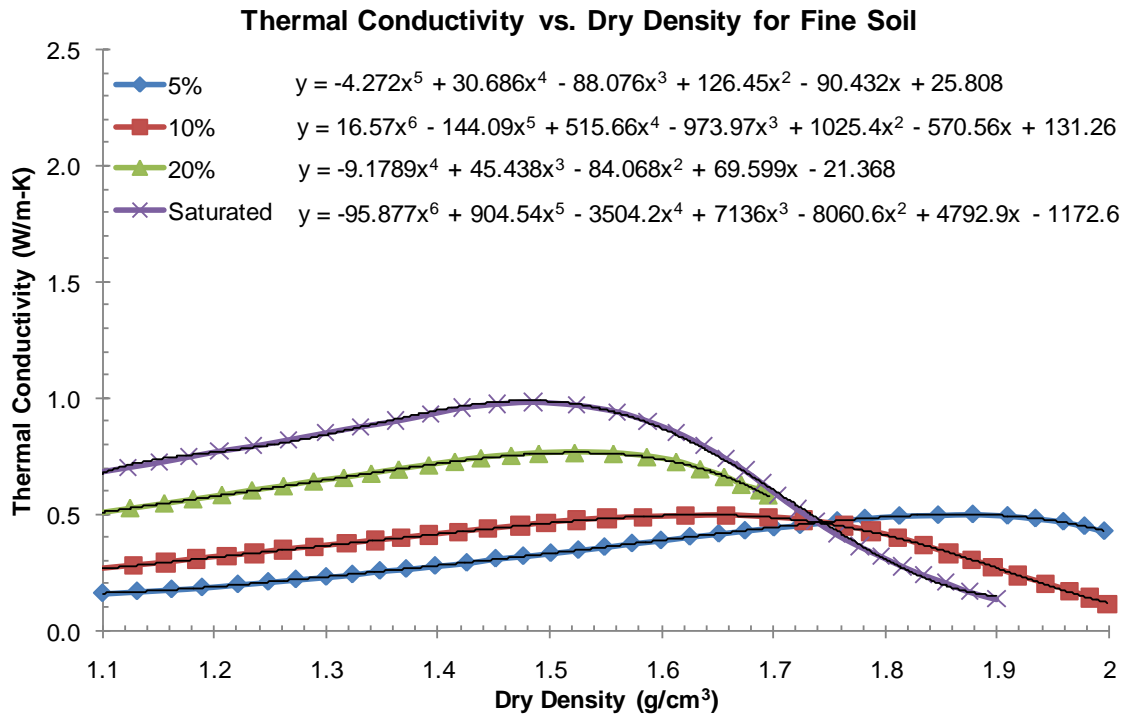
Figure 3.16: Thermal Conductivity vs. Density for a Fine Soil (Van Rooyen)

43
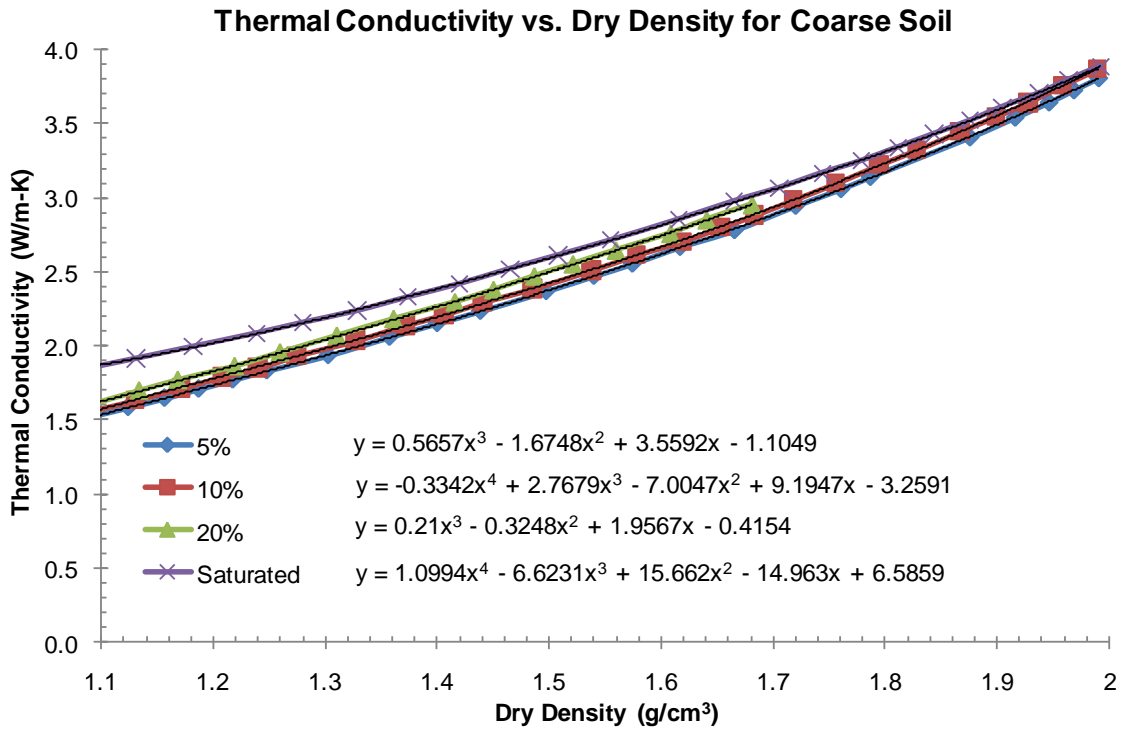
Figure 3.17: Thermal Conductivity vs. Density for a Coarse Soil (McGaw)
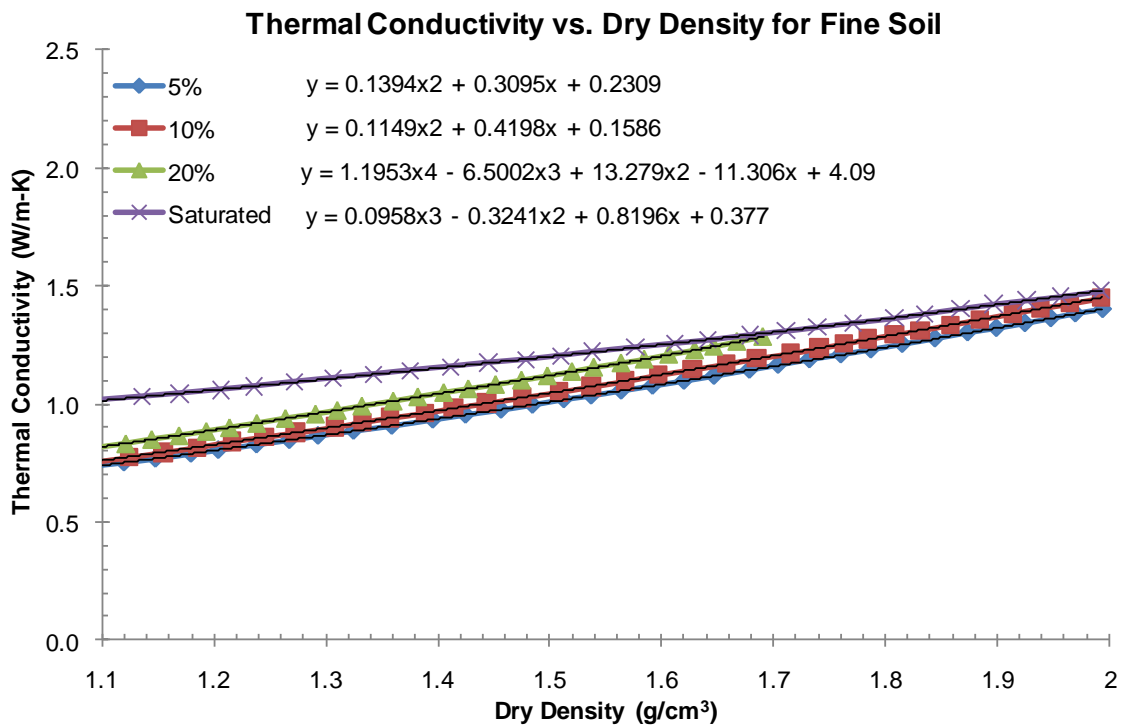
Figure 3.18: Thermal Conductivity vs. Density for a Fine Soil (McGaw)
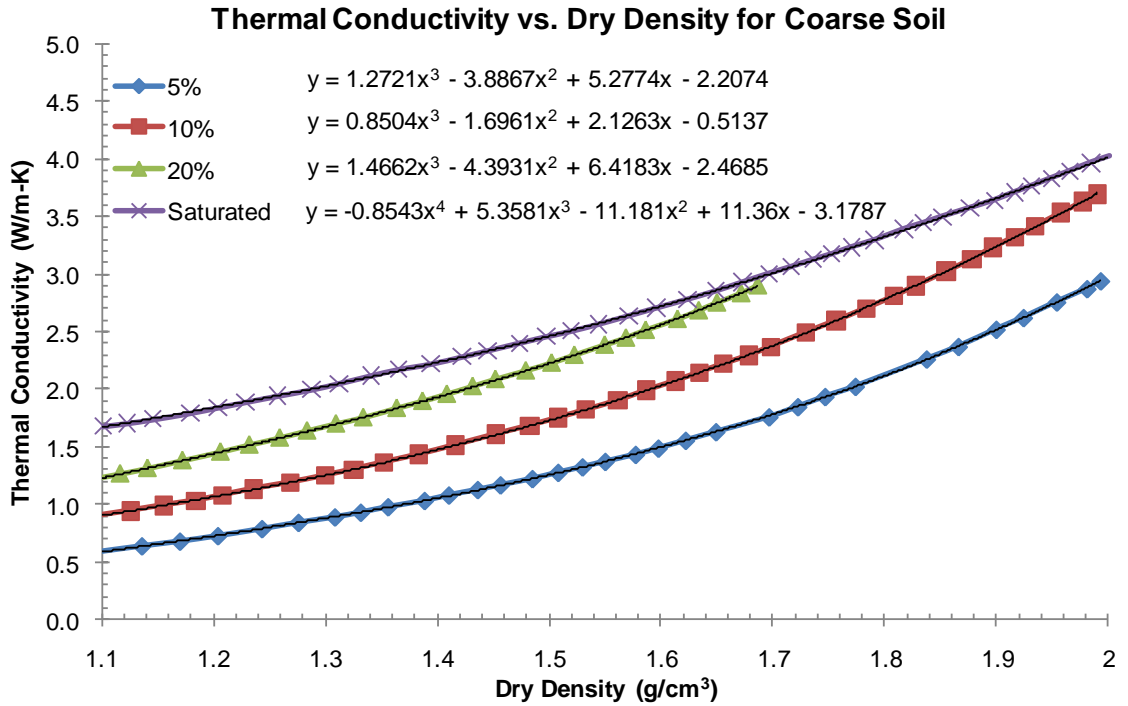
Figure 3.19: Thermal Conductivity vs. Density for a Coarse Soil (Johansen)

Thermal Conductivity vs. Dry Density for Coarse Soil

5% $y = 1.2721x^3 - 3.8867x^2 + 5.2774x - 2.2074$

10% $y = 0.8504x^3 - 1.6961x^2 + 2.1263x - 0.5137$

20% $y = 1.4662x^3 - 4.3931x^2 + 6.4183x - 2.4685$

Saturated $y = -0.8543x^4 + 5.3581x^3 - 11.181x^2 + 11.36x - 3.1787$
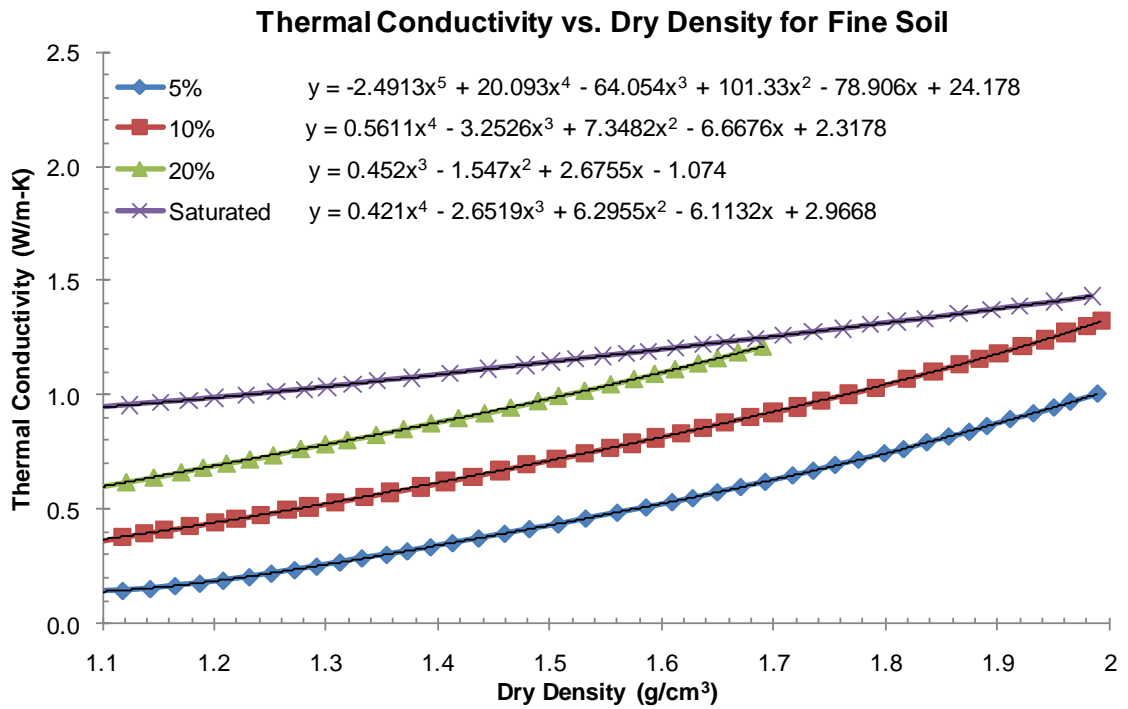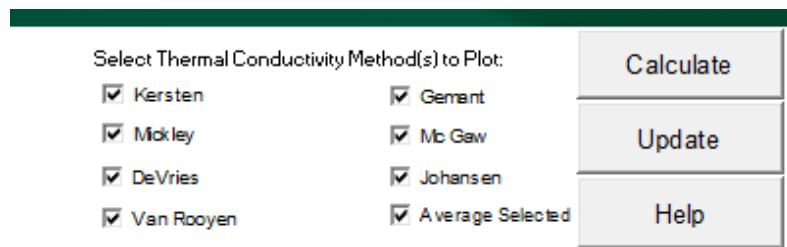
Figure 3.20: Thermal Conductivity vs. Density for a Fine Soil (Johansen)

Thermal Conductivity vs. Dry Density for Fine Soil

5% $y = -2.4913x^5 + 20.093x^4 - 64.054x^3 + 101.33x^2 - 78.906x + 24.178$

10% $y = 0.5611x^4 - 3.2526x^3 + 7.3482x^2 - 6.6676x + 2.3178$

20% $y = 0.452x^3 - 1.547x^2 + 2.6755x - 1.074$

Saturated $y = 0.421x^4 - 2.6519x^3 + 6.2955x^2 - 6.1132x + 2.9668$

3.6 Plotting

Plotting routines were developed to produce two graphs of the interpreted boring log data. The first and foremost is the thermal conductivity vs. depth graph. This graph shows the thermal conductivity changes with variations in depth and soil type. The second graph plots blow count vs. depth. This graph is plotted to allow the user to make comparisons between the thermal conductivity changes and the density changes throughout the boring log while also providing a visual confirmation of proper input.

All seven thermal conductivity methods are set to calculate each time the spreadsheet is run, but only to plot if they are selected. Check boxes were added and programmed so that if the check box is clicked when the graph is updated, the data for that method is plotted. An additional check box was added to plot the average of the selected methods. This was designated as a thicker black line on the graph to distinguish it from the rest. A screen shot of the check boxes is provided in Figure 3.21.

Figure 3.21: Plotting Preferences

Upon clicking the *Calculate* button, the graph will plot the selected methods. The default setting selects all the methods and the average, but any method can be selected or unselected simply by clicking on the name. The average of the selected methods will

automatically re-calculate, but the *Update* button must be clicked for the graph to update.

Figure 3.22 is a screen shot of the graphs resulting from the selection.
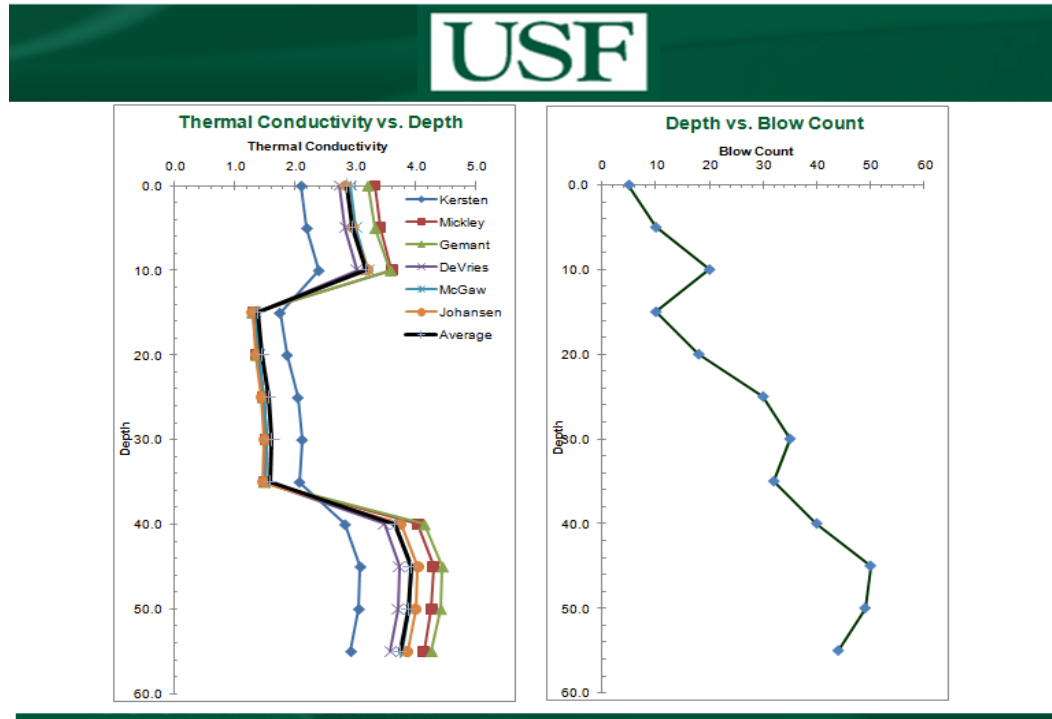
Figure 3.22: Plotting Results

Chapter 4 - Testing and Evaluation

For the laboratory testing portion of this thesis, a thermal probe was rented to perform thermal conductivity testing on selected soils. This was primarily to validate or dispel the previously published data being used to calculate thermal conductivity in the spreadsheet. The probe used for testing is described in the Section 4.1, *Equipment*, the information pertaining to the test procedures, results, and evaluation can be located in Sections 4.2, *Laboratory Testing and Evaluation*, and implementation of the spreadsheet, including a boring log example, is provided in Section 4.3*, Evaluation of Theoretical Algorithms*.

4.1 Equipment

The "KD2 Pro Thermal Properties Analyzer" was rented from Decagon Devices, Inc. The system comes with a handheld controller that records the data from one of three probes. Two of the probes (the KS-1 and the TR-1) are single-needle sensors used to measure thermal conductivity and resistivity for different mediums. The third probe, the SH-1, is a dual-needle sensor used to measure specific heat and diffusivity. Figure 4.1 shows the three needle probes.

Figure 4.1: Needle Probes: TR-1 (left), KS-1 (middle), SH-1 (right)

The KS-1 is a 60 mm long needle with a 1.3 mm diameter and its thermal conductivity range is from 0.02 W/m-K to 2.0 W/m-K with ± 5% accuracy. The TR-1 is the larger of the two single-needle probes. It is a 100 mm long needle with a 2.4 mm diameter. For thermal conductivity, its range is from 0.10 W/m-K to 4.00 W/m-K with an accuracy of ±10%. The SH-1 is the dual-needle probe that consists of two 30 mm long needles with 1.3 mm diameters, spaced 6 mm apart.

The KS-1 probe applies a smaller amount of heat for a shorter period of time than the TR-1 probe, making it more suitable for liquids and insulating materials. The dual-needle probe, SH-1, is primarily designed to read specific heat and diffusivity so this probe was not used for thermal conductivity testing. The TR-1 probe is designed for use in soil, concrete, rock, and other granular materials. Because of this, the TR-1 probe was chosen for all thermal conductivity testing.

Testing times for the TR-1 vary between 5 and 10 minutes. Heat is applied for the first half of the test and readings are taken every 5 or 10 seconds, depending on the chosen read time. A total of 60 measurements are taken during each test. The longer read time is suggested for dry granular materials, large grains, or solid samples. A minimum of 2.7 mm of the tested material must surround the probe in all directions to avoid errors while testing. The KD-2 system follows the specifications outlined in ASTM D5334-08.

4.2 Laboratory Testing and Evaluation

Three sets of tests were performed using the KD2 Pro device. The first were density variation tests which were done to determine the changes in the thermal conductivity of soils with increasing densities. The second were repeatability tests to check the accuracy of the probe when tests are consecutively conducted versus when tests are conducted with a fifteen minute break between each test. Third, tests were conducted to determine the change in thermal conductivity as the temperature of the soil changes. All three test series utilized the same soil; therefore, one sieve analysis was performed and can be located in Section 4.2.1. The density variation tests are discussed in Section 4.2.2 and analyzed in Section 4.2.3. The repeatability and temperature tests are presented in Section 4.2.4 and the results in Section 4.2.5.

4.2.1 Soil Classification

A soil sample was chosen for experimentation. The soil from the sample was dry to the touch but it was still placed in an oven at 105°C for 24 hours to assure that all the moisture had been removed. The sample was then cooled and weighed. The mass of the sample was 1750.10 grams. In order to classify the soil using the USCS specifications, the percentage of particles passing each sieve needed to be calculated. Table 4.1 provides the results of the sieve analysis. The equations used to calculate the values in the table for the mass retained, mass passing, and percent of particles passing each sieve are:

$$Mass_{retained} = Mass_{sieve+soil} - Mass_{sieve}$$

$$Mass_{passing} = Mass_{sample} - \sum_{largest\ sieve}^{current\ sieve} Mass_{retained}$$

$$\% \ Passing = \left(\frac{Mass_{passing}}{Mass_{sample}} \right) x \ 100\%$$

Table 4.1: Particle Size Distribution for Soil Sample

Sieve #	Sieve size (mm)	Mass of Sieve (g)	Mass of Sieve + Soil (g)	Mass Retained (g)	Mass Passing (g)	% passing
#4	4.76	669.25	669.25	0.00	1750.10	100.00
#10	2.00	487.63	495.90	8.27	1741.83	99.53
#40	0.42	338.10	1348.15	1010.05	731.78	41.81
#60	0.25	358.56	743.60	385.04	346.74	19.81
#100	0.15	347.30	643.10	295.80	50.94	2.91
#200	0.07	329.28	380.22	50.94	0.00	0.00

The entire sample passed the #4 sieve and was retained on the #200 sieve. According to the USCS classification chart (Table 2.2), this soil was classified as a sand.

4.2.2 Density Variation Testing

Density tests were performed using the KD2 Pro device and a vertically vibrating table in order to obtain thermal conductivity values that correspond to different densities. The procedure followed the Standard Test Method for Maximum Index Density and Unit Weight of Soils Using a Vibratory Table (ASTM D4253). The test set up conformed to the ASTM specifications, but modifications were made to the procedure to include incremental testing that would create a density vs. time curve instead of a linear trend between the minimum and maximum densities.

There was an option to use two different size molds, a 0.1 ft^3 or a 0.5 ft^3 mold. As the 0.1 ft^3 (172 in^3) mold is sufficient for all sands, clays, silts, and small rocks, it was chosen for this experiment. The height and diameter of the mold were measured using a caliper, and the empty mold was weighed. The cross-sectional area and volume were then calculated. The dimensions and mass of the mold are provided in Table 4.2, where

$$Area_{mold} = \frac{\pi d_{mold}^2}{4}$$

and,

$$Volume_{mold} = Height_{mold} \ x \ Area_{mold}$$

Table 4.2: Mold Dimensions

Mold Dimensions		
Height of Mold	6.12	In
Diameter of Mold	6.00	In
X-sectional Area of Mold	28.27	in^2
Volume of Mold (in3)	172.93	in^3
Volume of Mold (cm3)	2833.75	cm^3
Mass of Mold	3742.80	kg

For the dry tests, a scoop was used to gently place soil in the mold while keeping the soil as loosely packed as possible. Once the mold was filled, a leveling tool was used to create an even surface across the top of the mold. The mold with the soil was weighed, and the weight of the mold was subtracted in order to calculate the mass of dry soil.

The mold was then attached to the vibrating table (Figure 4.2). A minor amount of settling occurred while in transit, but the change in volume was negligible. To determine the thermal conductivity for the soil at its loosest state in the mold, the probe was inserted near the center of the soil sample and a 10 minute test was performed (Figure 4.3). Upon finishing the test, the probe was removed and the mold was tapped along the sides several times to allow the soil to settle enough to place the surcharge base plate uniformly on top of it (Figure 4.4). Once the base plate was applied, the guide sleeve was attached to the top of the mold. The surcharge weight was lowered through the sleeve and placed on top of the base plate (Figure 4.5). The complete assembled apparatus is displayed in Figure 4.6. Using a caliper, the distance from the top of the weight to the top of the sleeve was measured in two places 180° across from each other (Figure 4.7).

52

Figure 4.2: Placing Sand into Mold and Attaching it to the Vibrating Table

Figure 4.3: Performing Thermal Conductivity Test on Non-compacted Soil

Figure 4.4: Baseplate Placed on Mold

Figure 4.5: Placing Weight in Sleeve

Figure 4.6: Apparatus Set Up

Figure 4.7: Measuring Depth

The frequency of the vibrating table was set to 50 hertz and the table was turned on for one second. Before removing the surcharge weight, two more measurements between the top of the weight and top of the sleeve were taken with the caliper and averaged to provide a second depth measurement. This value, subtracted by the initial measurement, gives the displacement of the soil after one second of vibration.

After the measurements were taken, the weight and base plate were removed to expose the soil. A 10 minute test was done with the probe to determine the thermal conductivity corresponding to the calculated density. The base plate and weight were placed back on the mold and secured for the next test. Initially, the soil was placed loosely into the mold so it was expected that large changes in density would occur during the first few seconds. A total of 12 tests were conducted. To create an accurate density curve, the first four tests were done at one second intervals, and the subsequent tests increased up to a test that compacted for four minutes.

Each time the test was repeated, the vibrating table was turned on and run for the amount of time stated at that point in the testing matrix. Once the table was turned off, depth measurements were taken, and the weight and base plate were removed from the sleeve. At this point, a 10 minute thermal conductivity test was done. Finally, the base plate and weight were carefully placed back into the guide sleeve so that the next test was ready to begin.

Tests for wet and saturated soils were conducted as well. A specific moisture content was not needed for the wet soil test; therefore, small amounts of water were simply added to a portion of the soil sample until the soil had a heavily damp feel to it. A small sample was weighed and placed into the oven so that a moisture content test could

be done. The damp soil was loosely placed in the mold similar to the procedure for the dry soil. The procedure for the saturated tests differs slightly from the previous two in its initial steps. The mold was filled with water prior to the sand being placed into it. The soil was then added slowly, causing the excess water to be displaced over the sides of the mold (Figure 4.8). This allowed the water to saturate the soil as it settled to the bottom. When the mold was full, the excess soil was leveled off the top, and a water bottle was used to rinse off any excess that had spilled over the sides (Figure 4.9). The mold was then toweled dry and weighed. From this point on, the same procedure for the dry test was followed.

Figure 4.8: Saturated Test

Figure 4.9: Using a level and Water Bottle to Get Rid of Excess Soil

4.2.3 Results of Density Variation Tests

Moisture content tests were done for the dry and wet soil. For each test, an empty tare was weighed, filled with a sample of the soil, and weighed again. The difference of these two measurements provides the mass of the wet soil. The tare was then placed in an oven at 105°C for 24 hours. After this period of time it was removed and weighed. The mass of dry soil in the tare is simply the difference of this measurement and mass of the empty tare. To calculate the percentage of moisture for the sample, the difference between the mass of wet soil and the mass of dry soil is divided by the mass of the wet soil. The parameters and equation for moisture content (% Moisture) are:

$$Mass_{wet} = Mass_{wet+tare} - Mass_{tare} \qquad Mass_{dry} = Mass_{dry+tare} - Mass_{tare}$$

$$\% \, Moisture = \left(\frac{Mass_{wet} - Mass_{dry}}{Mass_{wet}} \right) x100\%$$

Calculating dry density of the soil is required to calculate thermal conductivity using the developed algorithms. The mass of dry soil in the mold is needed for this density calculation. Knowing both the weight of the wet soil in the mold and the moisture content of that soil, the mass of dry soil in the mold can be calculated.

$$Mass_{dry \, soil} = \frac{Mass_{wet \, soil}}{1 + \dfrac{\% \, moisture}{100}}$$

The moisture content results for the dry sand and the wet sand are provided in Table 4.3 and 4.4.

Table 4.3: Dry Soil Moisture Content

Dry Soil Test Moisture Content Results		
Mass Tare	31.20	kg
Mass Tare + Wet Soil	254.90	kg
Mass Tare + Dry Soil	254.60	kg
Moisture Content (%)	0.12	%
Mass of Dry Soil	4459.2	kg

Table 4.4 Wet Soil Moisture Content

Wet Soil Test Moisture Content Results		
Mass Tare	31.50	kg
Mass Tare + Wet Soil	203.60	kg
Mass Tare + Dry Soil	183.00	kg
Moisture Content (%)	10.12	%
Mass of Dry Soil	3907.45	kg

Tables were set up prior to testing with predetermined vibration lengths. Loose, dry soil compacts quicker than the wet soil, causing a steeper compaction curve. To account for this, a greater number of one second tests were performed for the dry soil than for the wet and saturated. Each time a test was executed and the soil was compacted, depth measurements were taken and a thermal conductivity test was performed. The data recorded during the dry, wet, and saturated tests is provided in Tables 4.5 through 4.7. A moisture content test was not conducted on the saturated soil; therefore, the soil was oven dried and the mass was determined after the test concluded. The results of the dried soil mass calculation are provided in Table 4.8.

Table 4.5: Dry Soil Test Results

Test Name	Time (s)	Total Time (s)	Depth 1 (in)	Depth 2 (in)	Thermal Conductivity (W/m-K)
D1	0	0	2.229	2.237	**0.356**
D2	1	1	2.543	2.54	**0.406**
D3	1	2	2.617	2.627	**0.424**
D4	1	3	2.642	2.665	**0.43**
D5	1	4	2.665	2.669	**0.467**
D6	4	8	2.701	2.713	**0.458**
D7	7	15	2.728	2.746	**0.456**
D8	15	30	2.777	2.759	**0.456**
D9	30	60	2.832	2.814	**0.465**
D10	60	120	2.868	2.818	**0.485**
D11	120	240	2.863	2.868	**0.507**
D12	240	480	2.885	2.963	**0.497**

Table 4.6: Wet Soil Test Results

Test Name	Time (s)	Total Time (s)	Depth 1 (in)	Depth 2 (in)	Thermal Conductivity (W-m-K)
T1	0	0	2.494	2.490	**1.925**
T2	1	1	2.975	2.943	**2.358**
T3	1	2	3.033	3.075	**2.534**
T4	2	4	3.183	3.206	**2.737**
T5	2	6	3.282	3.285	**2.942**
T6	4	10	3.319	3.329	**3.013**
T7	4	14	3.411	3.406	**3.025**
T8	8	22	3.478	3.447	**3.163**
T9	15	37	3.463	3.465	**3.155**
T10	30	67	3.543	3.503	**3.220**
T11	60	127	3.528	3.550	**3.256**
T12	120	247	3.513	3.681	**3.424**
T13	480	727	3.63	3.601	**3.274**

Table 4.7: Saturated Soil Test Results

Test Name	Time (s)	Total Time (s)	Depth 1 (in)	Depth 2 (in)	Thermal Conductivity (W-m-K)
S1	0	0	2.289	2.283	**4.009**
S2	1	1	2.399	2.400	**3.21**
S3	1	2	2.452	2.432	**3.018**
S4	2	4	2.486	2.494	**3.106**
S5	4	8	2.500	2.492	**2.822**
S6	8	16	2.587	2.548	**3.283**
S7	8	24	2.577	2.659	**3.844**
S8	16	40	2.644	2.616	**3.331**
S9	30	70	2.669	2.653	**3.578**
S10	60	130	2.663	2.706	**4.217**
S11	120	250	2.709	2.676	**3.855**
S12	240	490	2.728	2.706	**4.213**
S13	480	970	2.753	2.758	**3.234**
S14	960	1930	2.789	2.779	**3.449**

Table 4.8: Saturated Test – Soil Mass

Dried Soil Mass Calculation		
Mass of Pan	231.2	kg
Mass of Pan + Dry Soil	4399.8	kg
Mass of Dry Soil	4168.6	kg

The change in density over time is shown in the compaction curves provided in Figures 4.10 through 4.12. The curves are provided from zero to 100 seconds, where the majority of compaction occured.
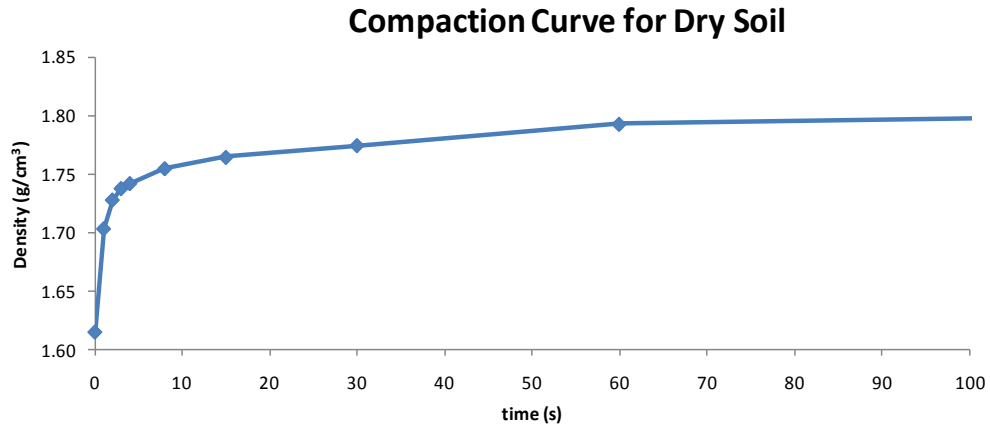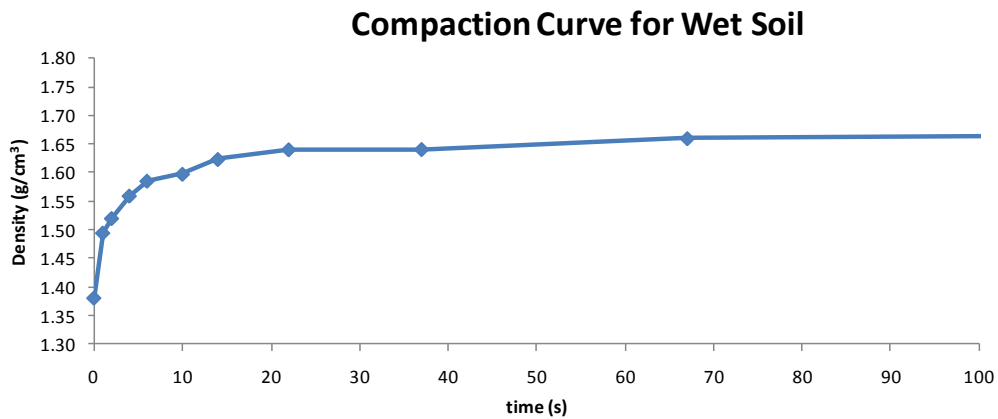
Compaction Curve for Dry Soil

Figure 4.10: Compaction Curve for Dry Soil Test

Compaction Curve for Wet Soil

Figure 4.11: Compaction Curve for Wet Soil Test

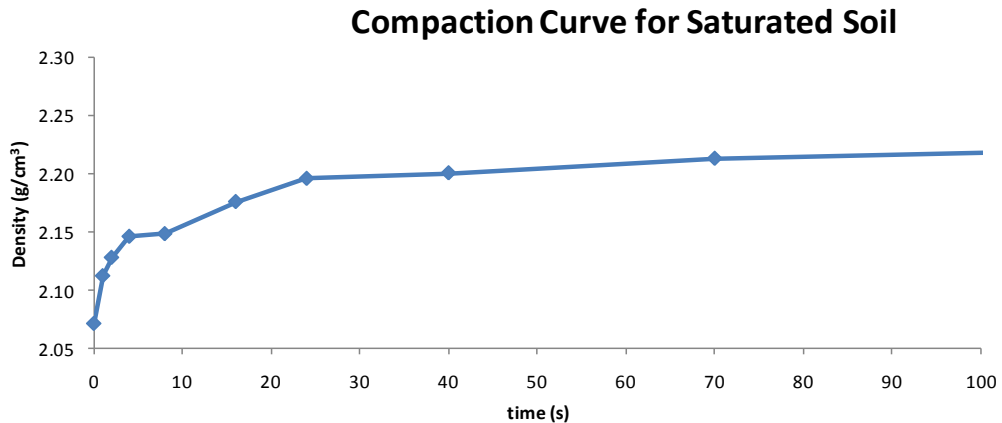**Compaction Curve for Saturated Soil**

Figure 4.12: Compaction Curve for Saturated Soil Test

60

The two depth measurements from the recorded data were averaged to account for uneven settling. To calculate the displacement of the soil from compaction, the initial average depth was subtracted from the average depth of the weight for each measurement taken. The average depth and soil displacement equations are:

$$Depth_{AVG} = \frac{(depth\ 1)(depth\ 2)}{2}$$

$$Soil\ Displacement = Depth_{AVG} - Depth_{AVG\ initial}$$

The height of the soil is simply the difference between the height of the mold and the soil displacement. Volume of the soil can then be calculated by multiplying the soil height by the cross-sectional area. The spreadsheet requires volume in SI units so this value was multiplied by the necessary conversion factor to get the result in cm^3. The equations used to calculate the height and volume of the soil in the mold each time compaction occurred are

$$Height_{soil} = Height_{mold} - Soil\ Displacement$$

$$Volume_{soil}(in^3) = Height_{soil}\ x\ Area_{mold}$$

$$Volume_{soil}(cm^3) = Volume_{soil}(in^3)x\ (2.54\ cm)^3/\ 1\ in^3$$

From the results of the moisture content test and the dried soil mass calculation, the mass of the dry soil was calculated. For the initial, non-compacted test, the volume of the soil was equivalent to the volume of the mold. Otherwise, the volume of the soil was calculated from the measured soil displacements. Mass of the dry soil and volume of the soil are the two parameters required to calculate dry density.

$$Dry\ Density = \frac{Mass_{dry\ soil}}{Volume_{soil}}$$

61

Using the data collected and the equations described in this section, dry density was computed for each test. These calculations are presented in tabular format for the dry, wet, and saturated tests in Tables 4.9 through 4.11.

Table 4.9: Dry Soil Test Calculations

Average Depth (in)	Displacement (in)	Height (in)	Volume (in³)	Volume (cm³)	Dry Density (g/cm³)
2.233	0.000	6.116	172.926	2833.747	**1.574**
2.542	0.309	5.808	164.203	2690.808	**1.657**
2.622	0.389	5.727	161.927	2653.510	**1.680**
2.654	0.421	5.696	161.036	2638.915	**1.690**
2.667	0.434	5.682	160.655	2632.660	**1.694**
2.707	0.474	5.642	159.524	2614.127	**1.706**
2.737	0.504	5.612	158.676	2600.227	**1.715**
2.768	0.535	5.581	157.799	2585.863	**1.724**
2.823	0.590	5.526	156.244	2560.380	**1.742**
2.843	0.610	5.506	155.678	2551.113	**1.748**
2.866	0.633	5.484	155.042	2540.688	**1.755**
2.924	0.691	5.425	153.388	2513.583	**1.774**

Table 4.10: Wet Soil Test Calculations

Average Depth (in)	Displacement (in)	Height (in)	Volume (in³)	Volume (cm³)	Dry Density (g/cm³)
2.492	0.000	6.116	172.926	2833.747	**1.379**
2.959	0.467	5.649	159.722	2617.370	**1.493**
3.054	0.562	5.554	157.036	2573.353	**1.518**
3.195	0.703	5.414	153.063	2508.255	**1.558**
3.284	0.792	5.325	150.547	2467.018	**1.584**
3.324	0.832	5.284	149.402	2448.253	**1.596**
3.409	0.917	5.200	147.012	2409.102	**1.622**
3.463	0.971	5.146	145.486	2384.082	**1.639**
3.464	0.972	5.144	145.443	2383.387	**1.639**
3.523	1.031	5.085	143.775	2356.050	**1.658**
3.539	1.047	5.069	143.323	2348.637	**1.664**
3.597	1.105	5.011	141.683	2321.763	**1.683**

Table 4.11: Saturated Soil Test Calculations

Average Depth (in)	Displacement (in)	Height (in)	Volume (in³)	Volume (cm³)	Dry Density (g/cm³)
2.286	0.000	6.116	172.926	2833.747	**1.471**
2.400	0.167	5.950	168.218	2756.602	**1.512**
2.442	0.209	5.907	167.016	2736.910	**1.523**
2.490	0.257	5.859	165.659	2714.670	**1.536**
2.496	0.263	5.853	165.490	2711.890	**1.537**
2.568	0.335	5.782	163.468	2678.762	**1.556**
2.618	0.385	5.731	162.040	2655.363	**1.570**
2.630	0.397	5.719	161.701	2649.803	**1.573**
2.661	0.428	5.688	160.824	2635.440	**1.582**
2.685	0.452	5.665	160.160	2624.552	**1.588**
2.693	0.460	5.657	159.934	2620.845	**1.591**
2.717	0.484	5.632	159.241	2609.493	**1.597**
2.756	0.523	5.594	158.152	2591.655	**1.608**
2.784	0.551	5.565	157.347	2578.450	**1.617**

The recorded test data was plotted against and compared with data from the methods provided by Kersten, Mickley, Gemant, De Vries, Van Rooyen, McGaw, and Johansen. The data for dry, coarse soil is provided in Figure 4.13. Comparing the data recorded by the KD2 device to the available data for dry, coarse soils, a consistent thermal conductivity trend can be observed. Aside from Mickley, dry soils with densities ranging from 1.6 to 1.9 g/cm³ have thermal conductivities between 0.2 and 0.5 W/m-K. The recorded test data fell within this range.

The data from the other two tests are shown in Figures 4.14 and 4.15. When analyzing these graphs, it can be deduced that the saturated condition introduced more variation in results. The soil with 10% moisture still showed a strong trend when compared to the other methods; however, the readings from the saturated test are on the higher end. This is most likely due to the longer heating time as noted by the ASTM guidelines. All thermal conductivity tests were performed at a length of 10 minutes. If

this time was reduced to 5 minutes, the reduced heating time might have provided a higher level of agreement and perhaps less variability.
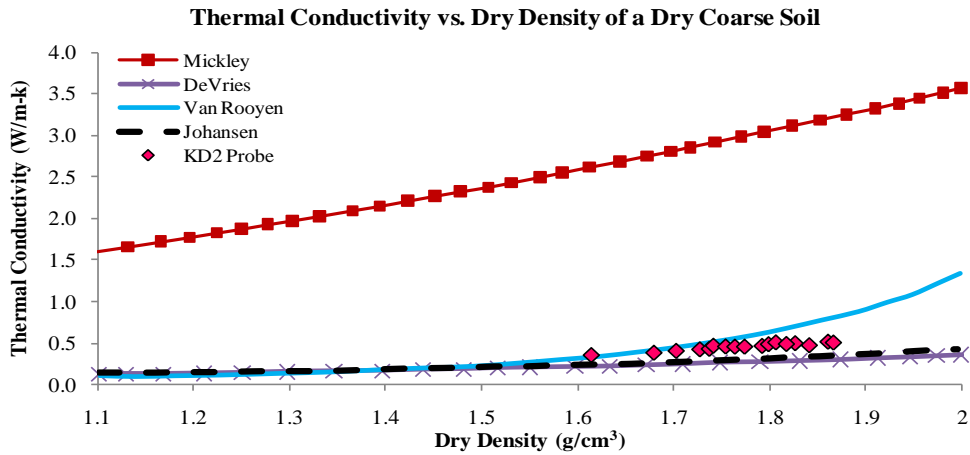

Figure 4.13: Thermal Conductivity vs. Dry Density for Dry Coarse Soil
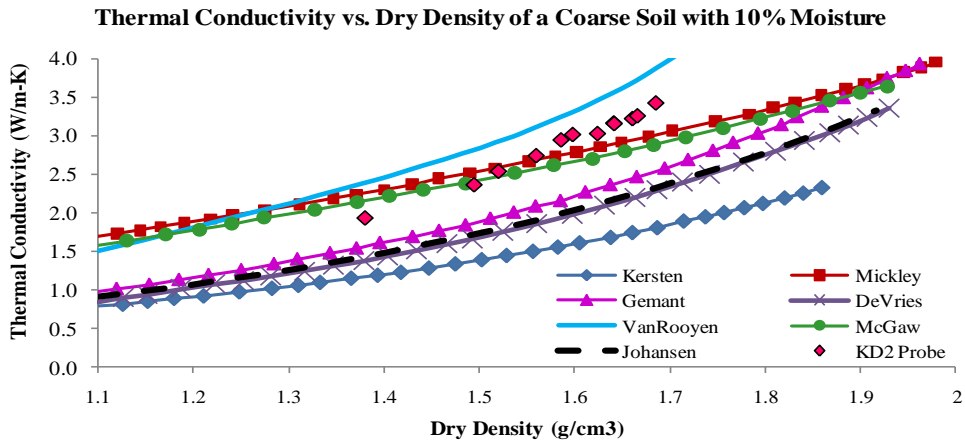

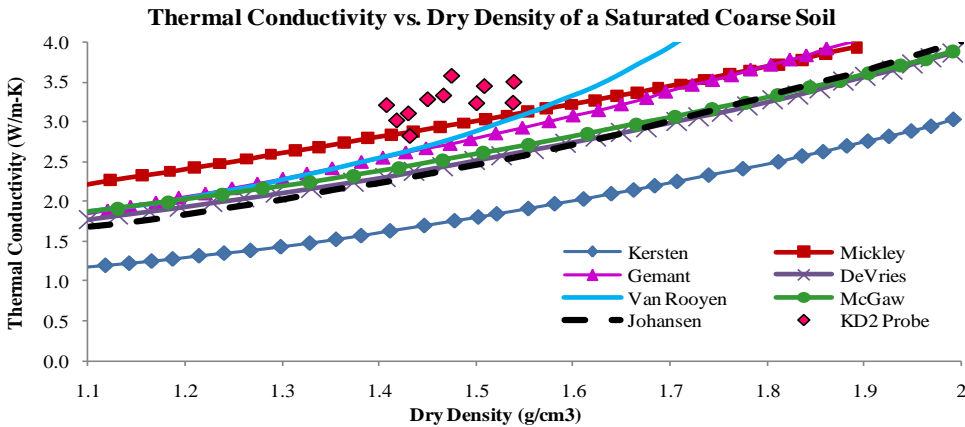Figure 4.14: Thermal Conductivity vs. Density for a Wet Coarse Soil

Figure 4.15: Thermal Conductivity vs. Density for a Saturated Coarse Soil

4.2.4 Repeatability and Temperature Tests

The repeatability and temperature tests utilized the same 0.10 ft^3 mold and soil from the same sample as the density tests. The mold was filled to the top with oven dried soil and compacted for 20 minutes using the vibrating table apparatus at a frequency of 50 hertz. This length of time was chosen to ensure a reasonably compacted soil. All tests were done without removing the probe from the compacted soil after its initial placement. This allows errors due to changing the location of the probe to be excluded from the analysis.

The KD2 probe manual suggests a 15 minute wait time between tests to obtain maximum accuracy. Tests were done to see how necessary this was. Several tests were set up to observe the changes in accuracy between continuous testing and testing with a 15 minute break in between. The consecutive tests were conducted at both the five and ten minute settings on the probe in order to see if there were variations in the results, whereas the longer tests were done at the 10 minute setting.

A refrigerator was used to control the temperature of the soil matrix. It was initially placed at its warmest setting and allowed to warm up for a period of 36 hours. The mold with the probe still inserted was then placed in the refrigerator with the cord from the probe connected to the data collection device located outside the refrigerator. At this point, the refrigerator was closed and was not opened until all testing was complete to prevent external temperatures from affecting the readings. The mold was left overnight at this setting to allow the soil to reach a stable temperature. Seven tests were done at three different refrigerator settings; low, medium, and high. One set was done each day

for three consecutive days. After the tests were completed each day, the refrigerator

would be turned to a colder setting and left overnight to cool down.

4.2.5 Repeatability and Temperature Test Results

The results for the repeatability tests are provided in Table 4.12. Temperature and

thermal conductivity are plotted against time in Figures 4.16 and 4.17. From the graph of

temperature vs. time, it can be seen that the 10 minute tests are run at a lower

temperature, both with and without wait time between. For the 10 minute test with the 15

minute wait time, the results appear to be linear whereas there are variations in the results

plotted from the data of the other tests; therefore, a 15 minute wait time provides more

consistent results and does appear to be more reliable. Assuming the data for the longer

tests with 15 minutes in between each is correct, the five minute tests under estimate the

thermal conductivity by approximately 12% and the continuous 10 minute tests slightly

over estimate the thermal conductivity.

Table 4.12: Results for Repeatability Tests

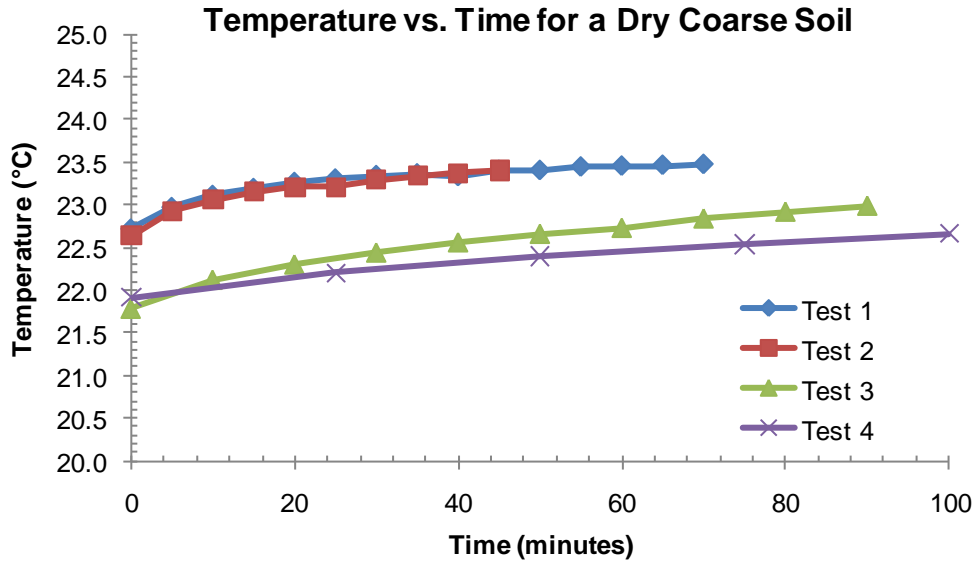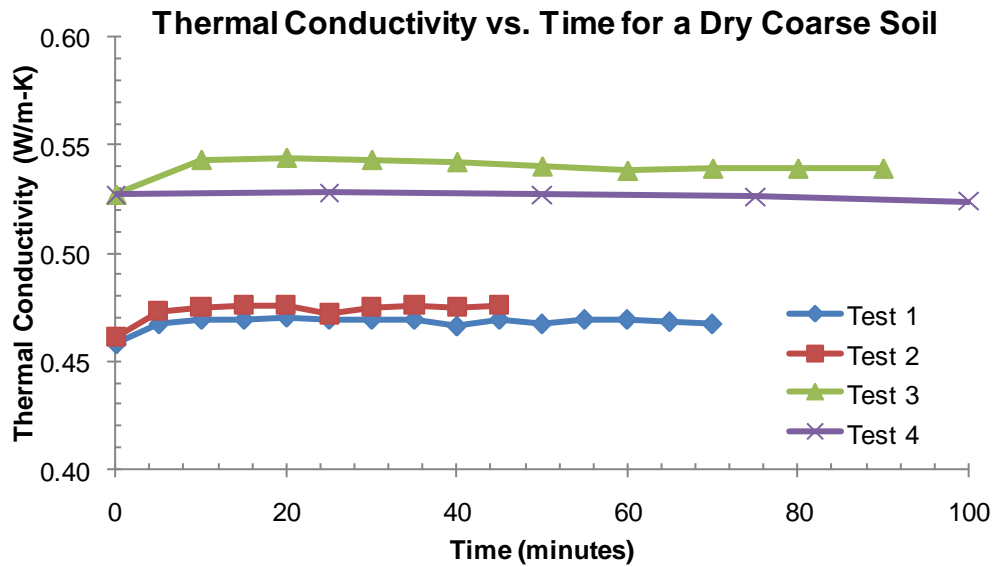|	Test 1 5 min tests no wait		Test 2 5 min tests no wait		Test 3 10 min tests no wait		Test 4 10 min tests 15 minute wait	
Test	T (°C)	λ (W/m-K)	T (°C)	λ (W/m-K)	T (°C)	λ (W/m-K)	T (°C)	λ (W/m-K)
T1	22.72	0.458	22.64	0.461	21.78	0.527	21.91	0.527
T2	22.97	0.467	22.93	0.473	22.12	0.543	22.20	0.528
T3	23.11	0.469	23.06	0.475	22.30	0.544	22.40	0.527
T4	23.19	0.469	23.15	0.476	22.44	0.543	22.54	0.526
T5	23.26	0.470	23.21	0.476	22.56	0.542	22.66	0.524
T6	23.30	0.469	23.21	0.472	22.66	0.540	22.75	0.524
T7	23.34	0.469	23.29	0.475	22.73	0.538	22.82	0.523
T8	23.36	0.469	23.34	0.476	22.84	0.539	22.89	0.523
T9	23.33	0.466	23.37	0.475	22.92	0.539		
T10	23.40	0.469	23.40	0.476	22.99	0.539		
T11	23.40	0.467						
T12	23.44	0.469						
T13	23.45	0.469						

Figure 4.16: Change in Temperature over Time

Figure 4.17: Change in Thermal Conductivity over Time

The data recorded from the temperature test is provided in Table 4.13. Temperature vs. time and thermal conductivity vs. time are plotted in Figures 4.18 and 4.19. Soil temperature remains reasonably constant over time at the four temperatures, but thermal conductivity increases slightly at the warmer temperatures and decreases slightly at the colder temperatures.

Table 4.13: Results for Temperature Tests

time (min)	Room Temperature		Setting 1 (warmest)		Setting 2		Setting 3 (coldest)	
	T (°C)	λ (W/m-K)	T (°C)	λ (W/m-K)	T (°C)	λ (W/m-K)	T (°C)	λ (W/m-K)
0	21.91	0.527	7.26	1.134	4.87	2.372	-3.36	3.280
25	22.20	0.528	7.37	1.180	4.85	2.437	-3.38	3.218
50	22.40	0.527	7.26	1.232	4.78	2.427	-3.37	3.148
75	22.54	0.526	7.23	1.258	4.85	2.249	-3.39	3.336
100	22.66	0.524	7.34	1.267	4.77	2.362	-3.70	3.136
125	22.75	0.524	7.35	1.320	4.79	2.260	-3.70	3.130
150	22.82	0.523	7.23	1.363	4.82	2.307	-3.55	3.170
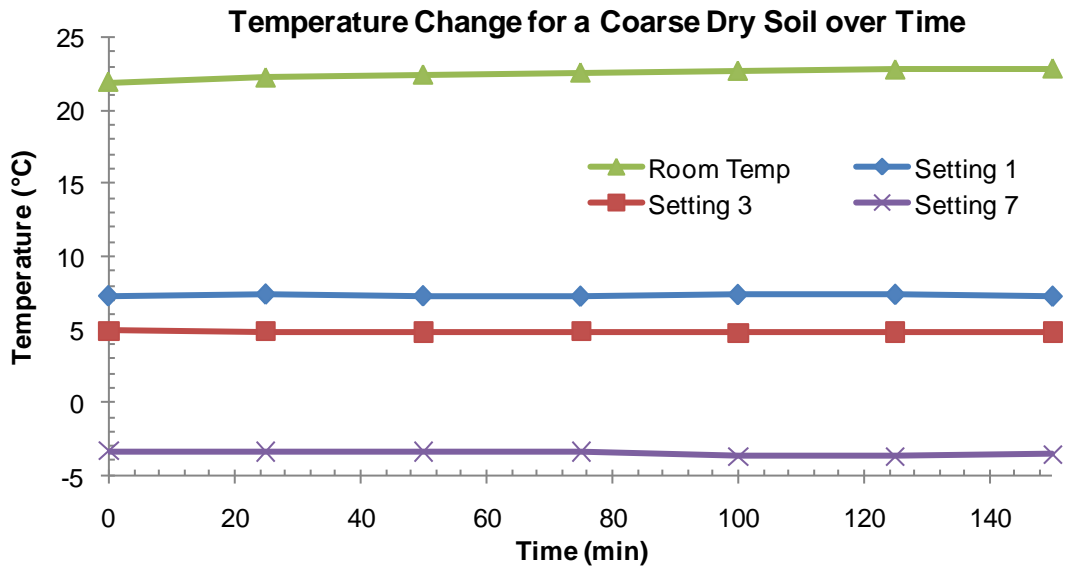
Figure 4.18: Change in Temperature over Time
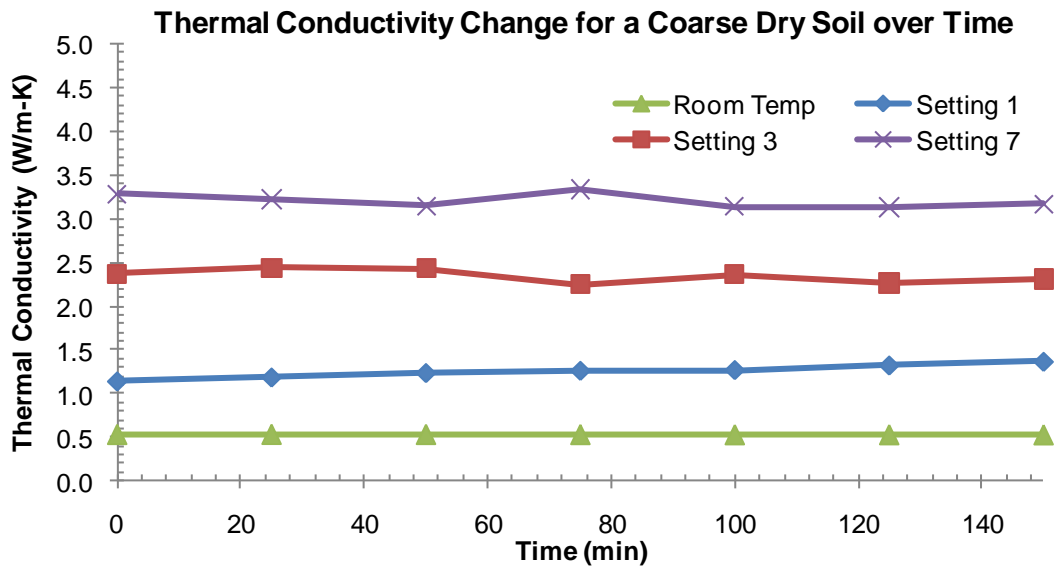
Figure 4.19: Change in Thermal Conductivity over Time

68

4.3 Evaluation of Theoretical Algorithms

A sample boring log is provided to aid as an example on how the spreadsheet

functions. Figure 4.20 shows a boring log for a soil boring performed for the

Crosstown/I-4 Connector project in Tampa, FL.
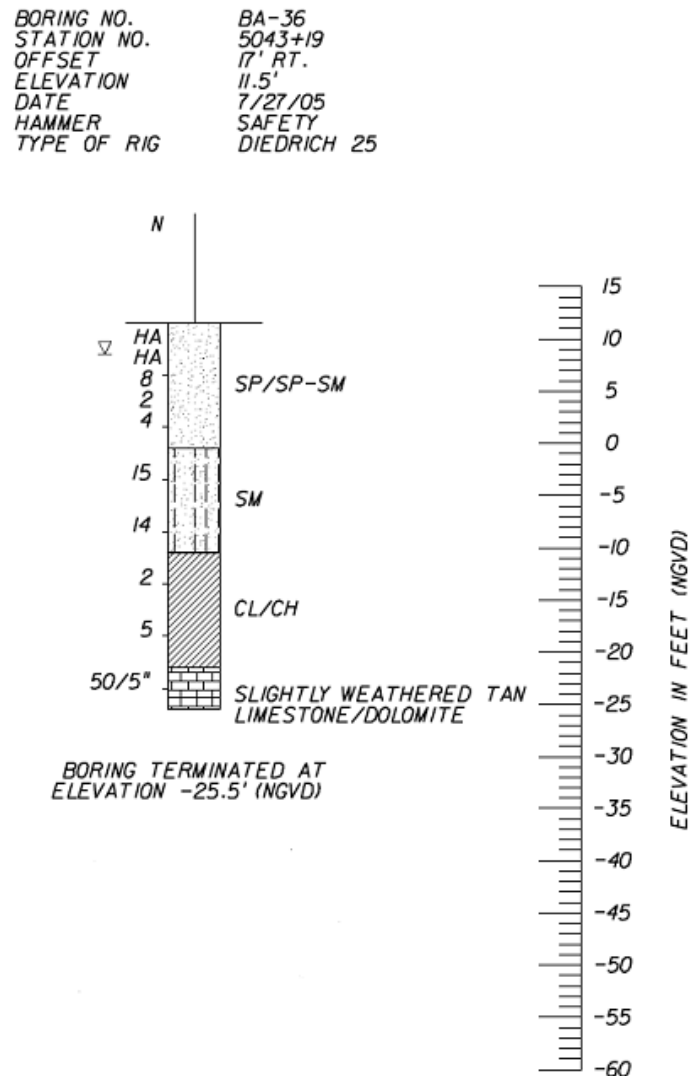
Figure 4.20: Boring Log for Boring BA-36

At the top of the spreadsheet are highlighted cells for project name, location,

boring ID, engineer's name, and date. Clicking on these cells will make them active so

that the project information can be input (Figure 4.21).

Figure 4.21: Inputting Project Information

To input the boring log data into the spreadsheet, the ground surface elevation and the elevation of the water table must be determined. Careful analysis of the boring log shows the ground surface elevation at 11.5 ft and the elevation of the water table at 8.5 ft. Figure 4.22 shows the elevations as they are input into the spreadsheet.

Figure 4.22: Inputting Elevations

This boring log is provided in terms of elevation, not depth; therefore, the depth of each input is the difference between the ground surface elevation and current elevation. Only elevations where blow counts were calculated should be input. Figures 4.23 through 4.25 show examples of the data being input for depth, blow count and soil type. Soil type is selected by clicking on the cell in the soil type column. This will bring up the drop-down menu with the different soil type options.

Boring Log Information				
Elevation	Depth	Blow Count	Soil Type	Density
ft	ft			g/cm3
	5			

Figure 4.23: Inputting Depth

Boring Log Information				
Elevation	Depth	Blow Count	Soil Type	Density
ft	ft			g/cm3
	5.0	8		

Figure 4.24: Inputting Blow Count

Boring Log Information				
Elevation	Depth	Blow Count	Soil Type	Density
ft	ft			g/cm3
	5.0	8		
			Sand	
			Limestone	
			Silt	
			Clay	
			Silty Sand	
			Clayey Sand	
			Silty Limestone	
			Clayey Limeston	

Figure 4.25: Inputting Soil Type

71

The blow count at a depth of 35 ft reads 50/5" which means that after 50 blows, the sampler only advanced 5 in. To account for this, the highest possible blow count, 60, is input to simulate a harder soil layer (Figure 4.26).

Boring Log Information				
Elevation ft	Depth ft	Blow Count	Soil Type	Density g/cm3
	5.0	8	Sand	
	7.5	2	Sand	
	10.0	4	Sand	
	15.0	15	Silty Sand	
	20.0	14	Silty Sand	
	25.0	2	Clay	
	30.0	5	Clay	
	35.0	60	Limestone	

Figure 4.26 – Inputted Boring Log

Upon completion of the depth, blow count, and soil type inputs for each boring log entry, clicking the *Calculate* button will calculate elevation, density, the 7 thermal conductivity methods, and the average of the selected methods. Figure 4.27 shows the results calculated when this button is clicked. To select which methods to plot and include in the average, the check boxes are clicked to be selected or deselected. Once the desired methods have been selected, clicking the *Update* button (Figure 4.28) will update the average and the thermal conductivity vs. depth graph. Six methods, including the average are selected and the resulting plots from the thermal conductivity vs. depth graph and the boring log plot are shown in Figure 4.29.

Figure 4.27: Results from Clicking the Calculate Button

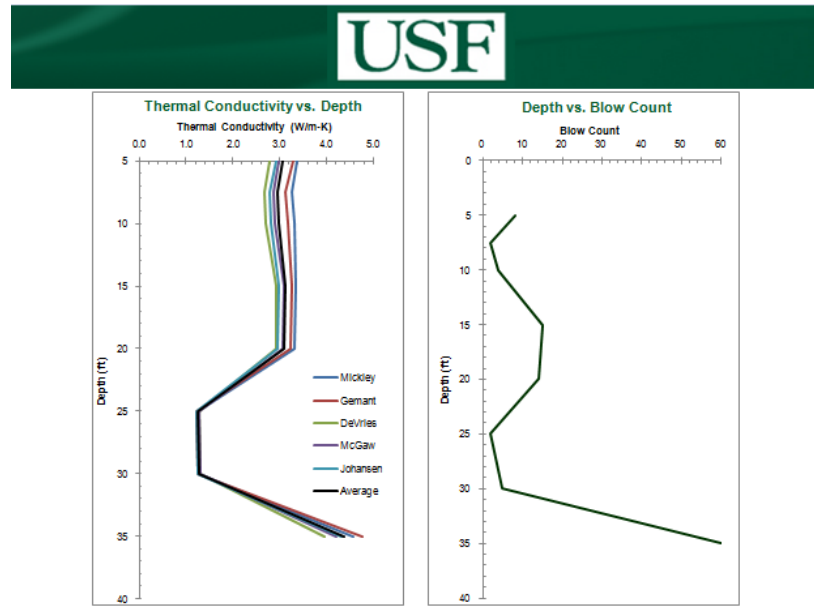Figure 4.28: Clicking Update after Selecting Desired Plotting Methods

Figure 4.29: Plot of Selected Methods and Plot of Boring Log

73

4.3.1 Heat Capacity

As the ultimate thermal property controlling diffusion is diffusivity, an additional module was created to compute the heat capacity from which the diffusivity can be calculated for each boring log entry using the following equation from chapter 2.

$$k = \frac{\lambda}{C}$$

Heat capacity, C, is a far less intense computation requiring only the fraction of air, water, and soil as well as the mineralogy. This is calculated using the equation for specific heat,

$$C = X_S C_S + X_W C_W + X_a C_a$$

where C_S, C_w, and C_a are the heat capacities of soil, water, and air, and X_S, X_W, and X_a are the volumetric fractions of soil, water, and air (Duarte 2006).

Chapter 5 - Conclusion

Thermal properties of soils vary drastically depending on the mineralogy, density, saturation state, and structure. Despite several decades of research on the topic, no rational correlations exist that predict thermal properties using common soil exploration methods. This thesis focused on assembling correlations from existing literature to close the gap between SPT sampling and thermal properties. The direct applications of defining the thermal properties of soils include both geothermal heating/cooling systems and those methods of foundation quality assurance involving thermal integrity profiling. The latter of which is discussed below.

5.1 Thermal Integrity Profiling

Thermal integrity profiling is a test method that assesses the intactness of cast-in-place concrete with emphasis on an underground structural element (e.g. drilled shaft or ACIP). The hydration energy of curing concrete is sufficient in magnitude to develop a temperature signature relative to the volume of concrete placed. In cases where the soil is uniform, the developed temperature is also uniform for a perfectly shaped cylinder. Variations in cross section can cause increases or decreases in the measured temperature proportional to bulges or necks, respectively.

Figures 5.1 through 5.3 show the temperature variation from TIP testing of shafts constructed with permanent casing in the upper portion along with the SPT blow counts. These three shafts provide an interesting case study for this thesis as the cross section is known not to have varied. As a result, the temperature variations recorded are largely the

effect of thermal properties which can be identified with the developed spreadsheet.

Therefore, this comparison is exclusively based on that portion above the bottom of
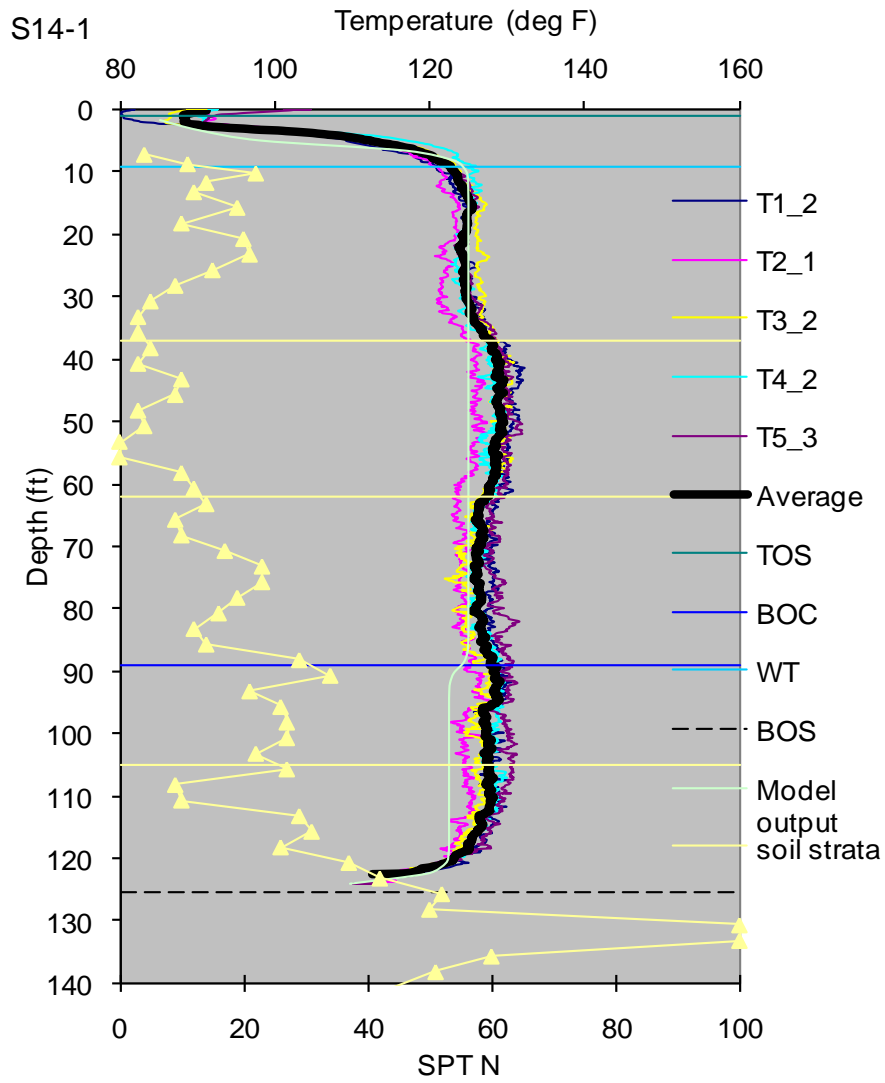
casing (BOC).
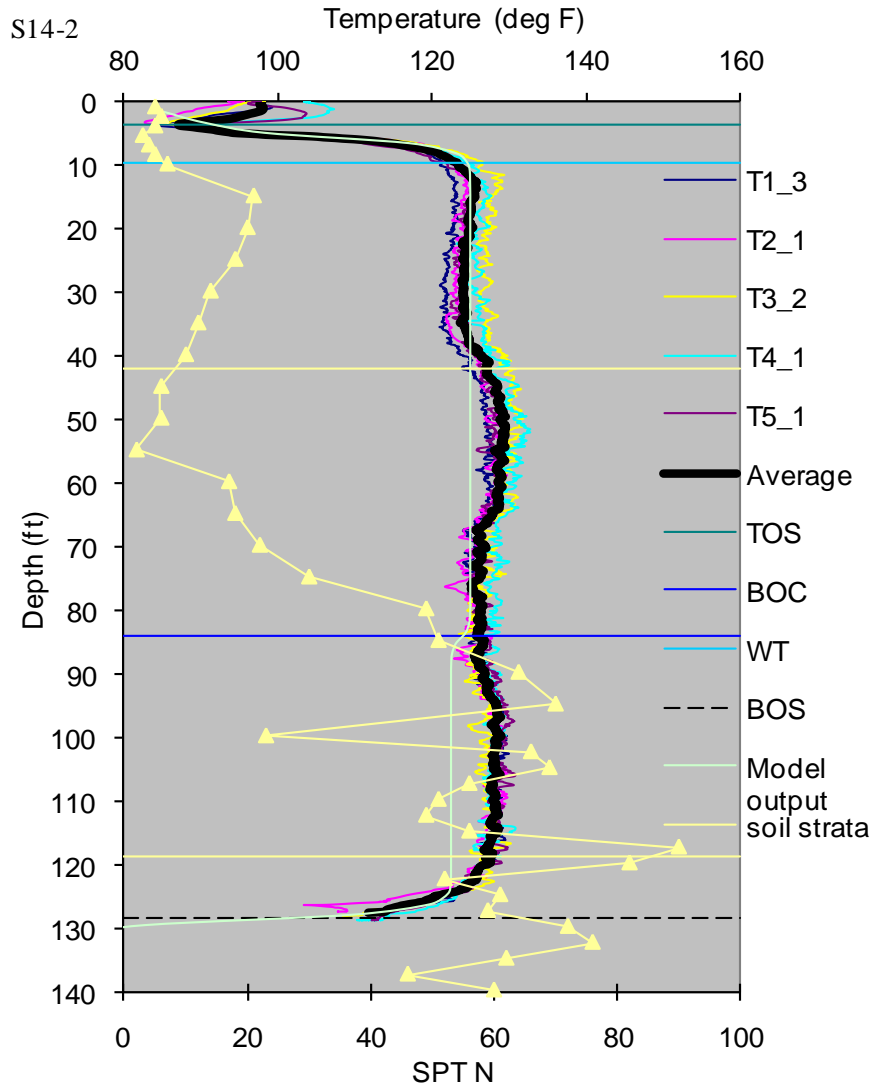

Figure 5.1: TIP Analysis – Shaft 14-1
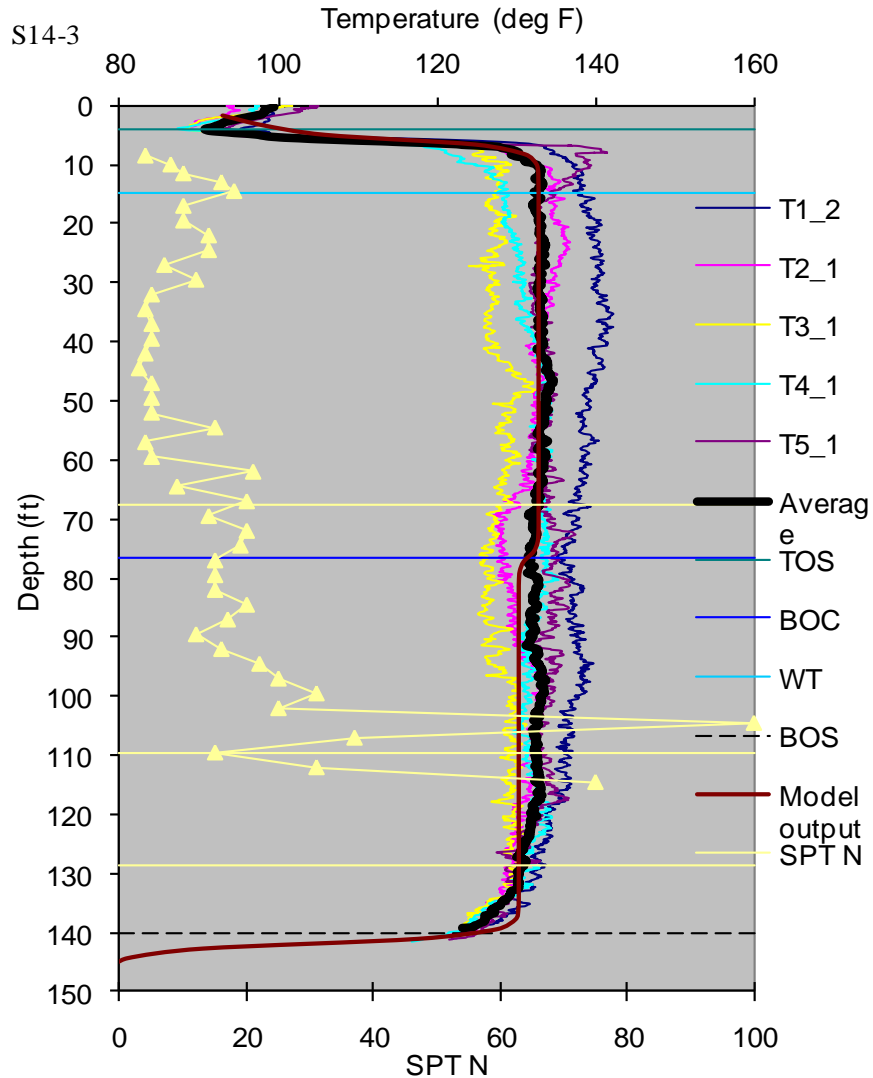
Figure 5.2: TIP Analysis – Shaft 14-2

Figure 5.3: TIP Analysis – Shaft 14-3

Figures 5.4 and 5.5 show the predicted thermal conductivity, heat capacity, and diffusivity along with the measured TIP results of the first shaft (14-1). In the cased region, an increased temperature trend is noted from 30 to 60 ft which corresponds to a reduction in the diffusivity. Figures 5.6 and 5.7 show the thermal conductivity, heat capacity, diffusivity, and TIP measurements of the second shaft (14-2). Again, an increased temperature trend and reduced diffusivity is noted in the cased region, in this case from 40 to 65 ft.
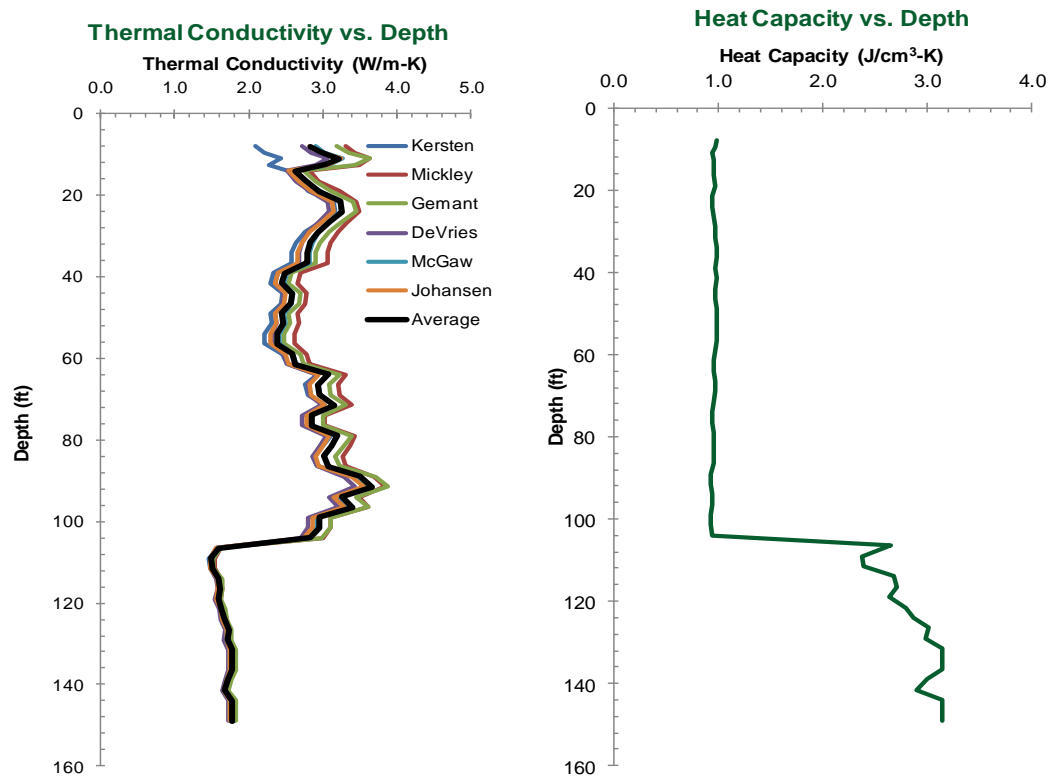
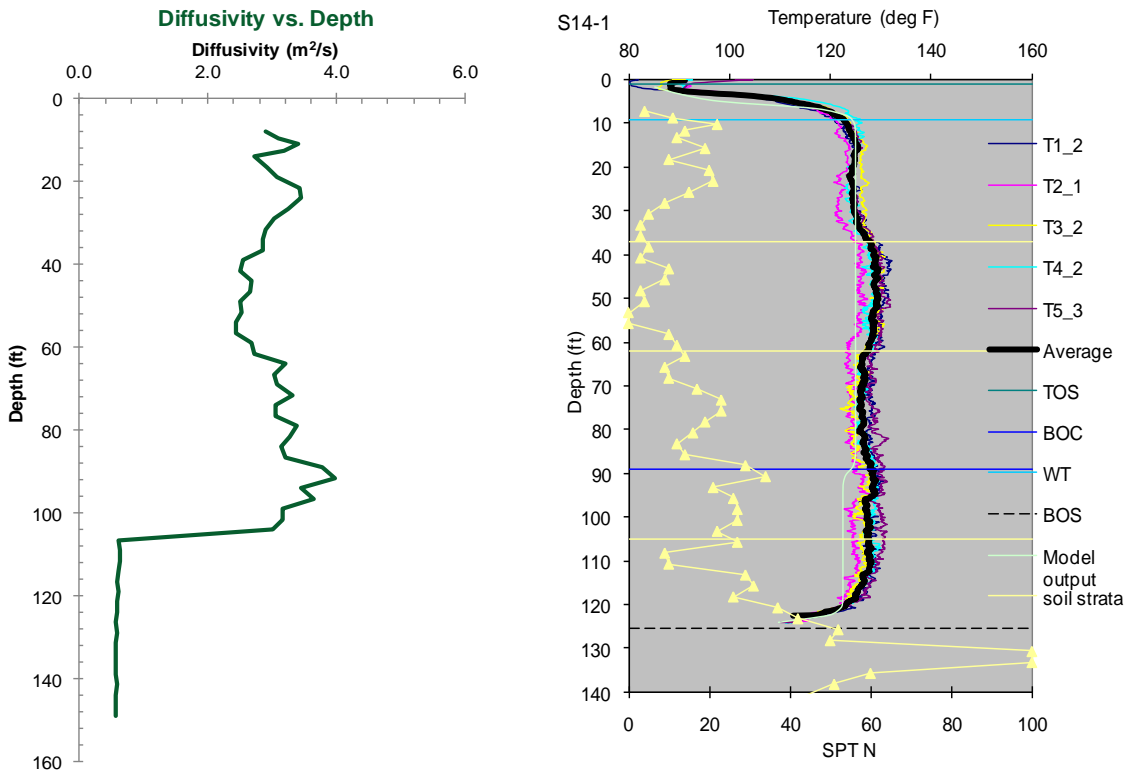Figure 5.4: Thermal Conductivity and Heat Capacity for Shaft 14-1

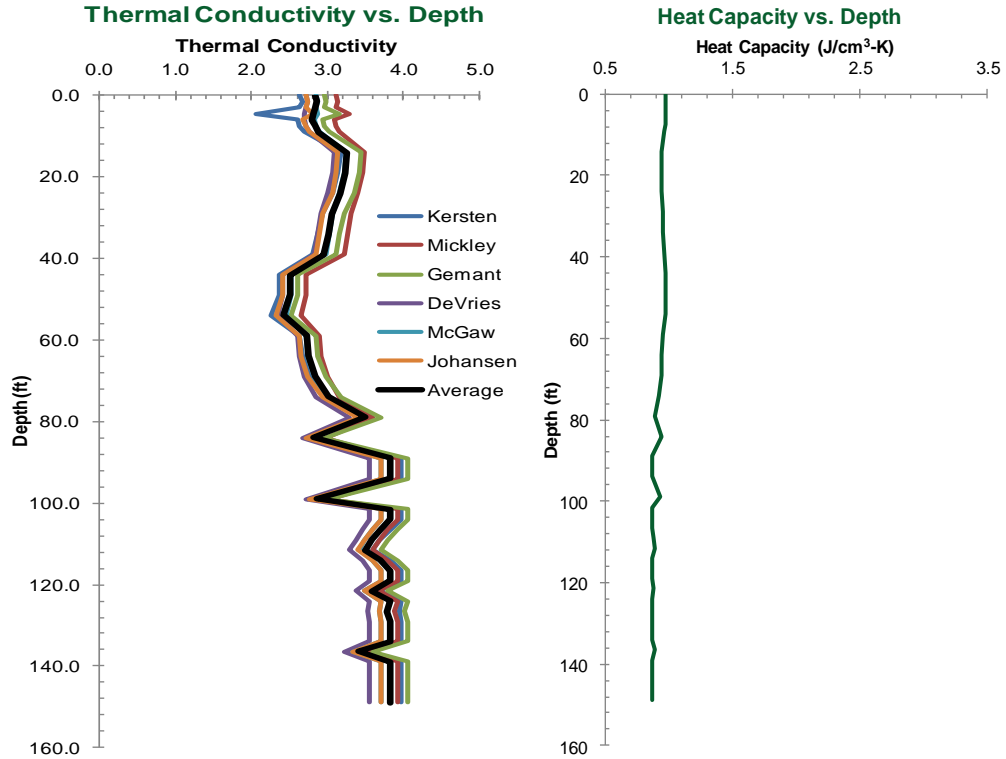Figure 5.5: Diffusivity and Temperature Profile for Shaft 14-1

79

Thermal Conductivity vs. Depth

Heat Capacity vs. Depth

Figure 5.6: Thermal Conductivity and Heat Capacity for Shaft 14-2
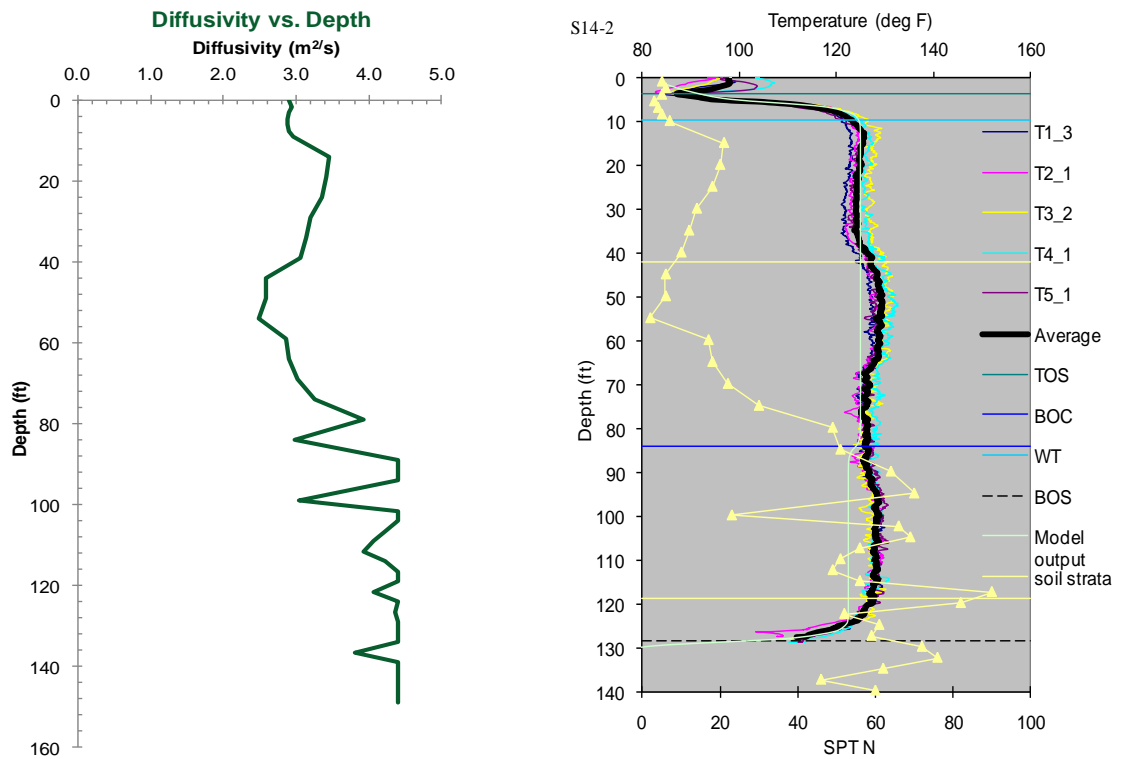
Diffusivity vs. Depth

Figure 5.7: Diffusivity and Temperature for Shaft 14-2

Conversely, Figures 5.8 and 5.9 show a nearly ideal temperature profile with the exception of a slight increased zone from 40 to 45 ft that appears to correspond to a reduced diffusivity at the same depth. The boring log consists entirely of either clayey or silty sands except for in this region, where the soil is labeled as sandy clay. The large increase in heat capacity and decreases in thermal conductivity and diffusivity could be due to a misclassification of the soils in this region. As an example, clayey sand was selected for this region instead of sandy clay and the modified results for diffusivity are plotted next to the temperature profile in Figure 5.10. This shows the sensitivity to soil classification.
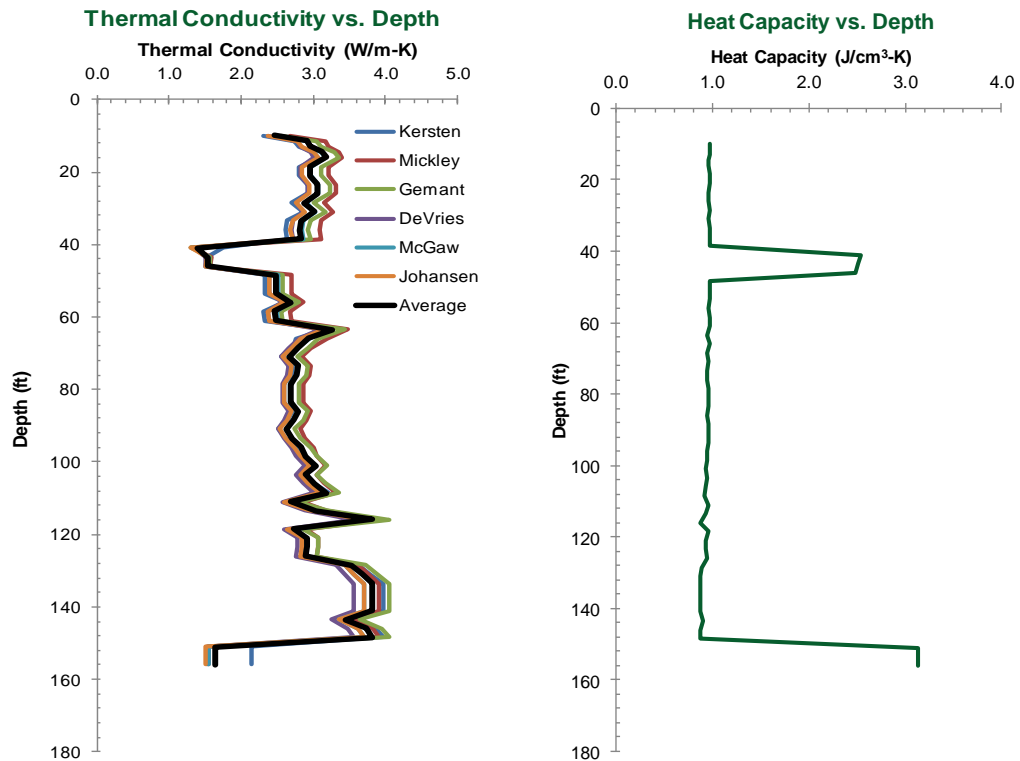
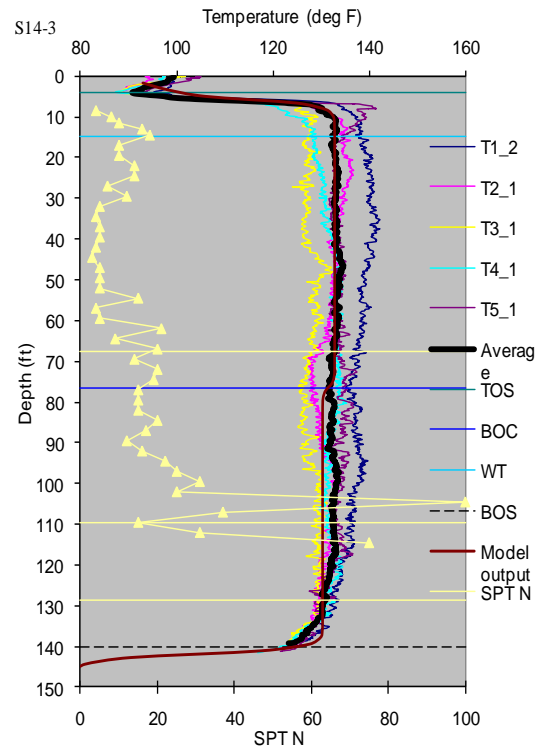

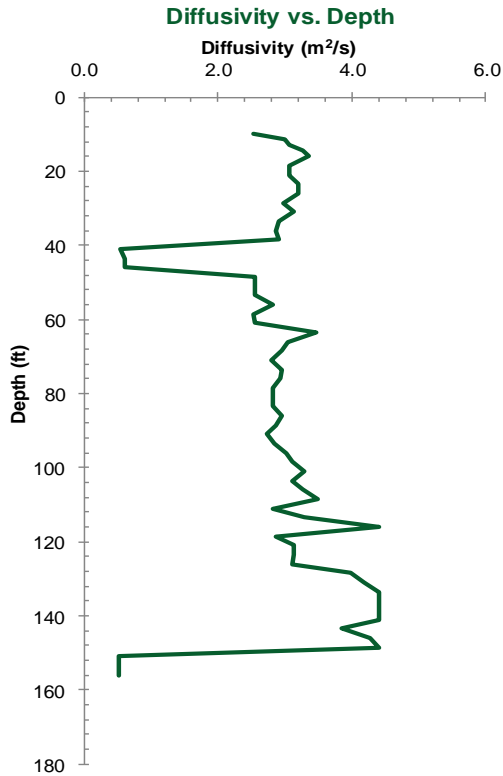Figure 5.8: Thermal Conductivity and Heat Capacity for Shaft 14-3

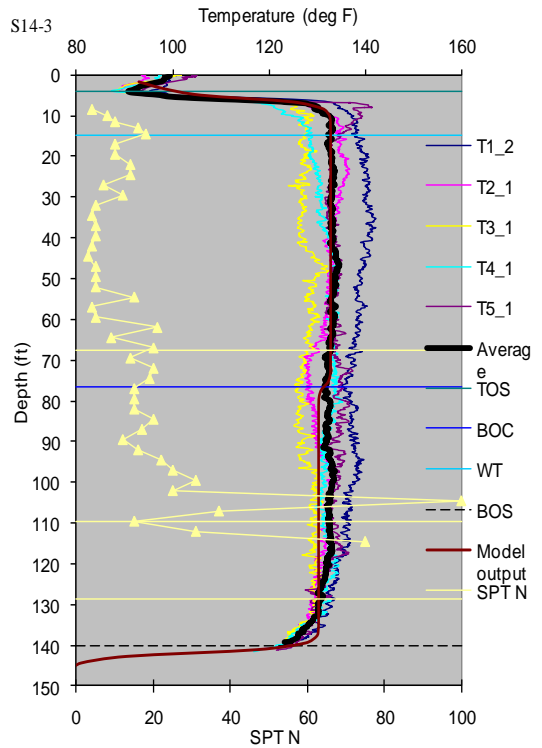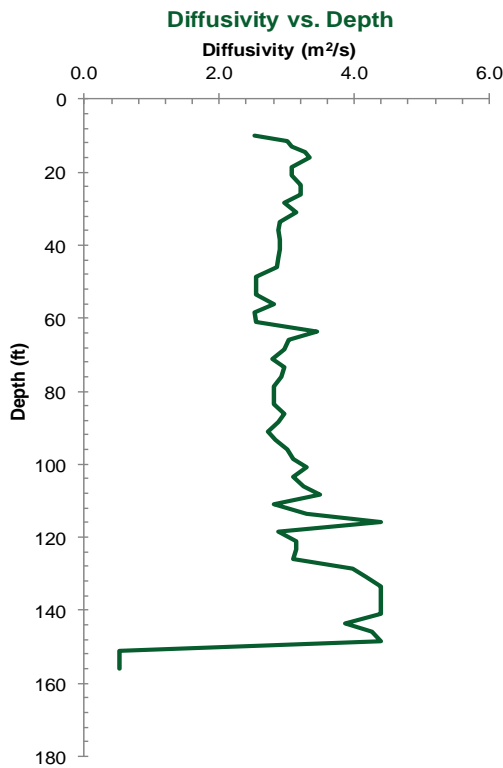Figure 5.9: Diffusivity and Temperature Profile for Shaft 14-3

Figure 5.10: Modified Diffusivity and Temperature Profile for Shaft 14-3

Obviously, limitations exist in such an approach in that often times the nearest boring log may not reflect the actual conditions. In those cases, construction logs can be used to explain subtle variations in soil mineralogy, but can only qualitatively assess the effect.

5.2 Future Studies

At present, efforts are underway to develop a CPT-based thermal conductivity probe. This has the potential to more readily quantify both the soil characteristics (i.e. strength, structure, and mineralogy) and the thermal conductivity with vertical depth resolution for more precise measurements (1 data point/cm) than the SPT wherein 1 data point per 1.5 ft is the absolute finest resolution attainable.

5.3 Summary

This thesis presents a new analysis tool for the purpose of quantifying the thermal properties of soil from commonly used SPT boring log data. It is thought to be the only such attempt to do so and as such will likely incur numerous changes and refinements in ensuing years. The applicability of the thesis findings are at present somewhat limited but predictive methods in these areas are receiving much needed attention and will benefit from the inroads developed herein.

List of References

ASTM (1996), "Annual Book of ASTM Standards", Vol. 4.08, D1586, D4253, D4318

ASTM (2008), "Annual Book of ASTM Standards", Vol. 4.08, D5334

Duarte, A., Campos, T., Araruna, J., and Filho, P., (2006). "Thermal Properties of Unsaturated Soils," *Unsaturated Soils*, GSP, ASCE, pp. 1707-1718.

Earth Temperature and Site Geology. Virginia Tech, Department of Mines Minerals and Energy. Web.
http://www.geo4va.vt.edu/A1/A1.htm

Farouki, O. (1982). "Evaluation of Methods for Calculating Soil Thermal Conductivity," Report 82-8, US Army Corps of Engineers Cold Regions Research and Engineering Laboratory, pp. 14-23

Farouki, O. (1966). "Physical Properties of Granular Materials with Reference to Thermal Resistivity," Highway Research Record 128, National Research Council, Washington, DC, pp. 25-44

Johansen, O. (1977). "Thermal Conductivity of Soils," U.S. Army Corps of Engineers Cold Regions Research and Engineering Laboratory. Hanover, NH, pp. 1-46

Johansen, O. (1975). "Thermal Conductivity of Soils and Rocks," Proceedings of the Sixth International Congress of the Foundation Francaise d'Etudes Nordigues, Vol. 2, pp.407-420

Kersten, M.S. (1949). "Thermal Properties of Soils," University of Minnesota Institute of Technology, Engineering Experiment Station, Vol. LII, No. 21.

Kranc, S.C. and Mullins, G. (2007). "Inverse Method for the Detection of Voids in Drilled Shaft Concrete Piles from Longitudinal Temperature Scans," Inverse Problems Design and Optimization Symposium, Miami, FL, April 16-18, 2007.

Kulhawy, F. H. and Mayne, P. W. (1990), "Manual on Estimating Soil Properties for Foundation Design," Technical Report EPRI-EL-6800, Electric Power Research Institute, Palo Alto, CA.

Limestone Properties. University of Florida. Bridge Software Institute. Web. http://bsi-web.ce.ufl.edu/downloads/files/MultiPier_Soil_Table.pdf

Maynard, Whitney (2010). "Monitoring and Evaluation of Geothermal Systems," Master's Thesis, University of South Florida, December.

Mullins, G., Winters, D., and Johnson, K., (2009), "Attenuating Mass Concrete Effects in Drilled Shafts," Final Report, FDOT Project BD544-39, September.
Mullins, G. and Kranc, S., (2007), "Thermal Integrity Testing of Drilled Shafts," Final Report, FDOT Project BD544-20, May.

Mullins, G. and Ashmawy, A., (2005), "Factors Affecting Anomaly Formation in Drilled Shafts," Final Report, FDOT Project BC353-19, March.

Mullins, A. G. and Kranc, S. C., (2004), "Method for Testing the Integrity of Concrete Shafts," US Patent 6,783,273.

Mullins, G. and Winters, D. (2004). "Post Grouting Drilled Shaft Tips - Phase II Final Report." Final Report submitted Florida Department of Transportation, June.

Trout, K. (2010). "Integrated North Tampa Bay Model Application of the Integrated Hydrologic Model," INTB Model Calibration Report, Tampa Bay Water. In press.